Chapter 4

THE ELECTROCHEMICAL BEHAVIOUR OF GOLD-BASED ALLOYS IN ACID SOLUTION WITHOUT ETHYLENE GLYCOL

4.1. Introduction

The heat treatments of the gold-based alloys were discussed in the previous chapter. By employing different heat treatments, different microstructures could be produced in alloys with the same composition. The purpose of this chapter is to investigate the electrochemical behaviour of all the electrodes in acid solution without ethylene glycol. Cyclic voltammetry was used to study electrode surface oxidation, oxide reduction and the oxygen and hydrogen gas evolution reactions. In order to have a better understanding of the electrochemical behaviour of alloy electrodes, experiments were also conducted with gold and platinum electrodes.

4.2. Experimental

The experimental work was performed with polycrystalline gold (99.9%), platinum (99.9%), 60Au-40Pt, 50Au-50Pt and Gold 990 electrodes. The electrodes were disc-shaped with 6mm diameter. All the electrodes were mounted in a resin by using a black phenolic thermosetting powder. Electrical contact was achieved by drilling a hole through the rear of the mounting and tapping M6 thread. A Pine analytical rotator was used as electrode rotator. The apparent surface area of 0.28 cm^2 was used in all cases to calculate current densities. The higher real surface areas of the porous electrodes are expected to give higher apparent current densities than the non-porous electrodes. This will give an indication on how the porosity of these electrodes will influence their electrochemistry.
A water-jacketed perspex electrochemical cell was used for all the experiments. The cell had an inside diameter of 90 mm and a height of 100 mm. Approximately 400 ml electrolyte was used. The distance between the working electrode and the bottom of the cell was about 60 mm. The temperature was controlled at 25°C. The cover of the perspex

cell had six openings which allowed the insertion of two counter electrodes, the working electrode, the Luggin capillary, the tube for nitrogen purging and a thermometer.

The experiments were conducted in 0.5 M H_2SO_4 solution. The solution was prepared by using CP grade H_2SO_4 from Chemical Suppliers (Pty) Ltd and double distilled water. Prior to each experiment, the solution was purged with nitrogen for 30 minutes to remove dissolved oxygen. The electrodes were polished before the experiments with diamond paste (down to 1 μm) and ultrasonically cleaned in 0.5 M H_2SO_4.

A Solartron 1287 Electrochemical Interface was used for the cyclic voltammetry experiments. The electrode potential was cycled between the values for onset of O_2 and H_2 evolution until the I-E curves were reproducible. It was found that approximately 15 cycles are needed to obtain reproducible I-E curves. The fifteenth cycle is used in all cyclic voltammograms shown in this chapter. The scan rate employed was 50 mV/s. The electrochemical experiments in acid solution without ethylene glycol were conducted without rotating the electrodes or stirring the solution. Platinum wire was used as counter electrode. All potentials quoted in this study are with respect to the silver/silver chloride reference electrode (SSC). Electrochemical impedance spectroscopy was performed with a Solartron 1250 Frequency Response Analyser.

4.3. Results and discussion

4.3.1. Gold

Cyclic voltammograms for gold are shown in Figure 4.1. These voltammograms agree well with those found in the literature (Fig. 2.1). Monolayer oxide formation commences at 1.05 V_{SSC} during the positive sweep followed by oxygen gas evolution at higher potentials. The surface oxide is reduced at 0.9 V_{SSC} during the negative sweep. More oxide is formed during the positive sweep when a higher upper potential limit is used. This results in a larger oxide reduction peak during the subsequent negative sweep. The potential for the oxide reduction peak is then also shifted to slightly more negative potentials (Fig. 4.1).

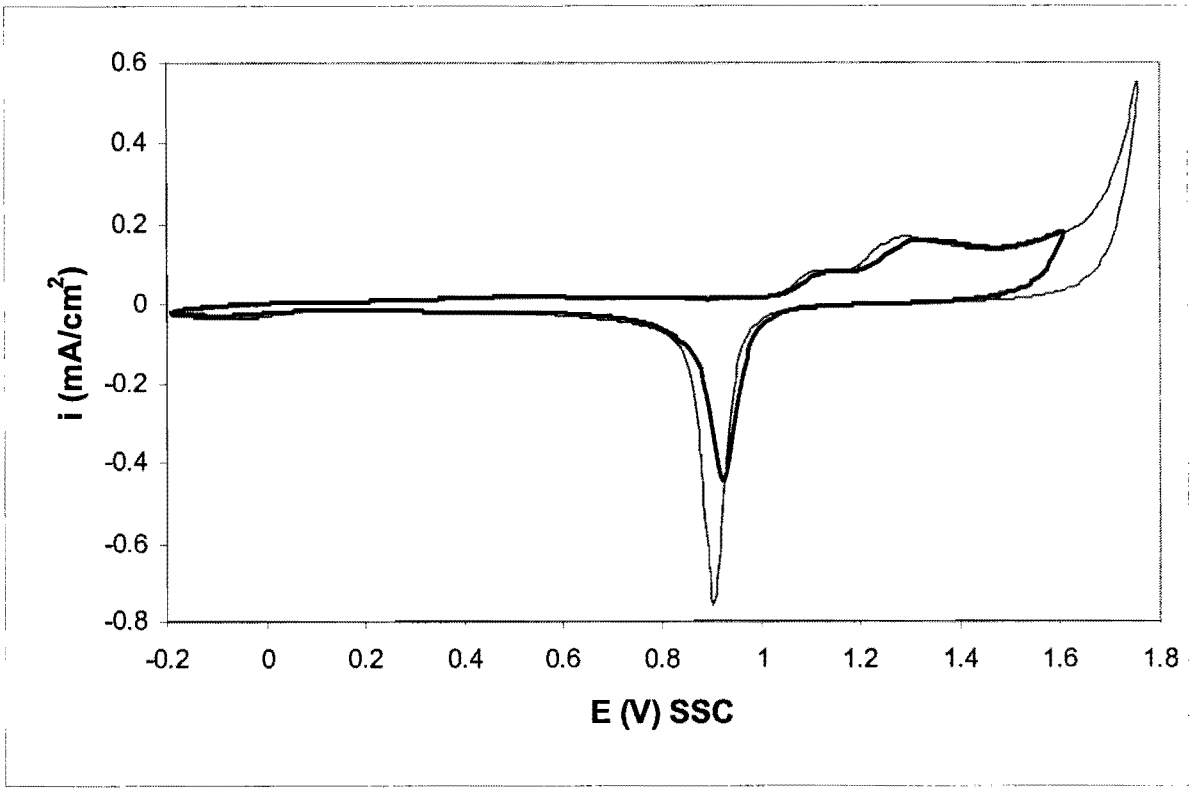

Figure 4.1. Cyclic voltammograms for gold in 0.5 M H_2SO_4. Scan rate 50 mV/s, 25°C.

4.3.2. Platinum

A cyclic voltammogram for platinum is shown in Figure 4.2. This voltammogram agrees well with those found in the literature (Fig. 2.9). Hydrogen desorption/adsorption occurs in the region of –0.2 to 0.1 V_{SSC}. Surface oxidation commences at approximately 0.55 V_{SSC}. The surface oxide is reduced during the negative sweep at 0.5 V_{SSC}.

Cyclic voltammograms for platinum with different upper potential limits (1.4 and 1.6 V_{SSC}) are shown in Figure 4.3. The higher upper potential limit leads to a much larger oxide reduction peak because more oxide is formed with a high upper potential limit. The peak is also shifted significantly to more negative potentials. Possibly some PtO_2 is formed with the high upper potential limit and only PtO with the low upper potential limit (Xia and Birss, 2000).

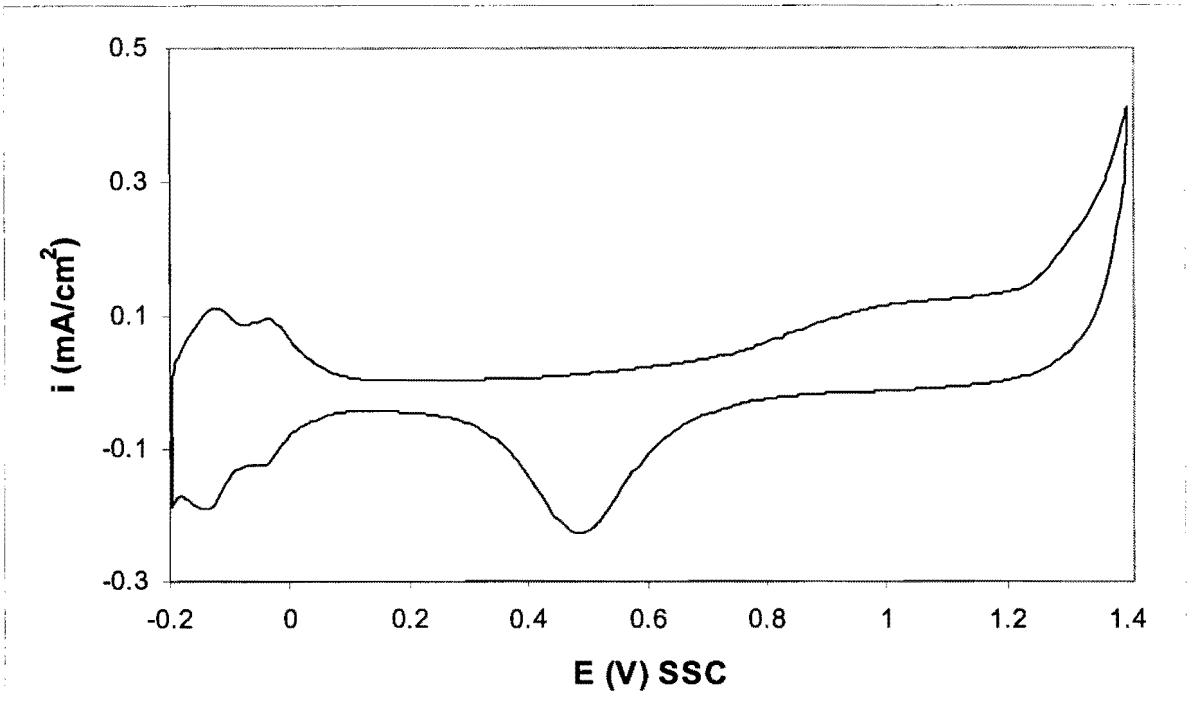

Figure 4.2. Cyclic voltammogram for platinum in 0.5 M H_2SO_4. Scan rate 50 mV/s, 25°C.

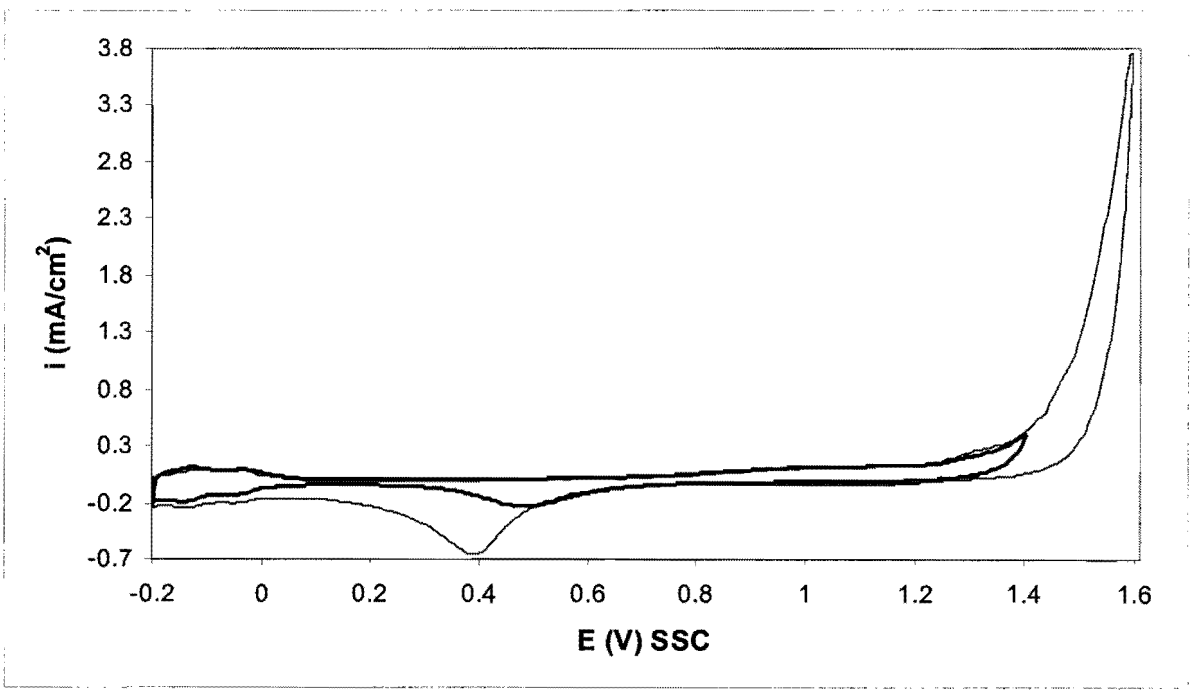

Figure 4.3. Cyclic voltammograms for platinum in 0.5 M H_2SO_4. Scan rate 50 mV/s, 25°C.

Cyclic voltammograms for gold and platinum with the same upper potential limit (E_{up} = 1.5 V) are shown in Figure 4.4. It is seen that oxygen gas evolution occurs at lower potentials on platinum than on gold. The lack of a hydrogen adsorption/desorption region on gold is also evident. A larger oxide reduction peak is found for platinum than gold. This is due to the fact that surface oxide formation commences at lower potentials on platinum.

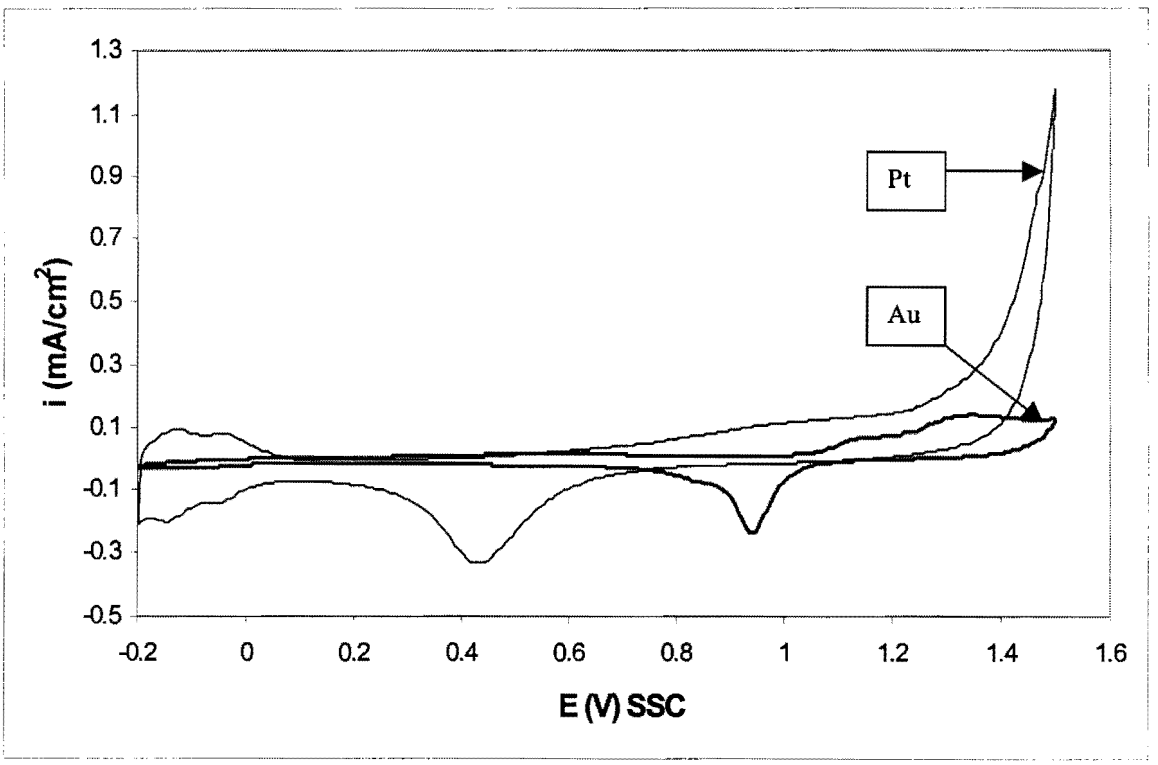

Figure 4.4. Cyclic voltammograms for platinum and gold in 0.5 M H_2SO_4. Scan rate 50 mV/s, 25°C. E_{up} = 1.5 V.

4.3.3. The 60Au-40Pt alloy

4.3.3.1. The 60Au-40Pt alloy in the 1300°C heat treatment condition

The two-phased microstructure of this alloy is shown in Figure 3.2. Cyclic voltammograms for the 1300°C treated electrode are shown in Figure 4.5 and features corresponding to both pure gold and platinum can be seen. The alloy has a hydrogen adsorption/desorption region (-0.2 to 0.1 V_{SSC}). Two oxide reduction peaks are found. The one peak corresponds to that of platinum and the other to gold. An increase in the upper potential limit causes an increase in the oxide reduction peaks and the peaks are shifted in the negative direction. The effect is more pronounced with the platinum (or platinum-rich) oxide reduction peak than with the gold (or gold-rich) oxide reduction peak. The current density for oxygen gas evolution at 1.6 V_{SSC} is higher than on pure gold, but lower than on pure platinum.

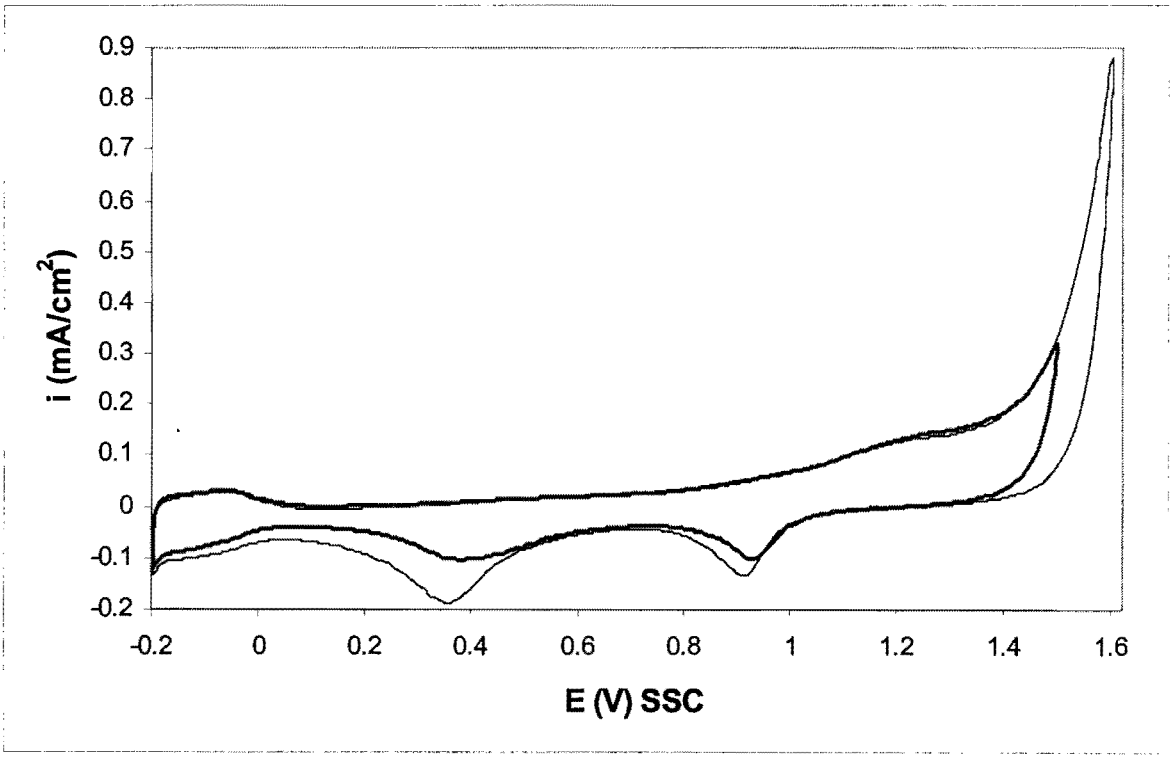

Figure 4.5. Cyclic voltammograms for the 1300°C heat treated sample (60Au-40Pt) in 0.5 M H_2SO_4. Scan rate 50 mV/s, 25°C.

4.3.3.2. The 60Au-40Pt alloy in the 1200°C (24 hours) heat treatment condition

The microstructure of this single-phased, but porous sample is shown in Figure 3.6. The sample was in the 1300°C treated condition prior to the heat treatment at 1200°C for 24 hours. Cyclic voltammograms for this electrode are shown in Figure 4.6. The apparent current densities obtained with this electrode are very high due to the porosity (the apparent surface area is used to calculate current density). Another interesting feature of the cyclic voltammograms is that two oxide reduction peaks are observed, even though the electrode is a solid solution of platinum in gold. The oxide reduction peaks occur at slightly more negative potentials than on the pure metals. Woods (1971) also found that gold-platinum solid solutions had two oxide reduction peaks. If one considers the mechanism of platinum oxide formation (Fig. 2.5), it is difficult to understand how platinum atoms surrounded by gold atoms can have an oxide reduction peak in the same potential region as pure platinum. The same applies to gold atoms that are surrounded by platinum atoms in a solid solution.

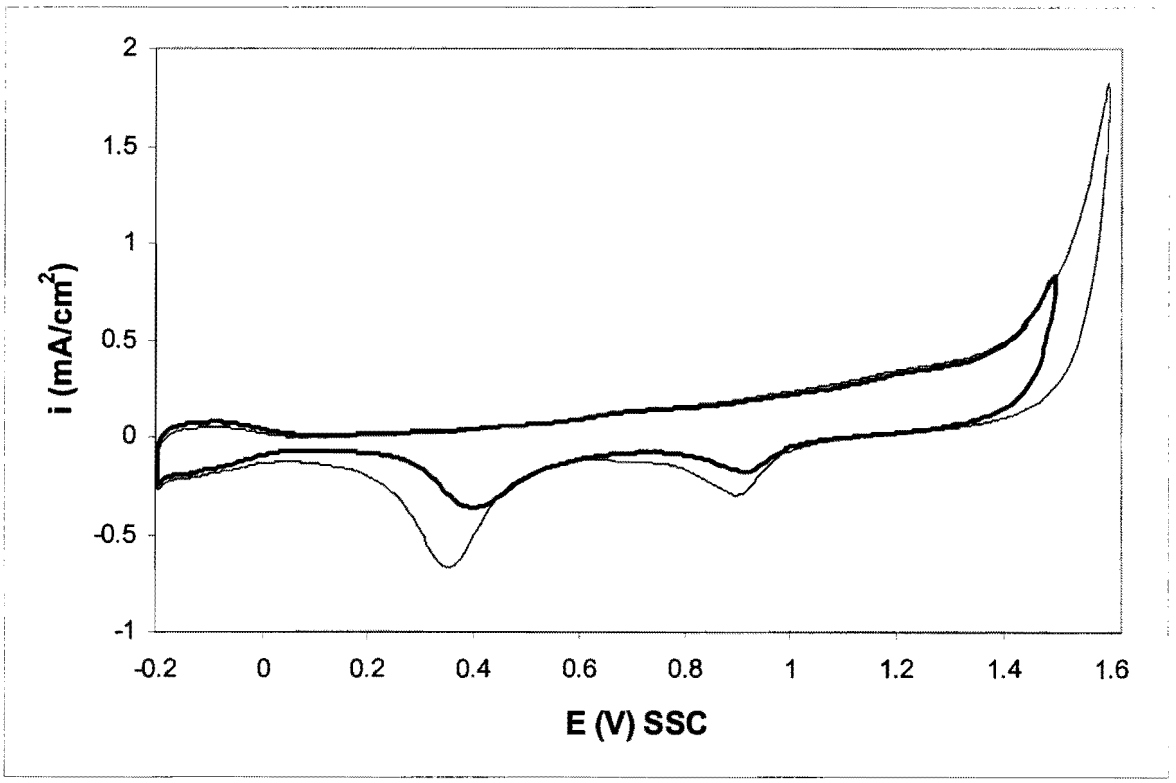

Figure 4.6. Cyclic voltammograms for the 1200°C- 24 hour heat treated sample (60Au-40Pt) in 0.5 M H_2SO_4. Scan rate 50 mV/s, 25°C.

Cyclic voltammograms for the non-porous 1300°C treated sample and the porous 1200°C sample heat treated for 24 hours are shown in Figure 4.7. From the increased apparent current density, it is clear that the porosity increases the surface area significantly.

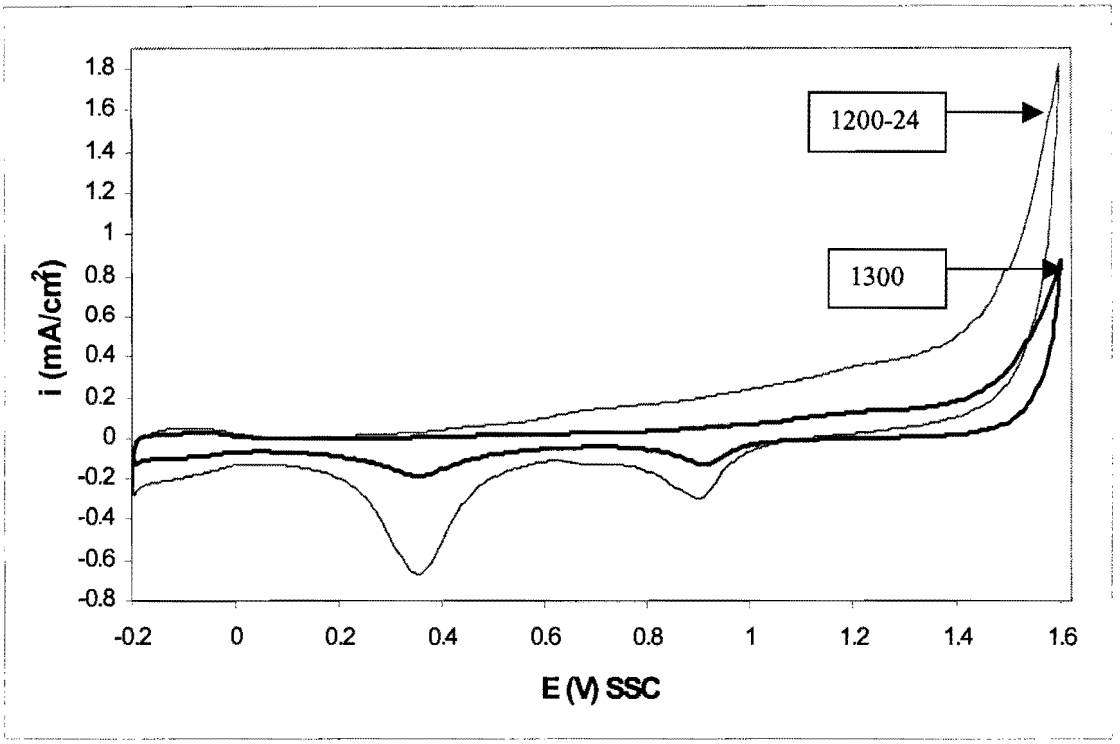

Figure 4.7. Cyclic voltammograms for the 1300°C heat treated sample and the 1200°C – 24 hour heat treated sample (60Au-40Pt) in 0.5 M H_2SO_4. Scan rate 50 mV/s, 25°C.

4.3.3.3. The 60Au-40Pt alloy in the 1200°C (168 hours) heat treatment condition

The microstructure of this sample is shown in Figure 3.8. The sample was in the 1300°C treated condition prior to the heat treatment at 1200°C for 168 hours. Cyclic voltammograms for this electrode are shown in Figure 4.8. Two oxide reduction peaks are also found for this solutionised sample.

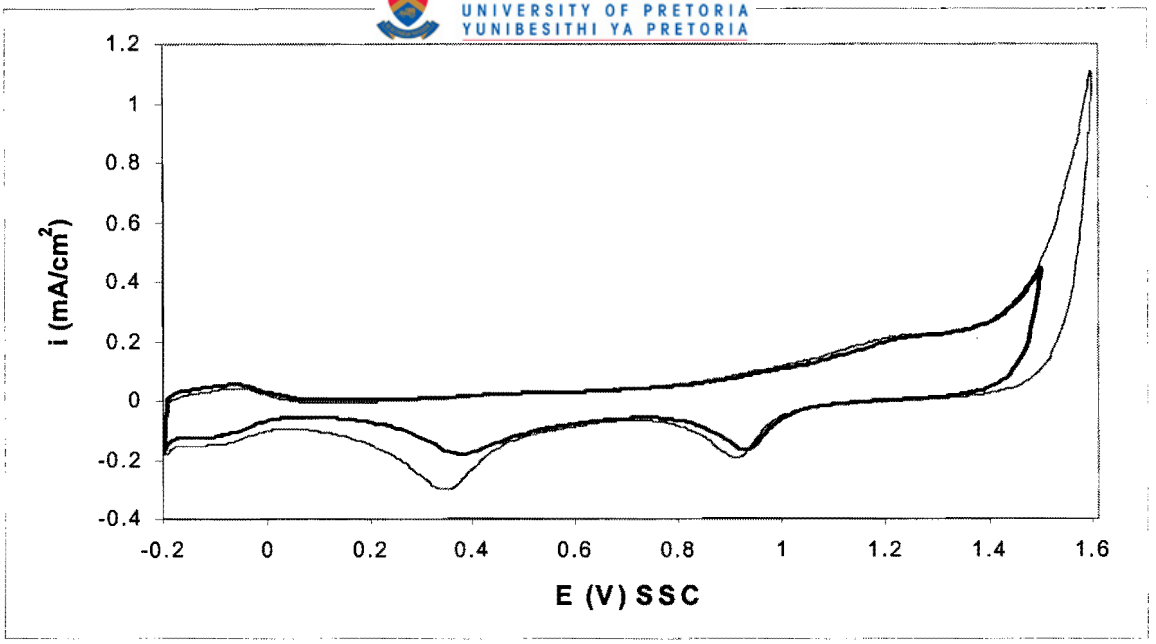

Figure 4.8. Cyclic voltammograms for the 1200°C – 168 hour heat treated sample (60Au-40Pt) in 0.5 M H_2SO_4. Scan rate 50 mV/s, 25°C.

The porosity of the sample heat treated for 168 hours appears to be less than for the sample heat treated for 24 hours (Figures 3.6 and 3.8). The same conclusion is reached when the cyclic voltammograms of the two samples are compared (Fig. 4.9), since the apparent current density is lower for the sample which received the longer heat treatment.

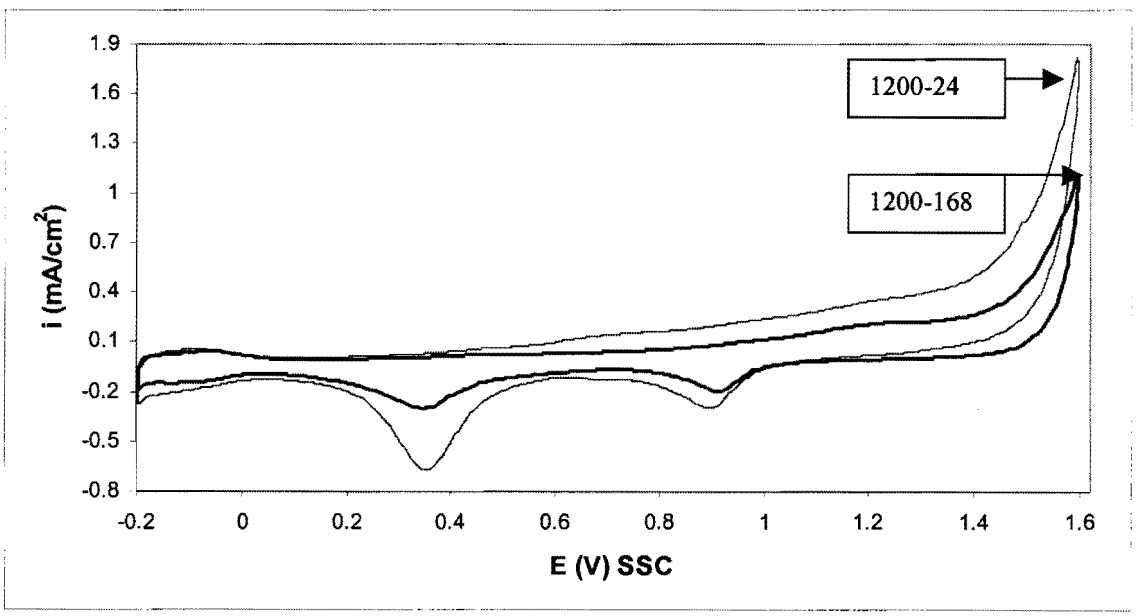

Figure 4.9. Cyclic voltammograms for the 1200°C heat treated samples (60Au-40Pt) in 0.5 M H_2SO_4. Scan rate 50 mV/s, 25°C.

Electrochemical Impedance Spectroscopy (EIS) can be used to compare surface areas of electrodes. An electrochemical double layer is formed at the interface between an electrode and an electrolyte at a given potential. In the absence of faradaic reactions, smooth and clean surfaces show ideal capacitive behaviour as described by (Song et al., 2000):

$$Z = 1/(j\omega C_d) \quad (1)$$

where the double layer capacitance C_d is independent of frequency (ω is the angular frequency). The ideal behaviour is represented as a vertical line in the Nyquist plot of impedance. However, the impedance of solid electrodes deviates from the purely capacitative behaviour. This causes a deviation of the vertical line in the Nyquist plot by a constant angle α, which falls in the range 0°-45°. For ideally smooth electrodes α should be 0°, whereas for extremely rough or porous surfaces, α should be close to 45° (Song et al., 2000).

The non-ideality or frequency dispersion (the term "frequency dispersion" indicates that the apparent capacitance is a function of the frequency, which is not the case for an ideal capacitor) has been described by the constant phase element (CPE) (Rammelt and Reinhard, 1990). The impedance of the CPE can be written as:

$$Z = 1/[(T(j\omega)^n] \quad (2)$$

where n is the roughness parameter (ranges between 0.5 and 1). $T = C_d$ only if n=1. T is expressed in units of farads per square centimetre per second to the power n.

n can be related to α by:

$$\alpha = (1-n)90° \quad (3)$$

The CPE element can be caused by several effects (Song et al., 2000): diffusion in a diffusion-limited system, geometric factors, sluggish processes such as adsorption of anions, surface reconstruction and transformation in adlayer, and crystallographic heterogeneity.

In cases of highly porous electrodes, geometric factors are the most important among the origins of frequency dispersion in the absence of faradaic reactions.

In Figure 4.10(a), the impedance as a function of frequency is shown for the 60Au-40Pt electrodes. Impedance spectroscopy was performed in 0.5 M H_2SO_4 at a potential of 0.1 V_{SSC}. This potential was chosen because the current at the electrode will then be a

minimum and reactions occurring at the electrode surface will be avoided. The phase angle (θ) as a function of the frequency is shown in Figure 4.10(b).

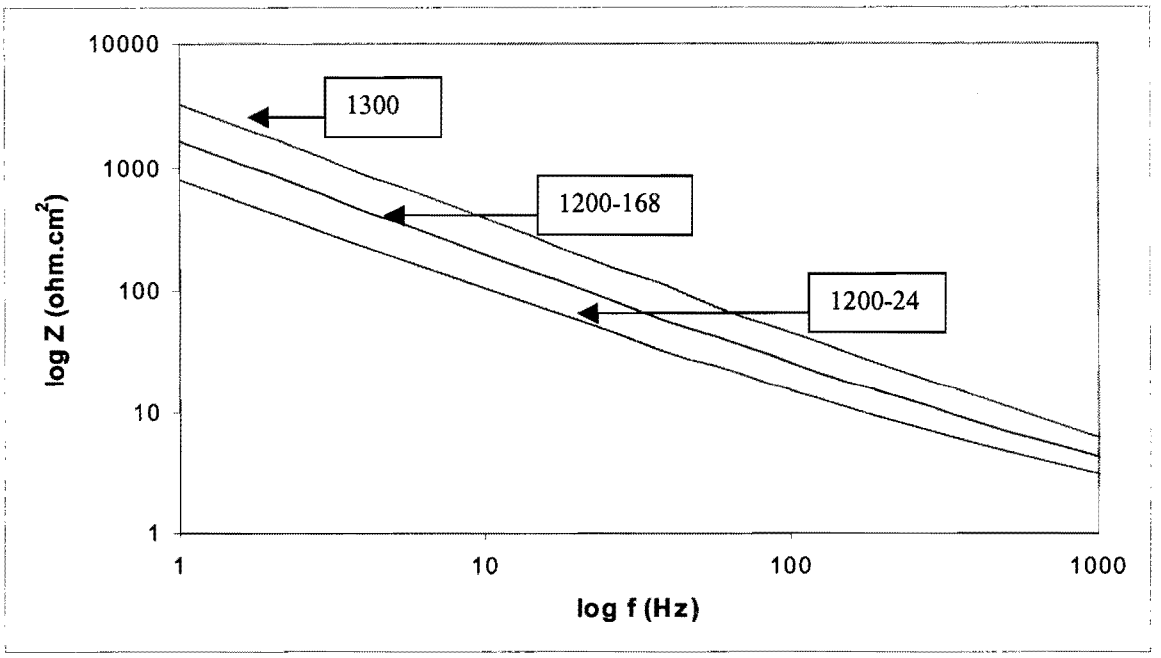

(a)

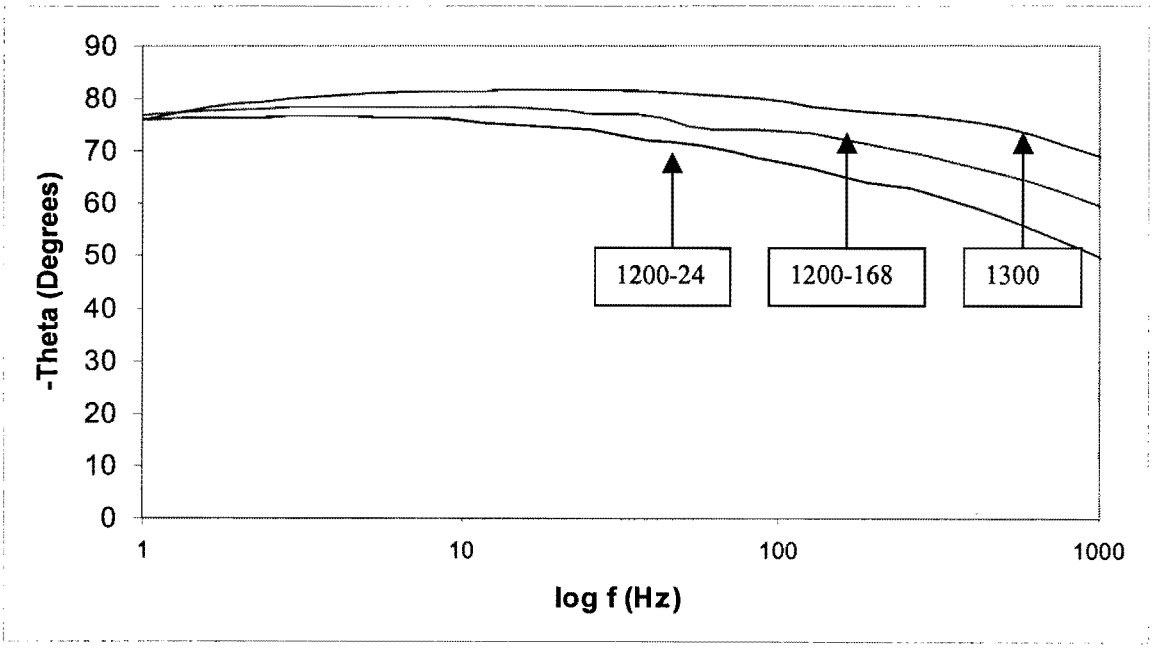

(b)

Figure 4.10. (a) Impedance spectroscopy at 0.1 V_{SSC} for the 60Au-40Pt samples in 0.5 M H_2SO_4; (b) the phase angle over the same frequency range.

The phase angles were fairly constant over the frequency range, dropping to lower values at higher frequencies (Fig. 4.10b). Purely capacitative behaviour is represented by a θ of -90°. A low Z value corresponds to a high surface area in the frequency range where the capacitance dominates the impedance. The phase angles in Figure 4.10(b) show that the capacitance dominated the impedance over most of this frequency range. Figure 4.10 confirms that the sample heat treated at 1200°C for 24 hours has a higher surface area than the sample heat treated for 168 hours. Both porous samples have higher surface areas than the non-porous 1300°C heat treated sample, as expected.

4.3.3.4. The 60Au-40Pt alloy in the 800°C heat treatment condition

The microstructure of this sample is shown in Figure 3.12. The sample was in the 1200°C-24h (porous, single-phased) heat treated condition prior to the heat treatment at 800°C for 50 hours. Cyclic voltammograms for this electrode are shown in Figure 4.11. The current densities of this sample are slightly higher than the solutionised sample heat treated at 1200°C for 24 hours. This suggests that the heat treatment at 800°C resulted in additional porosity or the linking up of the porosity already present before the heat treatment.

4.3.3.5. The 60Au-40Pt alloy in the 600°C heat treatment condition

The microstructure of this sample is shown in Figure 3.15. The sample was in the 1200°C-24h (porous, single-phased) heat treated condition prior to the heat treatment at 600°C for 100 hours. Cyclic voltammograms for this electrode are shown in Figure 4.12. The most notable feature of Figure 4.12 is the very high apparent current densities due to oxygen gas evolution. The equilibrium composition of the platinum-rich areas in this sample is 98Pt-2Au (Table 3.1). The fact that these areas are nearly pure platinum may explain the low oxygen gas evolution potential.

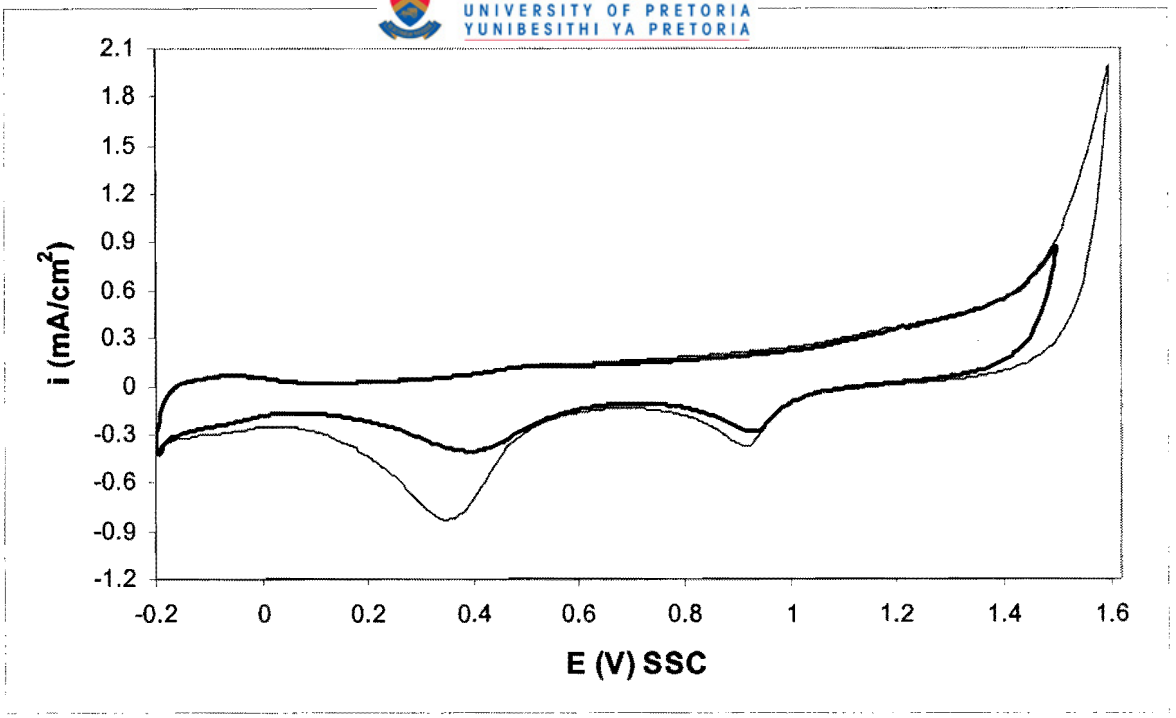

Figure 4.11. Cyclic voltammograms for the 800°C heat treated sample (60Au-40Pt) in 0.5 M H_2SO_4. Scan rate 50 mV/s, 25°C.

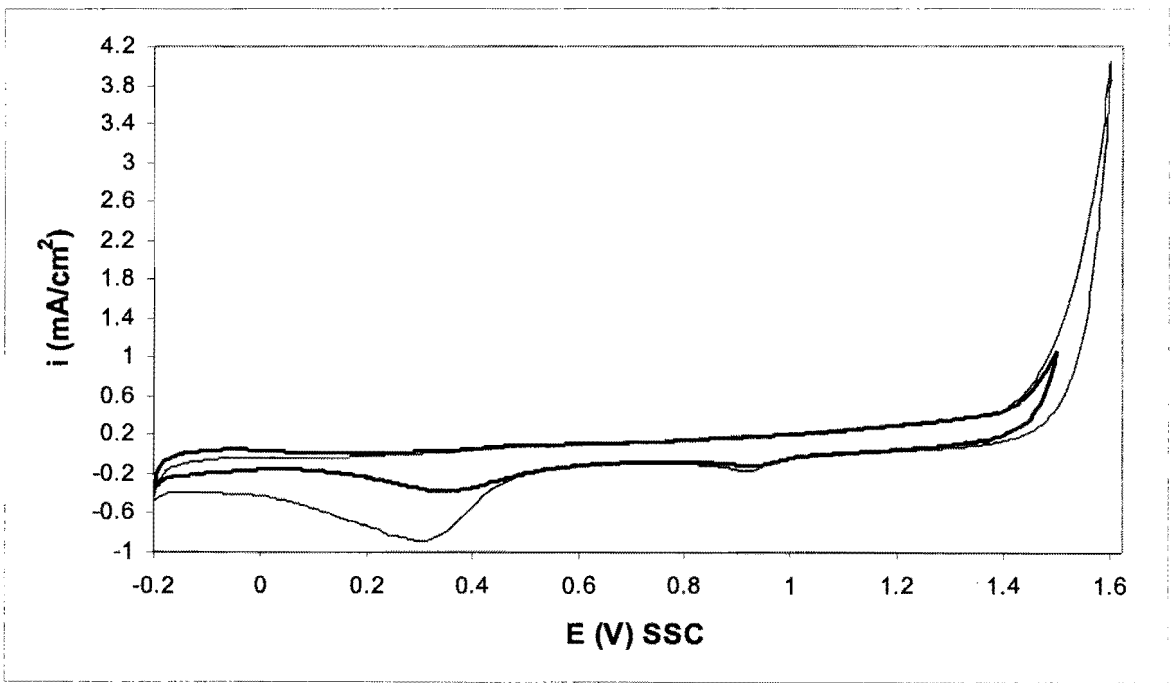

Figure 4.12. Cyclic voltammograms for the 600°C heat treated sample (60Au-40Pt) in 0.5 M H_2SO_4. Scan rate 50 mV/s, 25°C.

The equilibrium gold content of the platinum-rich phase in the 800°C heat treated sample is higher than that of the 600°C heat treated sample (Table 3.1). This causes the oxygen gas evolution reaction on the 800°C treated sample to be inhibited more than on the 600°C heat treated sample (Fig. 4.13).

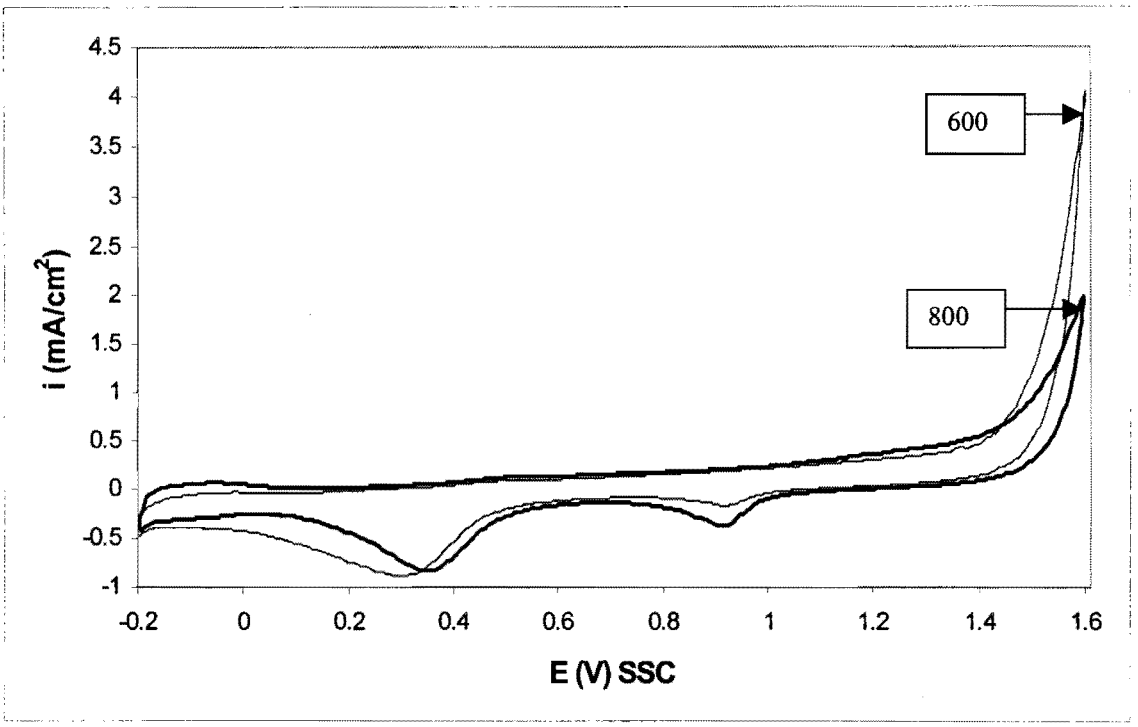

Figure 4.13. Cyclic voltammograms for the miscibility gap heat treated samples (60Au-40Pt) in 0.5 M H_2SO_4. Scan rate 50 mV/s, 25°C.

4.3.4. The 50Au-50Pt alloy

4.3.4.1. The 50Au-50Pt alloy in the "ductile" condition

The microstructure (two-phased, fine microstructure) of this sample is shown in Figure 3.17. Cyclic voltammograms for this electrode are shown in Figure 4.14. The current densities obtained on the ductile 50Au-50Pt sample are similar to the 60Au-40Pt electrode in the 1300°C (two-phased, coarse microstructure) heat treatment condition (Fig. 4.5).

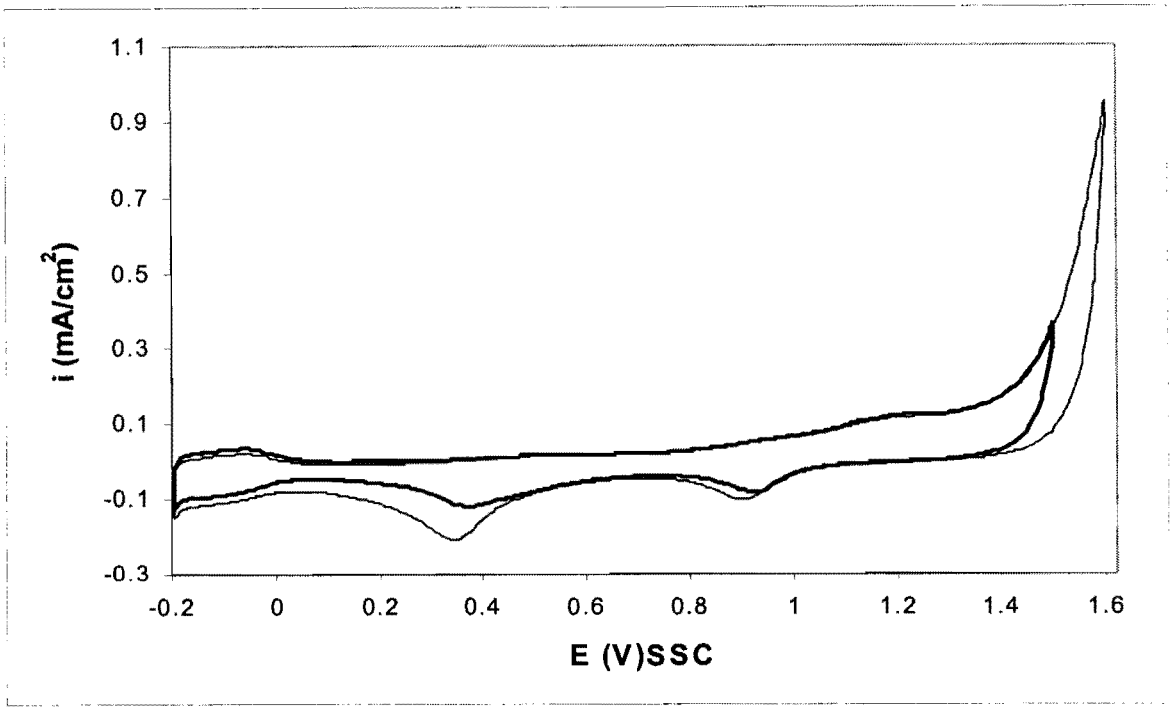

Figure 4.14. Cyclic voltammograms for the "ductile" heat treated sample (50Au-50Pt) in 0.5 M H_2SO_4. Scan rate 50 mV/s, 25°C.

4.3.4.2. The 50Au-50Pt alloy in the solid solution condition

The microstructure of this sample (single-phased, non-porous) is shown in Figure 3.19. Cyclic voltammograms for this electrode are shown in Figure 4.15. As was the case with the solutionised 60Au-40Pt electrodes, this sample also has two oxide reduction peaks.

Kirkendall porosity was not found in the sample after the solid solution heat treatment, and it can be seen that the two 50Au-50Pt samples have similar current densities (Fig. 4.16). The oxygen gas evolution reaction is inhibited on the solid solution sample compared to the ductile (two-phased) sample. If one considers the two temperature limits that were used for the "ductile" heat treatment (Fig. 3.16), it is seen that the Pt-rich areas of this sample have an equilibrium gold content of 5 to 10 %. The platinum atoms in the Pt-rich phase of this sample are therefore surrounded by fewer gold atoms than the platinum atoms in the solid solution sample. This results in oxygen evolution at a lower overpotential at the "ductile" sample.

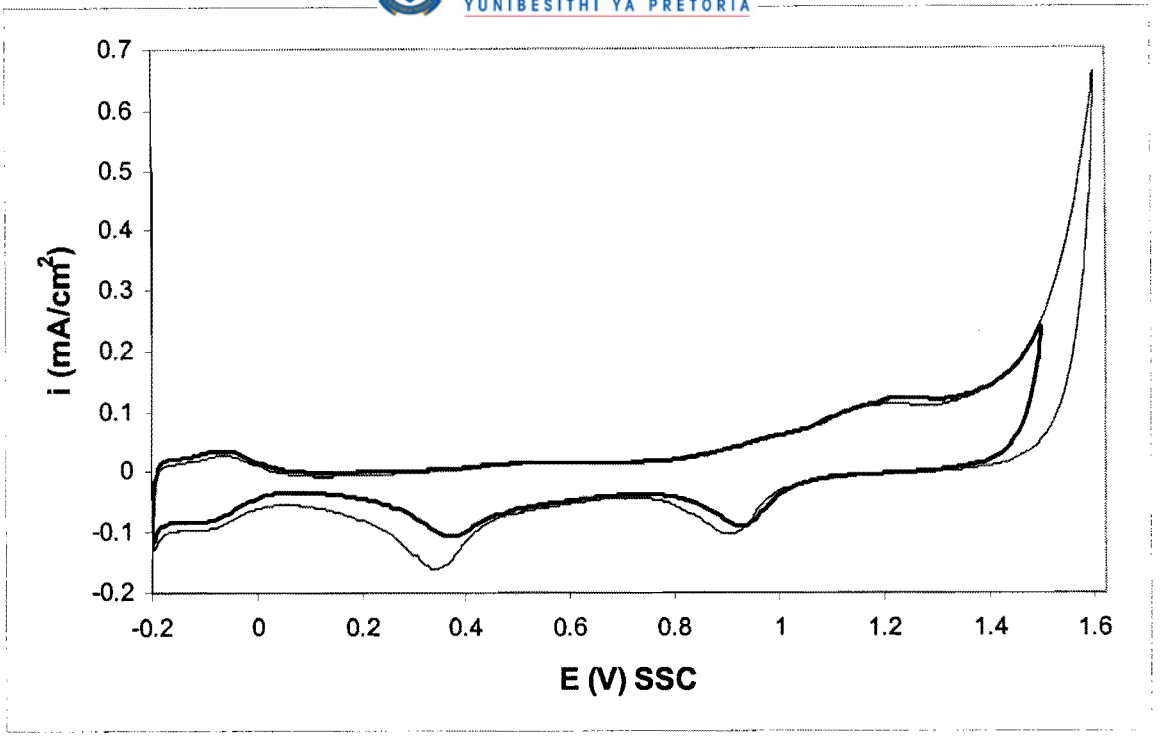

Figure 4.15. Cyclic voltammograms for the solutionised sample (50Au-50Pt) in 0.5 M H_2SO_4. Scan rate 50 mV/s, 25°C.

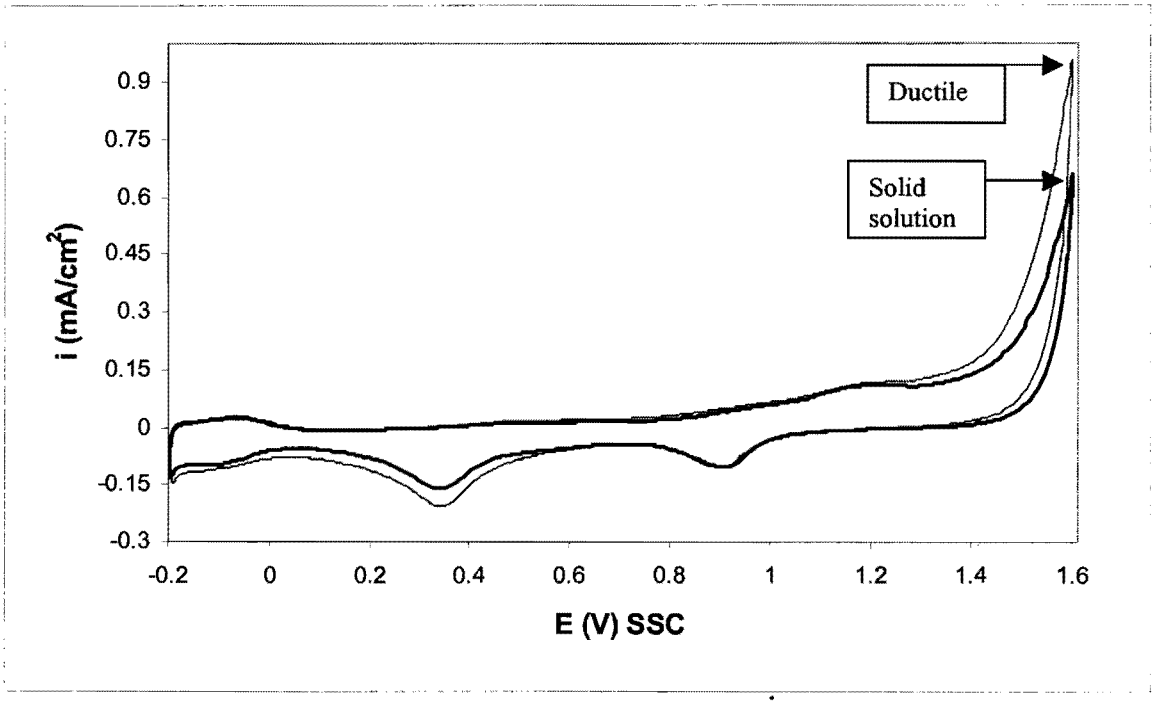

Figure 4.16. Cyclic voltammograms for the 50Au-50Pt samples in 0.5 M H_2SO_4. Scan rate 50 mV/s, 25°C.

Impedance spectroscopy was performed in 0.5 M H_2SO_4 at a potential of 0.1 V_{SSC}. In Figure 4.17(a), the impedance as a function of frequency is shown for the 50Au-50Pt electrodes. The phase angle (θ) as a function of the frequency is shown in Figure 4.17(b). The 60Au-40Pt sample in the 1300°C heat treatment condition is included for comparison. Figure 4.17 shows that the surface areas of the 50Au-50Pt electrodes are similar. This confirms that Kirkendall porosity was not formed during the solid solution heat treatment. The impedance of the 60Au-40Pt sample in the 1300°C heat treatment condition is also similar to the 50Au-50Pt alloy electrodes. This implies that the impedance of Au-Pt alloys in 0.5 M H_2SO_4 at a potential of 0.1 V_{SSC} is not influenced much by composition, but rather by the surface area.

4.3.5. The Gold 990 alloy

4.3.5.1. The Gold 990 alloy in the solid solution condition

This sample has 1 wt% (4 at%) titanium in solid solution with the gold. The Vickers hardness of the sample in this condition is $HV_5 = 50$ kg/mm^2. Cyclic voltammograms for this sample are shown in Figure 4.18. The behaviour of Gold 990 in the solid solution condition is similar to pure gold (Fig. 4.1).

4.3.5.2. The Gold 990 alloy in the precipitation-hardened condition

This sample is hardened by the presence of small Au_4Ti precipitates. The Vickers hardness of the sample in this condition is $HV_5 = 150$ kg/mm^2. Cyclic voltammograms for this sample are shown in Figure 4.19. The behaviour of Gold 990 in the precipitation-hardened condition is also similar to pure gold (Fig. 4.1).

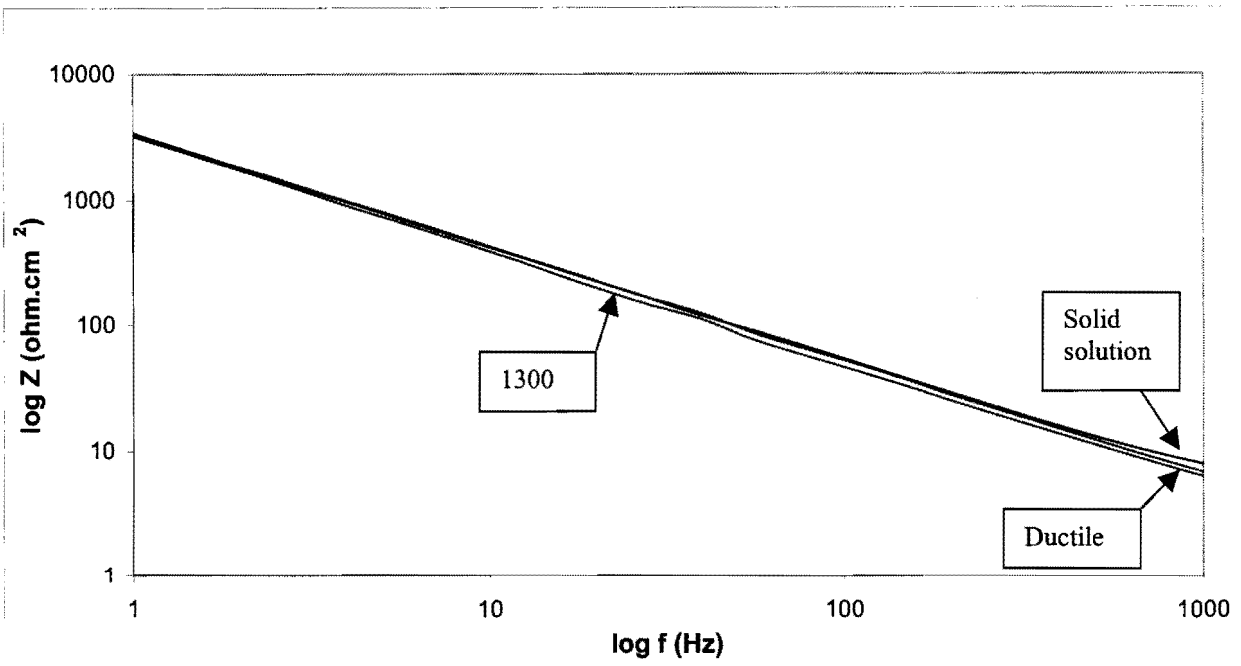

(a)

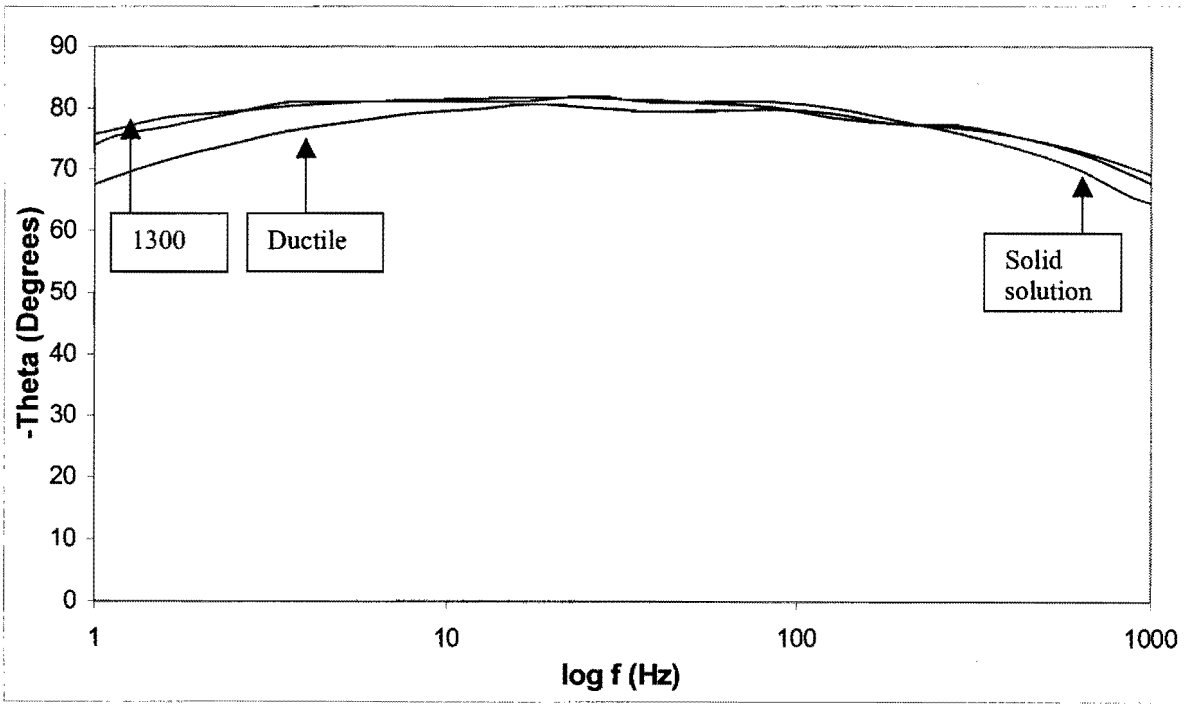

(b)

Figure 4.17. (a) Impedance spectroscopy at 0.1 V_{SSC} for the 50Au-50Pt samples in 0.5 M H_2SO_4; (b) the phase angle over the same frequency range. The 1300°C heat treated sample (60Au-40Pt) is included for comparison.

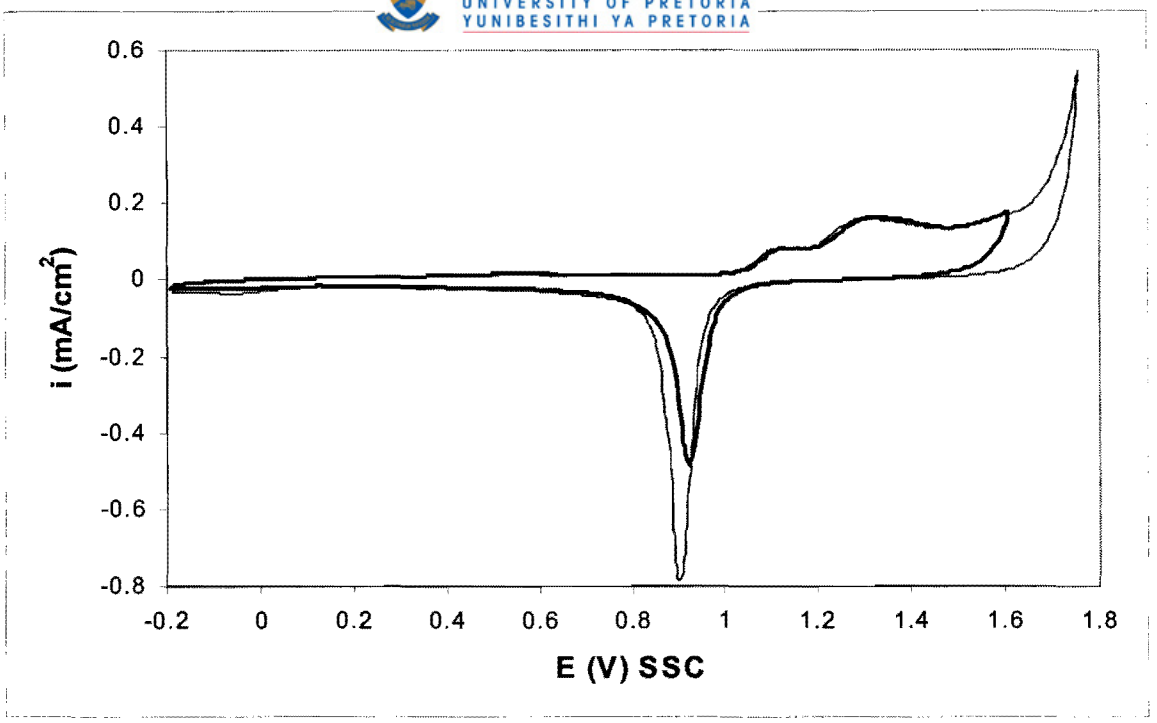

Figure 4.18. Cyclic voltammograms for the Gold 990 sample in the solid solution condition in 0.5 M H_2SO_4. Scan rate 50 mV/s, 25°C.

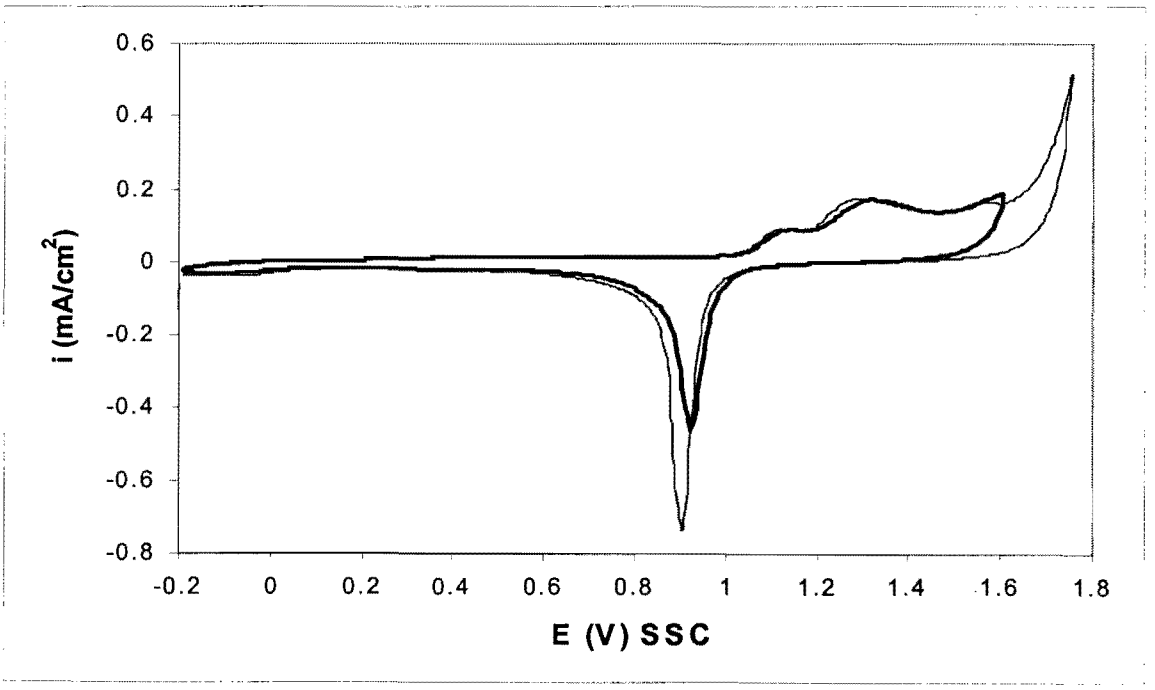

Figure 4.19. Cyclic voltammograms for the Gold 990 sample in the precipitation hardened condition in 0.5 M H_2SO_4. Scan rate 50 mV/s, 25°C.

The cyclic voltammograms for the two Gold 990 electrodes and pure gold are compared in Figure 4.20. The cyclic voltammograms of the three electrodes are similar to such a degree that they are difficult to distinguish in Figure 4.20.

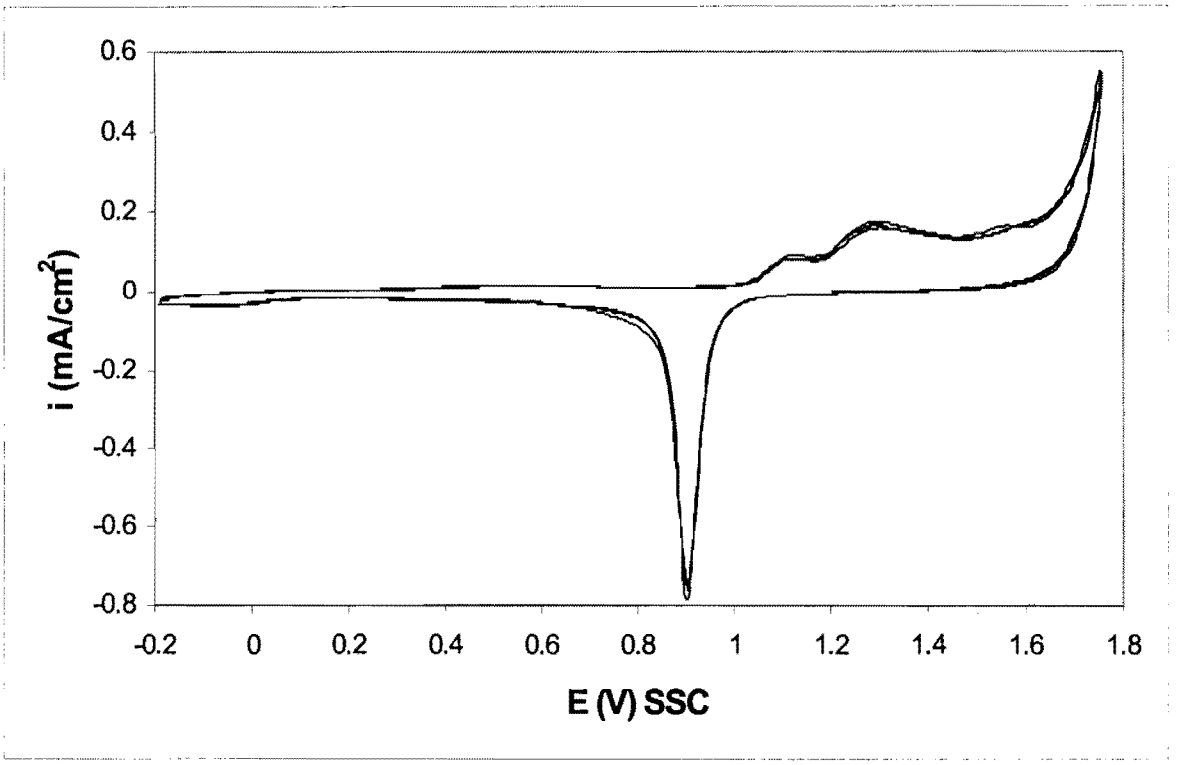

Figure 4.20. Cyclic voltammograms for gold and the Gold 990 samples in 0.5 M H_2SO_4. Scan rate 50 mV/s, 25°C.

The similarities may be due to the following possible reasons:

- The titanium content of 4 at% may be too low to have a significant influence on the electrochemical behaviour of gold.
- The titanium may be in the passive condition (Fig 2.21).
- The titanium may have dissolved selectively from the Gold 990 alloy resulting in a pure gold surface.

4.4. Conclusions

The electrochemical behaviour of the investigated gold-based alloys in 0.5 M H_2SO_4 can be summarised by the following conclusions:

- The cyclic voltammograms of the Au-Pt alloys have features corresponding to both pure gold and platinum.
- The Au-Pt alloys in the solid solution condition have two oxide reduction peaks. The one peak corresponds to oxide reduction of platinum and the other to oxide reduction of gold.
- The high surface areas of the porous electrodes result in higher currents. The current densities of these electrodes are therefore higher when the apparent surface area is considered.
- The 60Au-40Pt alloy electrode in the 600°C heat treatment condition has a lower oxygen evolution overpotential than the other Au-Pt alloys. This can be explained by the fact that the platinum-rich areas in this sample only contain 2 % gold.
- The surface areas of the 50Au-50Pt alloy electrode in the "ductile" condition and in the solid solution condition are similar. Kirkendall porosity is absent in the 50Au-50Pt solutionised alloy.
- The cyclic voltammograms of pure gold and the Gold 990 electrodes are similar.

The electrochemical behaviour of the electrodes in alkaline solution is discussed in the next chapter.

Chapter 5

THE ELECTROCHEMICAL BEHAVIOUR OF GOLD-BASED ALLOYS IN ALKALINE SOLUTION WITHOUT ETHYLENE GLYCOL

5.1. Introduction

The electrochemical properties of the Au-Pt and Gold 990 electrodes in acid solution without ethylene glycol were discussed in the previous chapter. Cyclic voltammetry was used to study electrode surface oxidation, oxide reduction and the oxygen and hydrogen gas evolution reactions. The purpose of this chapter is to present results of similar electrochemical experiments in alkaline solution without ethylene glycol. In order to have a better understanding of the electrochemical behaviour of the alloy electrodes, experiments were also conducted with gold and platinum electrodes.

5.2. Experimental

The experimental work was performed with polycrystalline gold (99.99%), platinum (99.99%), 60Au-40Pt, 50Au-50Pt and Gold 990 electrodes. The electrodes were disc-shaped with 6mm diameter. All the electrodes were mounted in a resin by employing a black phenolic thermosetting powder. Electrical contact was achieved by drilling a hole through the rear of the mounting and tapping M6 thread. A Pine analytical rotator was used as electrode rotator. The apparent surface area of 0.28 cm^2 was used in all cases to calculate current densities. The higher real surface areas of the porous electrodes are expected to give higher apparent current densities than the non-porous electrodes.

A water-jacketed perspex electrochemical cell was used for all the experiments. A water-jacketed perspex electrochemical cell was used for all the experiments. The cell had an inside diameter of 90 mm and a height of 100 mm. Approximately 400 ml electrolyte was used. The distance between the working electrode and the bottom of the cell was about 60 mm. The temperature was controlled at 25°C. The cover of the perspex cell had six

openings which allowed the insertion of two counter electrodes, the working electrode, the Luggin capillary, the tube for nitrogen purging and a thermometer.

The experiments were conducted in 0.5 M NaOH solution. The solution was prepared by using double distilled water and CP grade NaOH pellets from Associated Chemical Enterprises (Pty) Ltd. Prior to each experiment, the solution was purged with nitrogen for 30 minutes to remove dissolved oxygen. The electrodes were polished before the experiments with diamond paste (down to 1 μm) and ultrasonically cleaned in 0.5 M NaOH. A Solartron 1287 Electrochemical Interface was used for the cyclic voltammetry experiments. The electrode potential was cycled between the values for onset of O_2 and H_2 evolution until the I-E curves were reproducible. It was found that approximately 15 cycles are needed to obtain reproducible I-E curves. The fifteenth cycle is used in all cyclic voltammograms shown in this chapter. The scan rate employed was 50 mV/s. The electrochemical experiments in alkaline solution without ethylene glycol were conducted without rotating the electrodes or stirring the solution. Platinum wire was used as counter electrode. All potentials quoted in this study are with respect to the silver/silver chloride reference electrode (SSC). Electrochemical impedance spectroscopy was performed with a Solartron 1250 Frequency Response Analyser.

5.3. Results and discussion

5.3.1. Gold

Cyclic voltammograms for gold are shown in Figure 5.1. These voltammograms agree well with those found in the literature (Fig. 2.2). Monolayer oxide formation commences at 0.1 V_{SSC} during the positive sweep followed by oxygen gas evolution at higher potentials. The surface oxide is reduced at 0.06 V_{SSC} during the negative sweep. It is seen that the reactions occur at lower potentials in base than in acid (Fig. 4.1). A small cathodic peak at –0.18 V_{SSC} is also observed during the negative sweep. This peak is thought to be due to the reduction of hydrous gold oxide species formed on the gold surface at the upper end of the cycle (Burke and Nugent, 1997).

More oxide is formed during the positive sweep when a higher upper potential limit is used. This results in a larger oxide reduction peak during the subsequent negative sweep.

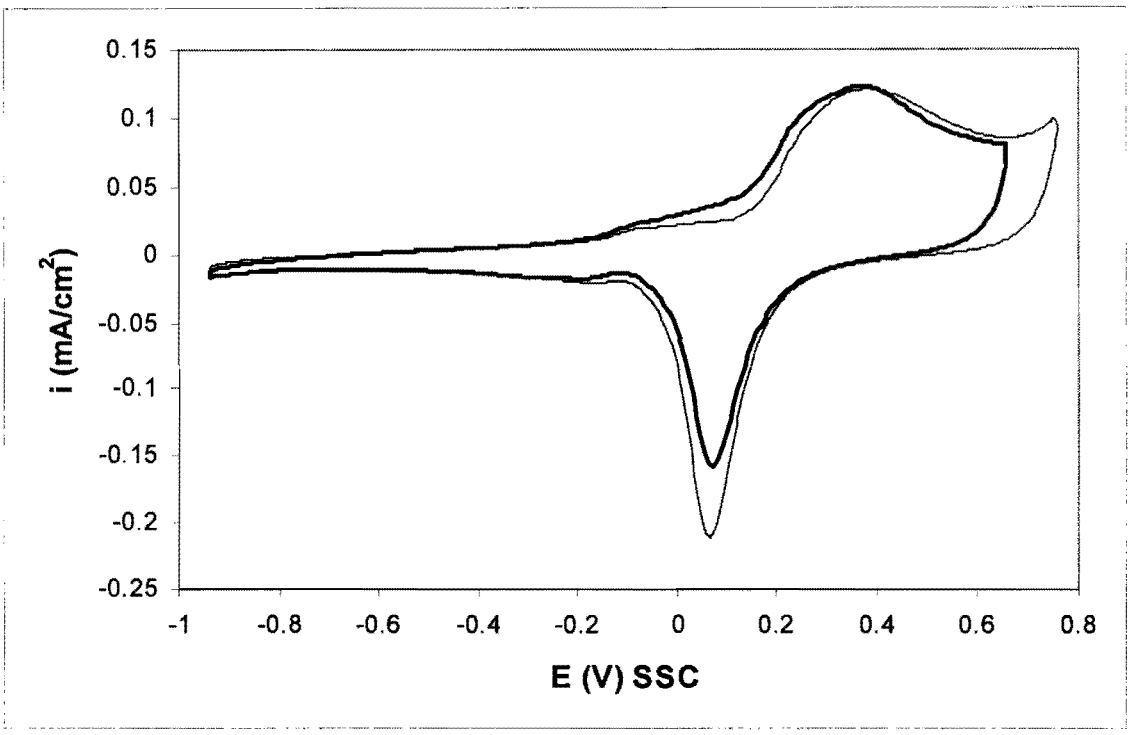

Figure 5.1. Cyclic voltammograms for gold in 0.5 M NaOH. Scan rate 50 mV/s, 25°C.

5.3.2. Platinum

A cyclic voltammogram for platinum is shown in Figure 5.2. This voltammogram agrees well with those found in the literature (Fig. 2.6). Hydrogen desorption/adsorption occurs in the region of –0.9 to –0.55 V_{SSC}. Surface oxidation commences at approximately -0.4 V_{SSC}. The surface oxide is reduced during the negative sweep at -0.3 V_{SSC}. Hydrogen gas evolution occurs at potentials negative of –0.9 V_{SSC}.

Cyclic voltammograms for platinum with different upper potential limits (0.65 and 0.75 V_{SSC}) are shown in Figure 5.3. The higher upper potential limit leads to a larger oxide reduction peak because more oxide is formed. The peak is not shifted to more negative potentials as was found for platinum in acid solution (Fig. 4.3). A higher upper potential limit than those used here is probably needed to form PtO_2 rather than PtO.

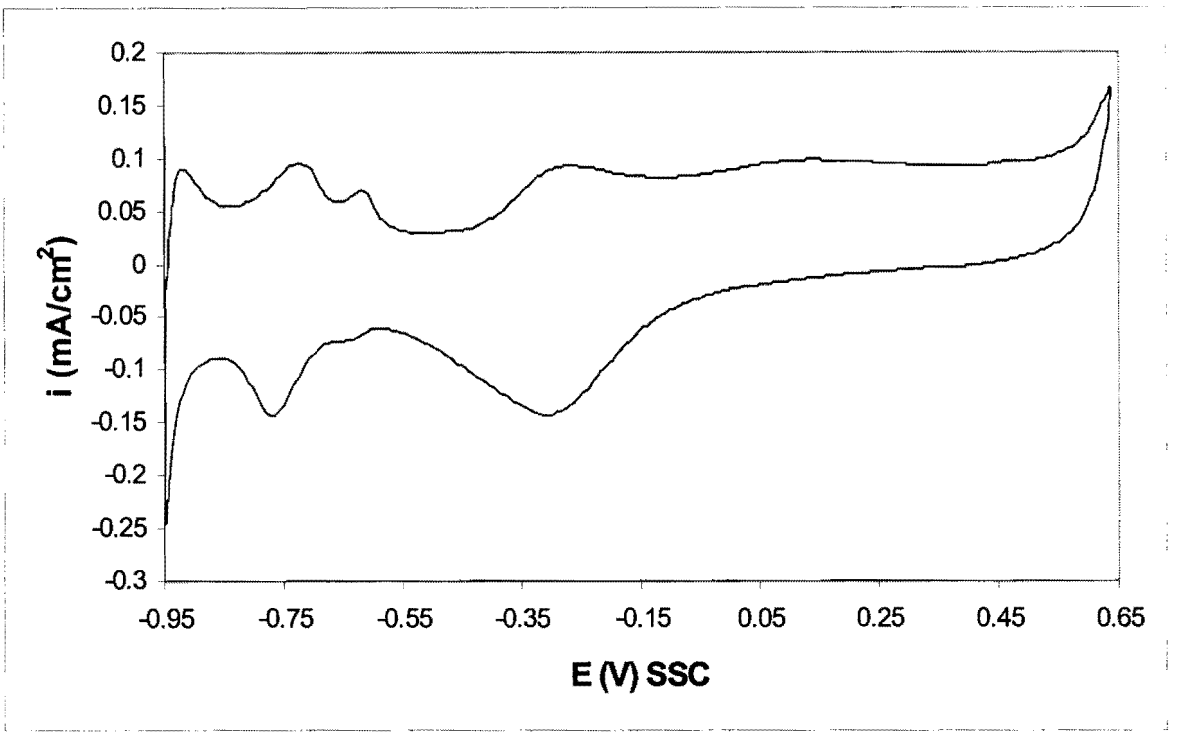

Figure 5.2. Cyclic voltammogram for platinum in 0.5 M NaOH. Scan rate 50 mV/s, 25°C.

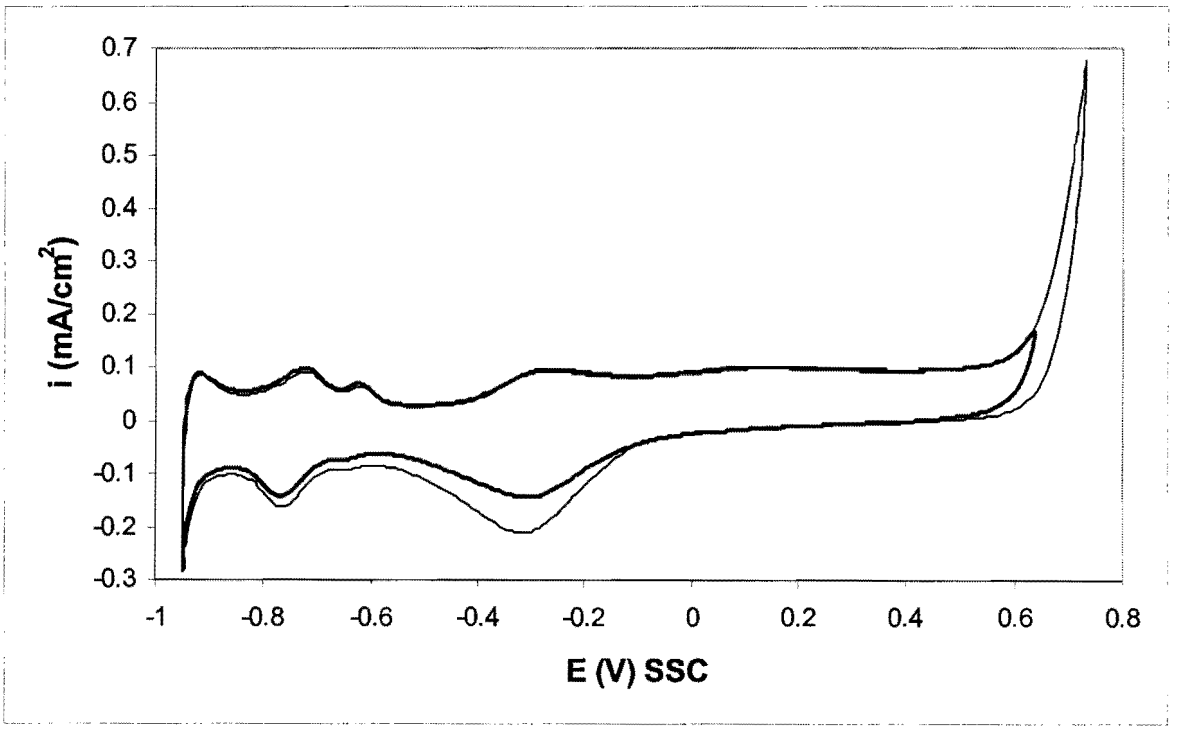

Figure 5.3. Cyclic voltammograms for platinum in 0.5 M NaOH. Scan rate 50 mV/s, 25°C.

Cyclic voltammograms for gold and platinum with the same upper potential limit (E_{up} = 0.75 V) is shown in Figure 5.4. It is seen that oxygen gas evolution occurs at lower potentials on platinum than on gold. The lack of a hydrogen adsorption/desorption region on gold is also evident. The same observations were made for gold and platinum in acid solution (Fig. 4.4).

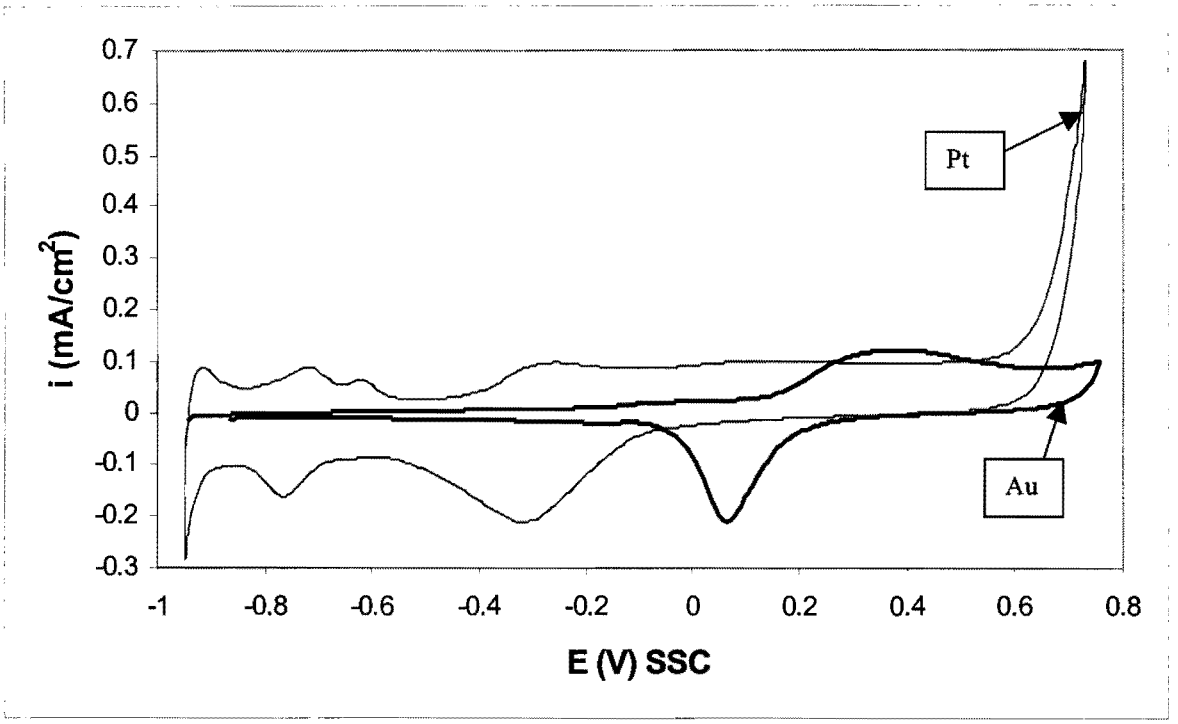

Figure 5.4. Cyclic voltammograms for platinum and gold in 0.5 M NaOH. Scan rate 50 mV/s, 25°C. E_{up} = 0.75 V.

5.3.3. The 60Au-40Pt alloy

5.3.3.1. The 60Au-40Pt alloy in the 1300°C heat treatment condition

The two-phased microstructure of this alloy is shown in Figure 3.2. Cyclic voltammograms for the 1300°C treated electrode are shown in Figure 5.5 and features corresponding to both pure gold and platinum can be seen. The alloy has a hydrogen adsorption/desorption region (-0.9 to -0.55 V_{SSC}). Surface oxide forms at platinum or

(platinum-rich areas) at –0.4 V_{SSC} during the positive sweep. Surface oxide formation at gold (or gold-rich areas) commences at 0.1 V_{SSC}. Two oxide reduction peaks are found in the same potential regions for oxide reduction on pure platinum and pure gold. An increase in the upper potential limit causes an increase in the oxide reduction peak, once again due to more oxide formation with the higher upper potential limit. The current density for oxygen gas evolution at 0.75 V is higher than on pure gold, but lower than on pure platinum. Hydrogen gas evolution occurs at potentials negative of –0.9 V_{SSC}.

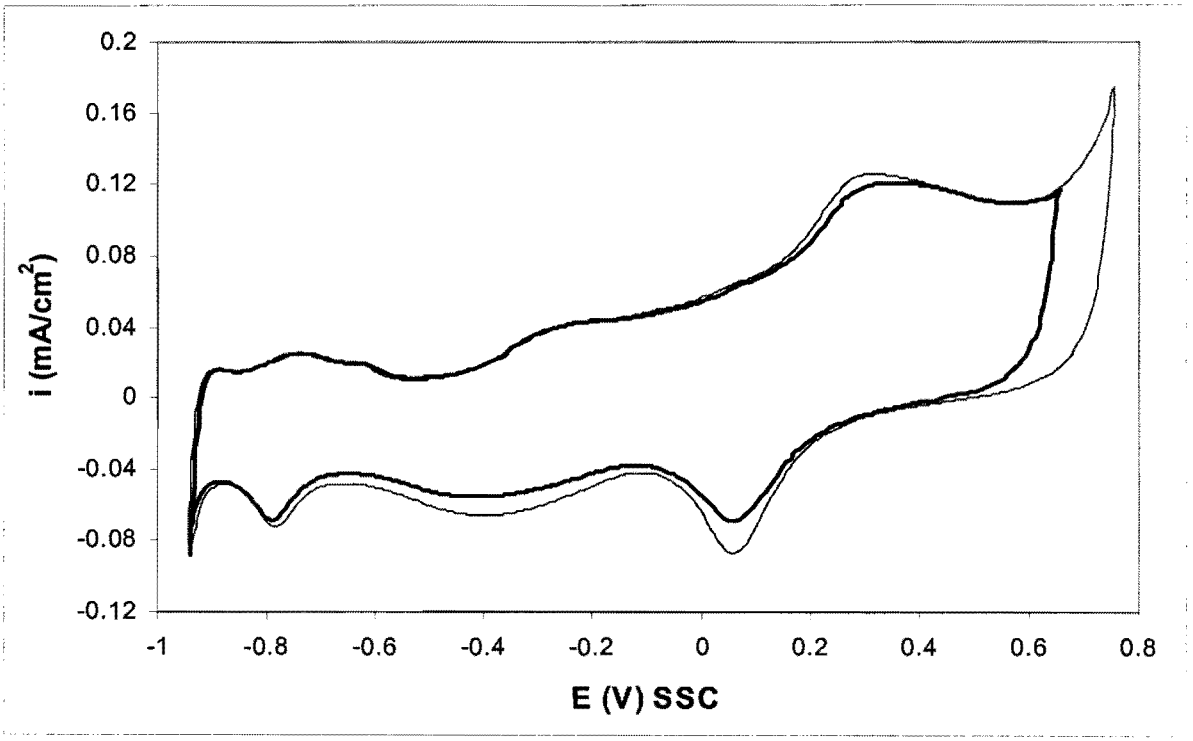

Figure 5.5. Cyclic voltammograms for the 1300°C heat treated sample (60Au-40Pt) in 0.5 M NaOH. Scan rate 50 mV/s, 25°C.

5.3.3.2. The 60Au-40Pt alloy in the 1200°C (24 hours) heat treatment condition

The microstructure of this sample (single-phased, porous) is shown in Figure 3.6. The sample was in the 1300°C treated condition prior to the heat treatment at 1200°C for 24 hours. Cyclic voltammograms for this electrode are shown in Figure 5.6. The apparent current densities obtained with this electrode are very high due to the porosity (the

apparent surface area is used to calculate current density). As was the case in acid solution (Fig. 4.6), two oxide reduction peaks are observed, even though the electrode is a solid solution of platinum in gold.

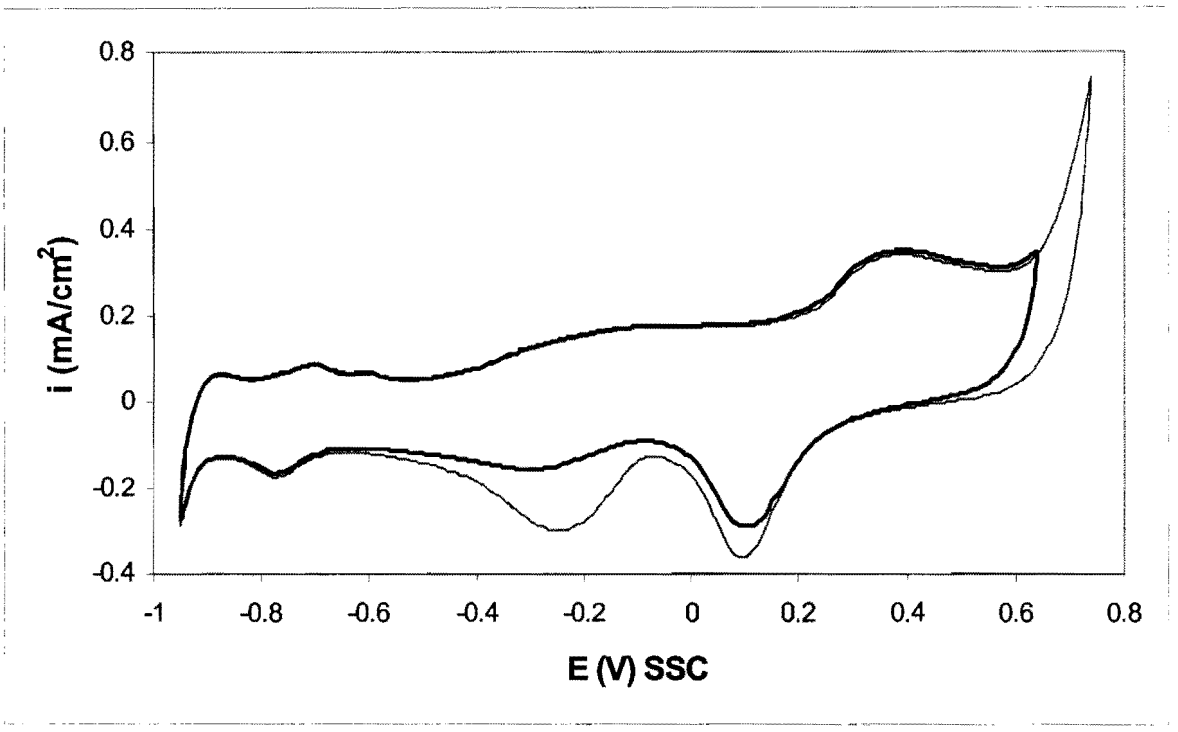

Figure 5.6. Cyclic voltammograms for the 1200°C - 24 hour heat treated sample (60Au-40Pt) in 0.5 M NaOH. Scan rate 50 mV/s, 25°C.

Cyclic voltammograms for the non-porous 1300°C treated sample and the porous 1200°C sample heat treated for 24 hours are shown together in Figure 5.7. From the increased apparent current density it is clear that the porosity increases the surface area significantly. The same effect was observed in acid (Fig. 4.7).

5.3.3.3. The 60Au-40Pt alloy in the 1200°C (168 hours) heat treatment condition

The microstructure of this sample (single-phased, porous) is shown in Figure 3.8. The sample was in the 1300°C treated condition prior to the heat treatment at 1200°C for 168

hours. Cyclic voltammograms for this electrode are shown in Figure 5.8. Two oxide reduction peaks are also found for this solutionised sample.

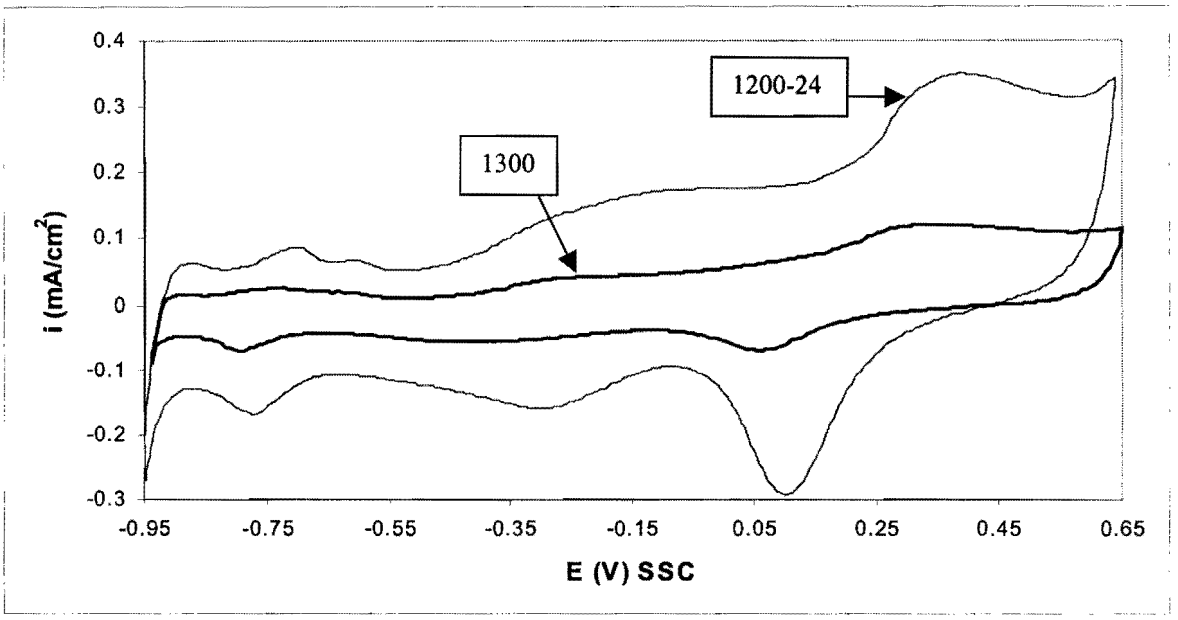

Figure 5.7. Cyclic voltammograms for the 1300°C heat treated sample and the 1200°C – 24 hour heat treated sample (60Au-40Pt) in 0.5 M NaOH. Scan rate 50 mV/s, 25°C.

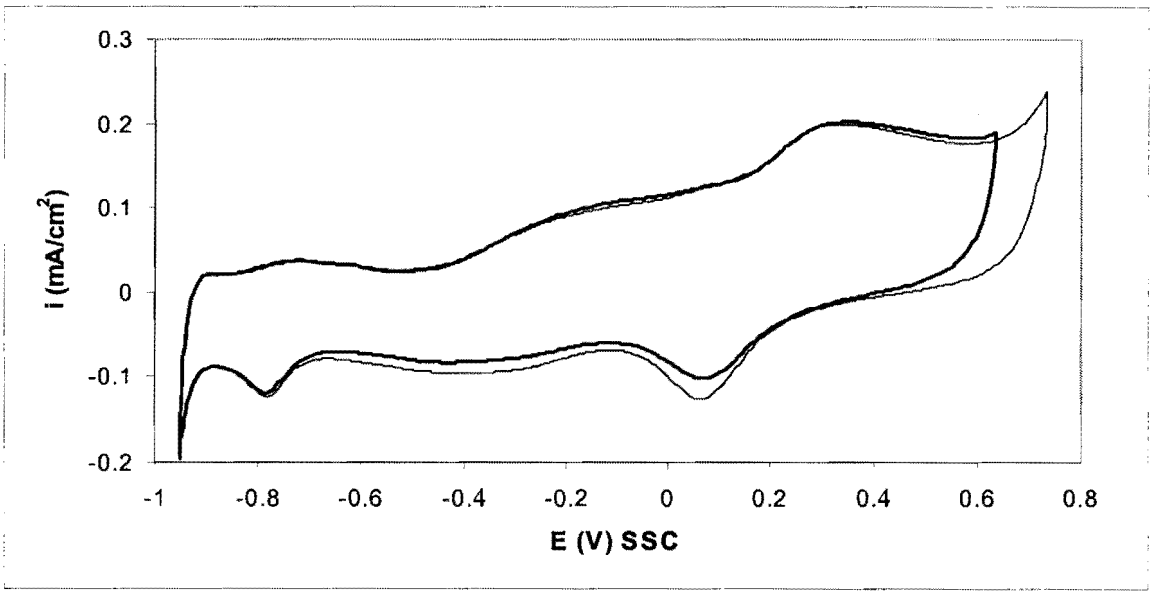

Figure 5.8. Cyclic voltammograms for the 1200°C – 168 hour heat treated sample (60Au-40Pt) in 0.5 M NaOH. Scan rate 50 mV/s, 25°C.

The apparent current densities obtained with the 1200°C – 24h sample are larger than with the 1200°C – 168h sample in acid (Fig. 4.9) and in base (Fig. 5.9). The porosity of the sample heat treated for 168 hours therefore appears to be less than for the sample heat treated for 24 hours (Figures 3.6 and 3.8).

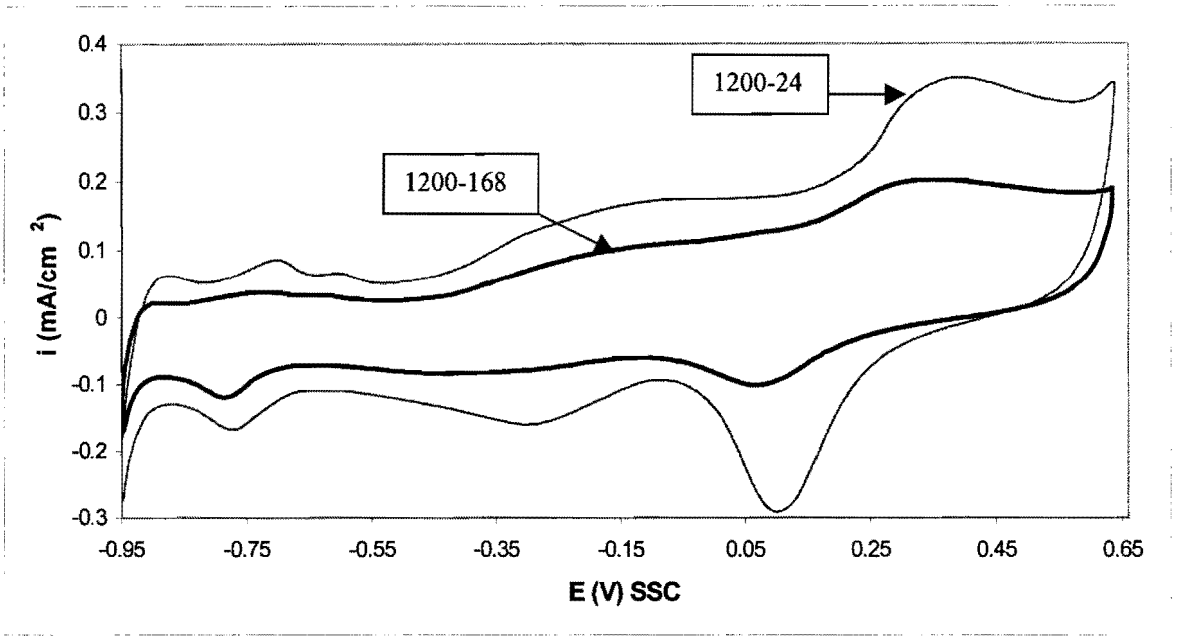

Figure 5.9. Cyclic voltammograms for the 1200°C heat treated samples (60Au-40Pt) in 0.5 M NaOH. Scan rate 50 mV/s, 25°C.

Electrochemical Impedance Spectroscopy (EIS) was used in 0.5 M H_2SO_4 to compare the surface areas of the electrodes (Fig. 4.10). The experiments were repeated in 0.5 M NaOH and the impedance as a function of frequency is shown for the 60Au-40Pt electrodes in Figure 5.10(a). Impedance spectroscopy was performed at a potential of –0.5 V_{SSC}. This potential was chosen because the current at the electrode will then be a minimum and reactions occurring at the electrode surface will be avoided.

The phase angle (θ) as a function of the frequency is shown in Figure 5.10(b). The phase angles were fairly constant over the frequency range, dropping to lower values at higher frequencies. Purely capacitative behaviour is represented by a θ of -90°.

A low Z value corresponds to a high surface area in the frequency range where the capacitance dominates the impedance. The phase angles in Figure 5.10(b) show that the

capacitance dominated the impedance over most of this frequency range. Figure 5.10(a) therefore indicates that the 1200°C-24h electrode has a higher surface area than the 1200°C-168h electrode. The porous electrodes have higher surface areas than the non-porous electrode.

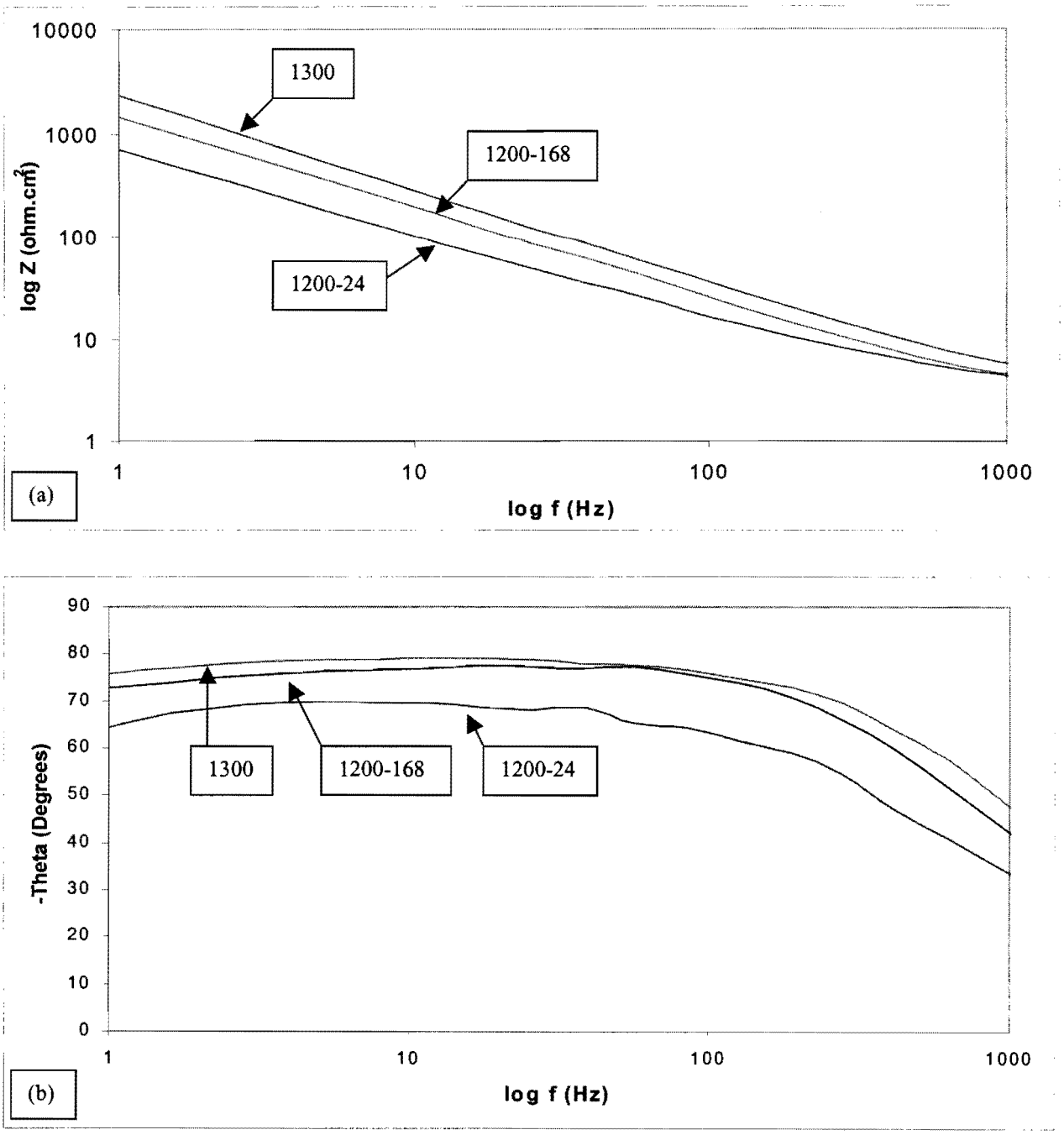

Figure 5.10.(a) Impedance spectroscopy at -0.5 V_{SSC} for the 60Au-40Pt samples in 0.5 M NaOH (b) the phase angle over the same frequency range.

5.3.3.4. The 60Au-40Pt alloy in the 800°C heat treatment condition

The microstructure of this sample is shown in Figure 3.12. The sample was in the 1200°C (24 h) porous, but single-phase heat treated condition prior to the heat treatment at 800°C for 50 hours. Cyclic voltammograms for this electrode are shown in Figure 5.11. The oxygen gas evolution overpotential is low on this electrode (Fig. 5.9). The low equilibrium gold content of the platinum-rich areas (Table 3.1) is probably responsible for this observation. The platinum oxide reduction peak is very large when the upper potential limit is 0.75 V (Fig. 5.11). This may be related to oxygen gas evolution at the upper end of the cycle. It must also be remembered that platinum-rich areas nucleated at the pores during the heat treatment at 800°C (Fig. 3.13). The surface area of the pores is therefore probably platinum-rich.

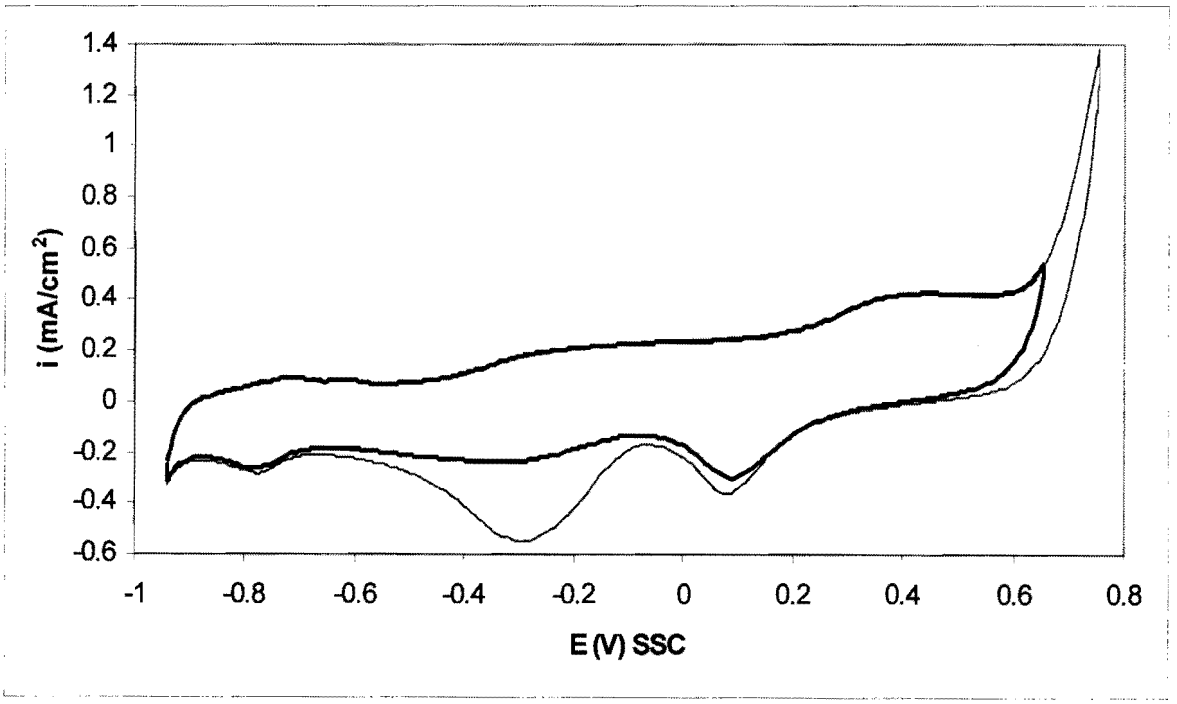

Figure 5.11. Cyclic voltammograms for the 800°C heat treated sample (60Au-40Pt) in 0.5 M NaOH. Scan rate 50 mV/s, 25°C.

5.3.3.5. The 60Au-40Pt alloy in the 600°C heat treatment condition

The microstructure of this sample is shown in Figure 3.15. The sample was in the 1200°C (24 h) heat treated condition prior to the heat treatment at 600°C for 100 hours. Cyclic voltammograms for this electrode are shown in Figure 5.12. High current densities due to oxygen gas evolution are also obtained. The equilibrium composition of the platinum-rich areas in this sample is 98Pt-2Au (Table 3.1). The fact that these areas are nearly pure platinum may explain the low oxygen gas evolution potential.

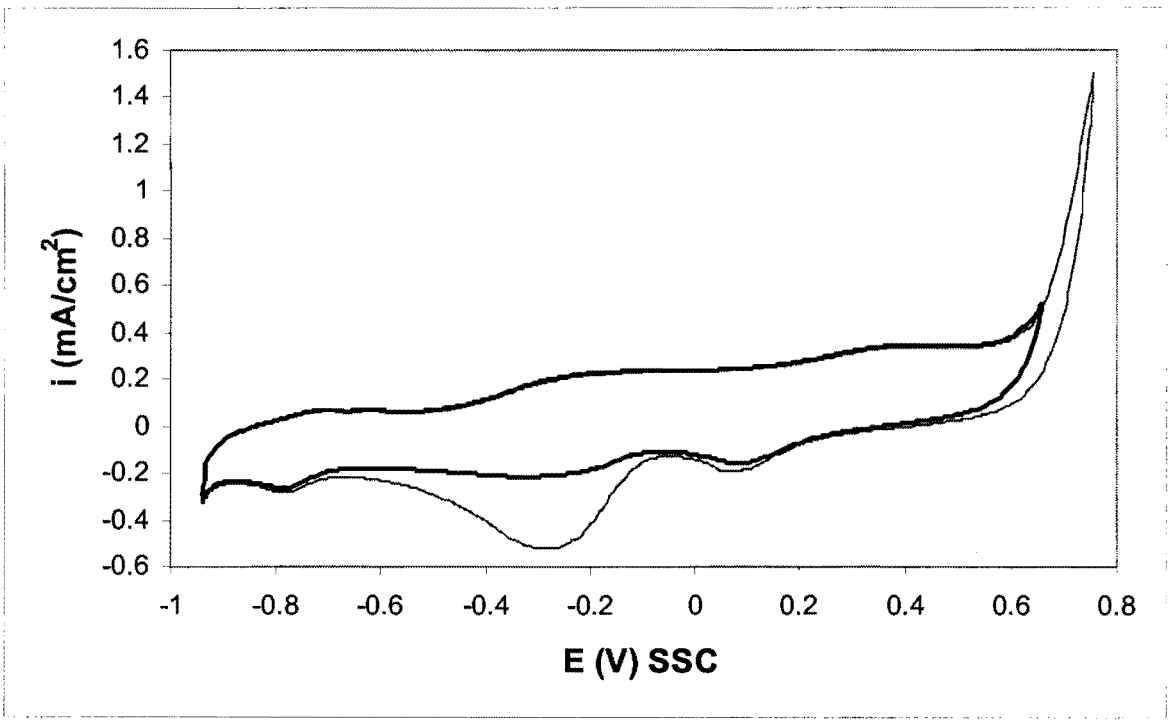

Figure 5.12. Cyclic voltammograms for the 600°C heat treated sample (60Au-40Pt) in 0.5 M NaOH. Scan rate 50 mV/s, 25°C.

In acid solution, it seems as if only a few percent of gold in platinum is needed to inhibit the oxygen gas evolution reaction. There is only 5 % Au in the platinum-rich areas in the 800°C heat treated sample, but the oxygen gas evolution reaction on this sample is inhibited more than on the 600°C heat treated sample in acid (Fig 4.13). The oxygen gas evolution reaction in alkaline solution is not inhibited on the 800°C heat treated sample

compared to the 600°C heat treated sample (Fig. 5.13). This implies that the presence of gold in the platinum-rich phase is not as effective in inhibiting the oxygen evolution reaction in base. The oxygen gas evolution reaction at gold in acid commences at approximately 1.65 V_{SSC} (Fig. 4.1) and in base at 0.75 V_{SSC} (Fig. 5.1). The corresponding values for oxygen evolution at platinum are 1.25 V_{SSC} in acid (Fig. 4.2) and 0.60 V_{SSC} in base (Fig. 5.2). These values compare well with those found in the literature. Burke and Nugent (1997) found that oxygen evolution starts at gold in acid at 1.7 V_{SSC} (1 M H_2SO_4, 25°C) and in base at 0.7 V_{SSC} (1 M NaOH, 25°C). Heyd and Harrington (1992) found a potential of 1.28 V_{SSC} for the onset of oxygen evolution at platinum in acid (0.5 M H_2SO_4, 25°C). For platinum in base (0.1 M NaOH, 25°C), a potential of 0.62 V_{SSC} was found by Xia and Birss (2000). The difference in potential at which oxygen starts to be evolved at gold and platinum is generally about 0.40 V in acid and 0.10 - 0.15 V in base. Burke and Nugent (1997) postulated that oxygen gas evolution at gold in base over the range 0.7 – 1.0 V_{SSC} is catalysed in a transient manner by some type of hydrous gold oxide species. They pointed out that regular oxygen gas evolution at gold in base occurs only above 1.0 V_{SSC}. The presence of gold in the platinum-rich areas will therefore be not so effective in inhibiting the oxygen evolution reaction in base as it is in acid. This is unfortunate, as oxygen gas evolution lowers the current efficiency during the electro-oxidation of organic compounds (Bock and MacDougall, 2000).

5.3.4. The 50Au-50Pt alloy

5.3.4.1. The 50Au-50Pt alloy in the "ductile" condition

The microstructure of this sample (two-phased, fine microstructure) is shown in Figure 3.17. Cyclic voltammograms for this electrode are shown in Figure 5.14. The current densities obtained on the ductile 50Au-50Pt sample are similar to the 60Au-40Pt electrode in the 1300°C (two-phased, non-porous) heat treatment condition (Fig. 5.5).

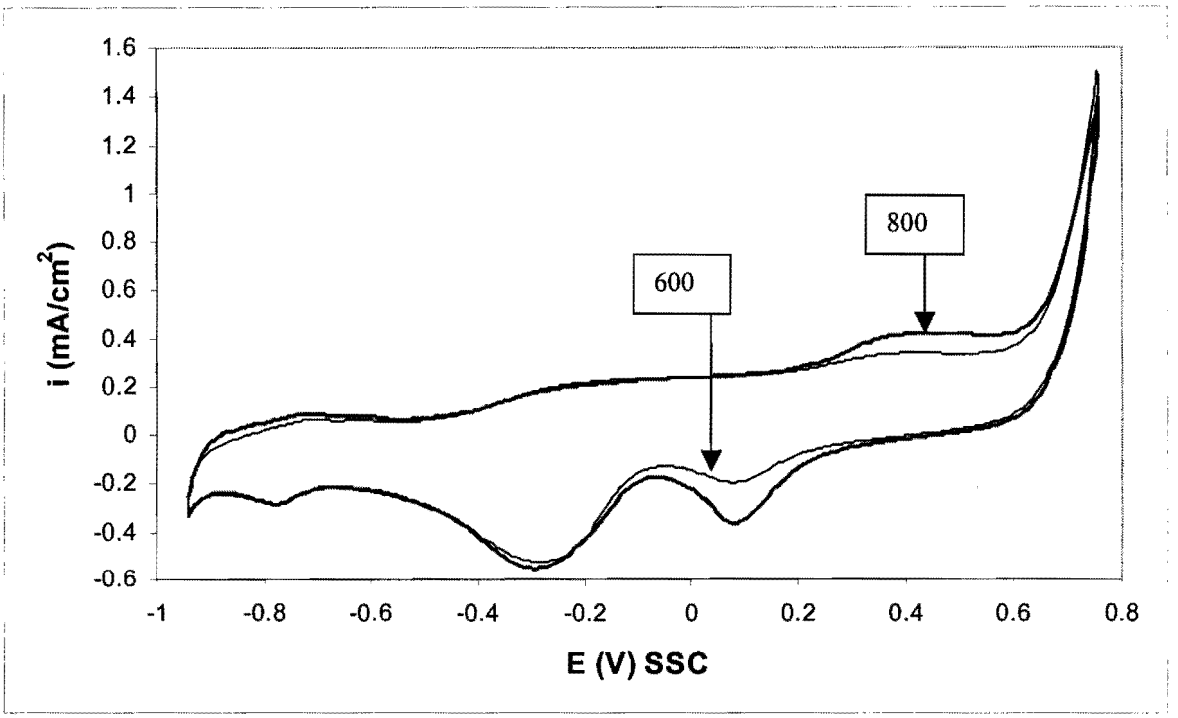

Figure 5.13. Cyclic voltammograms for the miscibility gap heat treated samples (60Au-40Pt) in 0.5 M NaOH. Scan rate 50 mV/s, 25°C.

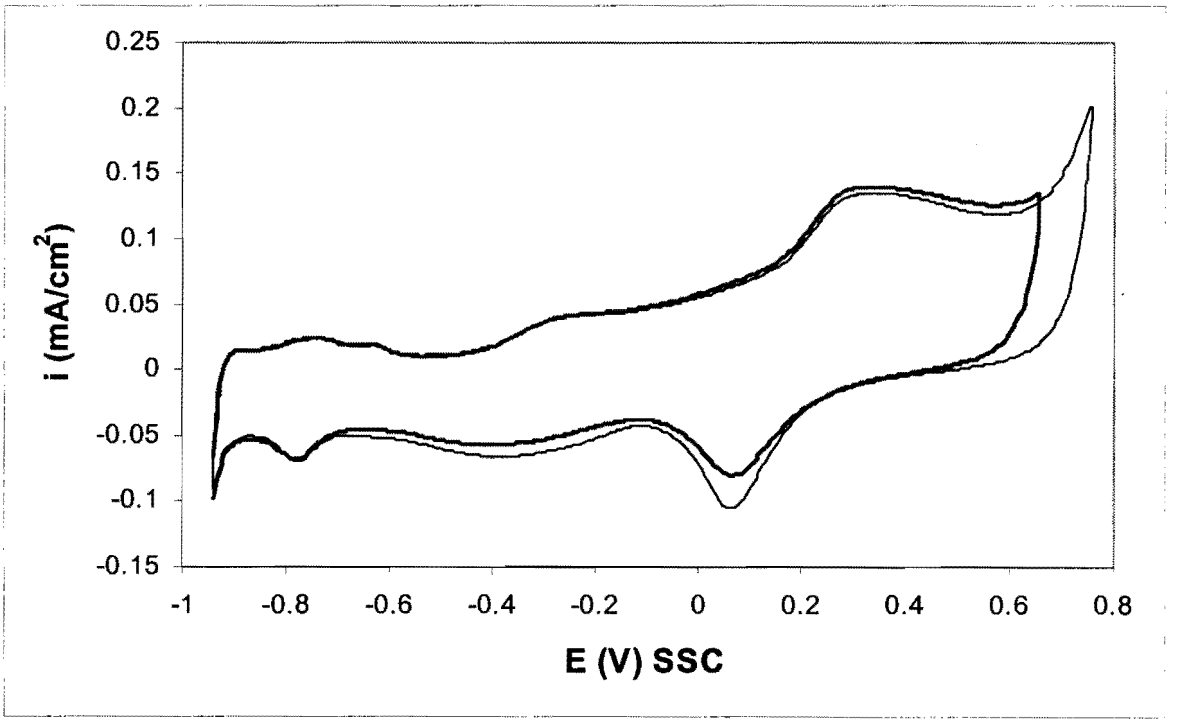

Figure 5.14. Cyclic voltammograms for the "ductile" heat treated sample (50Au-50Pt) in 0.5 M NaOH. Scan rate 50 mV/s, 25°C.

5.3.4.2. The 50Au-50Pt alloy in the solid solution condition

The microstructure of this sample is shown in Figure 3.19. Cyclic voltammograms for this electrode are shown in Figure 5.15. This electrode also has two oxide reduction peaks, despite being in the solid solution condition.

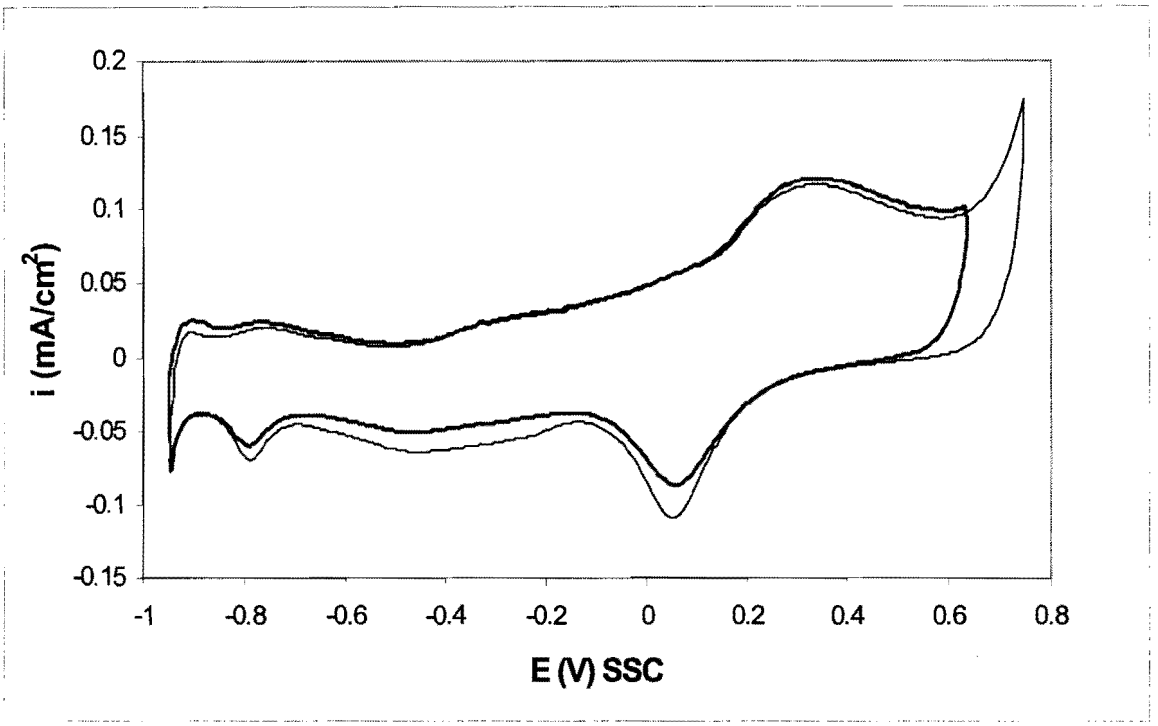

Figure 5.15. Cyclic voltammograms for the solutionised sample (50Au-50Pt) in 0.5 M NaOH. Scan rate 50 mV/s, 25°C.

The two 50Au-50Pt samples have similar current densities (Fig. 5.16). A similar result was obtained in acid (Fig. 4.16) and the reason once again is the absence of Kirkendall porosity in the sample after the solid solution heat treatment. The oxygen gas evolution reaction at the two electrodes is similar in base (Fig. 5.16). This was not the case in acid, where the oxygen evolution reaction was inhibited more at the solid solution electrode compared to the two-phased "ductile" sample (Fig. 4.16). This observation is in line with that in the previous section, namely that gold is less effective at inhibiting oxygen evolution in base than in acid.

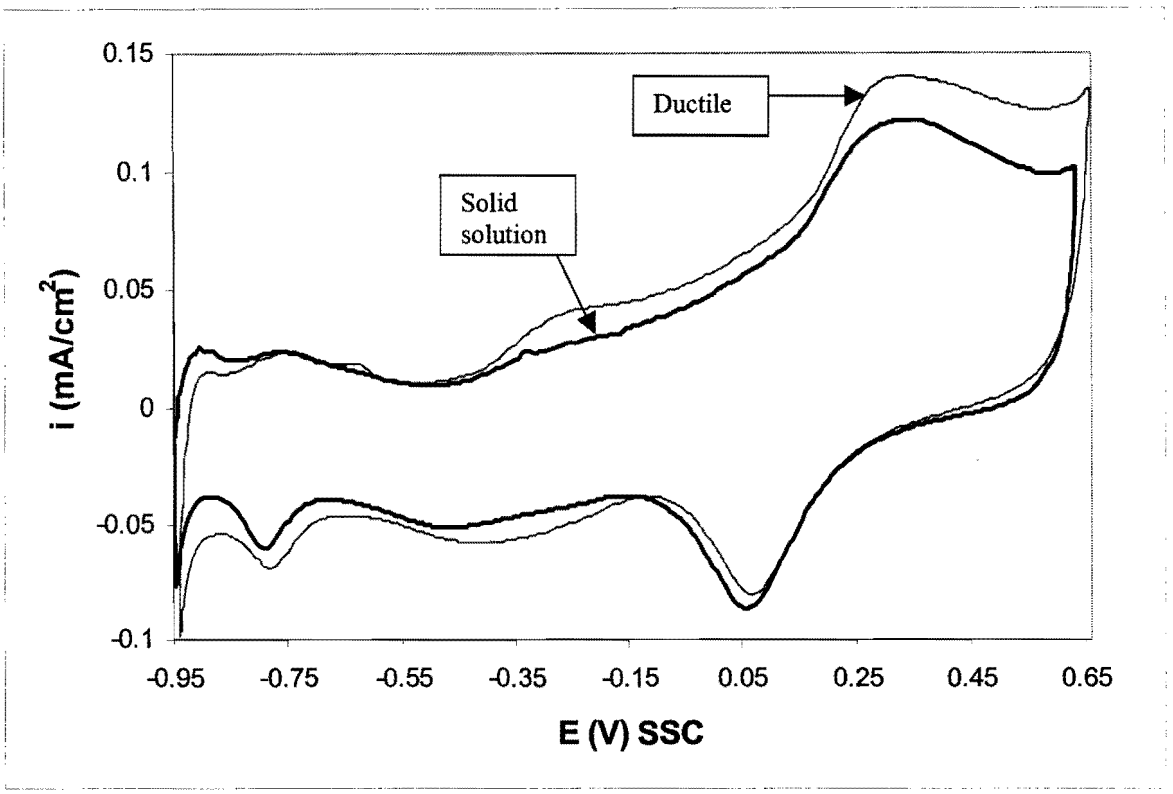

Figure 5.16. Cyclic voltammograms for the 50Au-50Pt samples in 0.5 M NaOH. Scan rate 50 mV/s, 25°C.

Impedance spectroscopy was performed in 0.5 M NaOH at a potential of –0.5 V_{SSC}. In Figure 5.17(a), the impedance as a function of frequency is shown for the 50Au-50Pt electrodes. The phase angle (θ) as a function of the frequency is shown in Figure 5.17(b). The phase angles were fairly constant over the frequency range, dropping to lower values at higher frequencies. The 60Au-40Pt sample in the 1300°C heat treatment condition is included for comparison. Figure 5.17 shows that the surface areas of the 50Au-50Pt electrodes in both heat treatment conditions are similar. The impedance of the 60Au-40Pt sample in the 1300°C heat treatment condition is also similar to the 50Au-50Pt alloy electrodes. This confirms the results of the impedance spectroscopy performed in acid (Fig. 4.17).

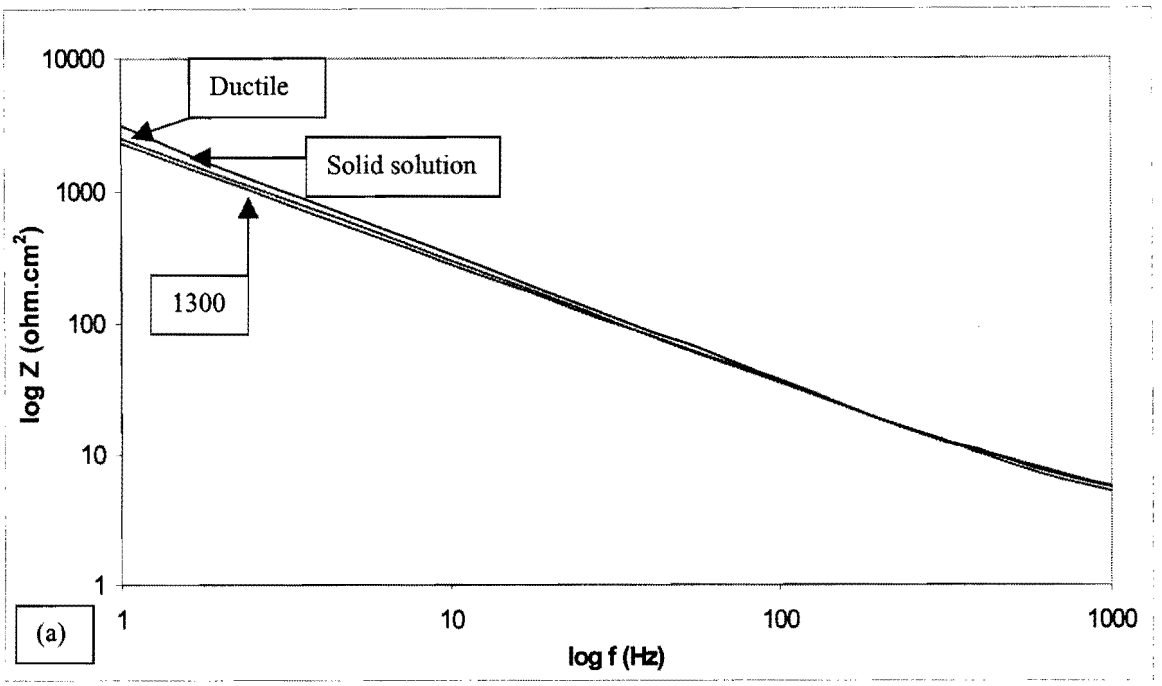

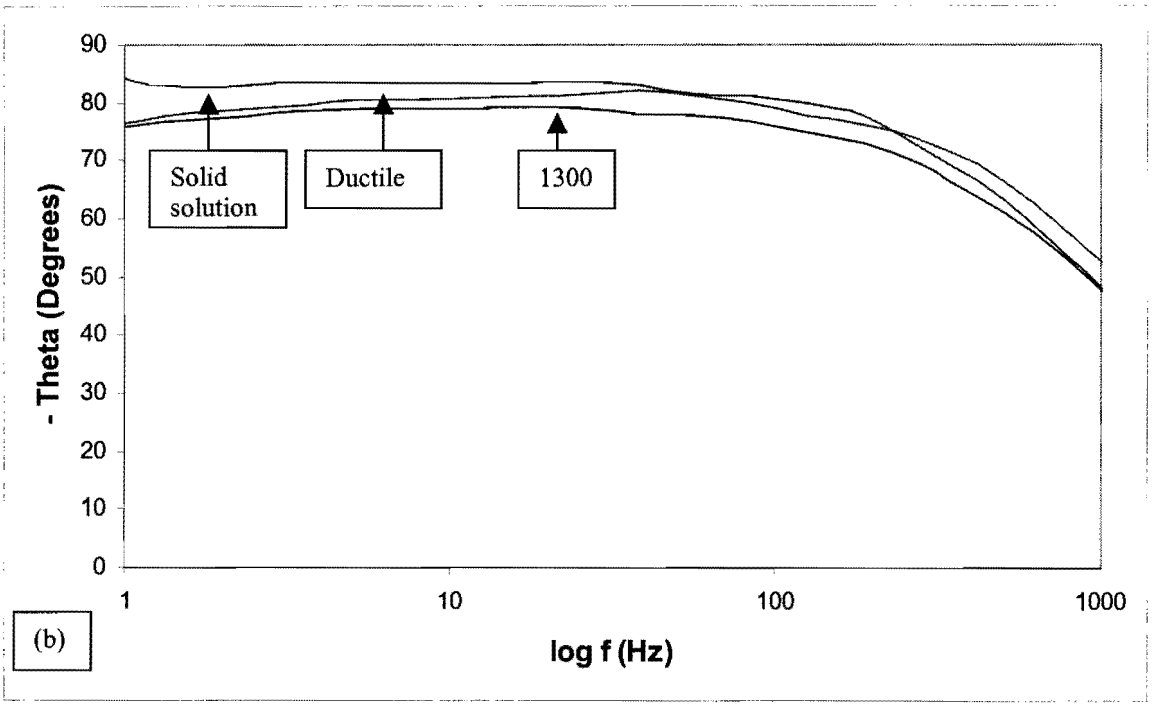

Figure 5.17. (a) Impedance spectroscopy of the 50Au-50Pt samples in 0.5 M NaOH at –0.5 V_{SSC}. (b) The phase angle over the same frequency range. The 1300°C heat treated sample (60Au-40Pt) is included for comparison.

5.3.5. The Gold 990 alloy

5.3.5.1. The Gold 990 alloy in the solid solution condition

This sample has 1 wt% (4 at%) titanium in solid solution with the gold. The Vickers hardness of the sample in this condition is HV_5 = 50 kg/mm^2. Cyclic voltammograms for this sample are shown in Figure 5.18. The behaviour of Gold 990 in the solid solution condition is similar to pure gold (Fig. 5.1), as was the case in acid solutions (Fig. 4.18).

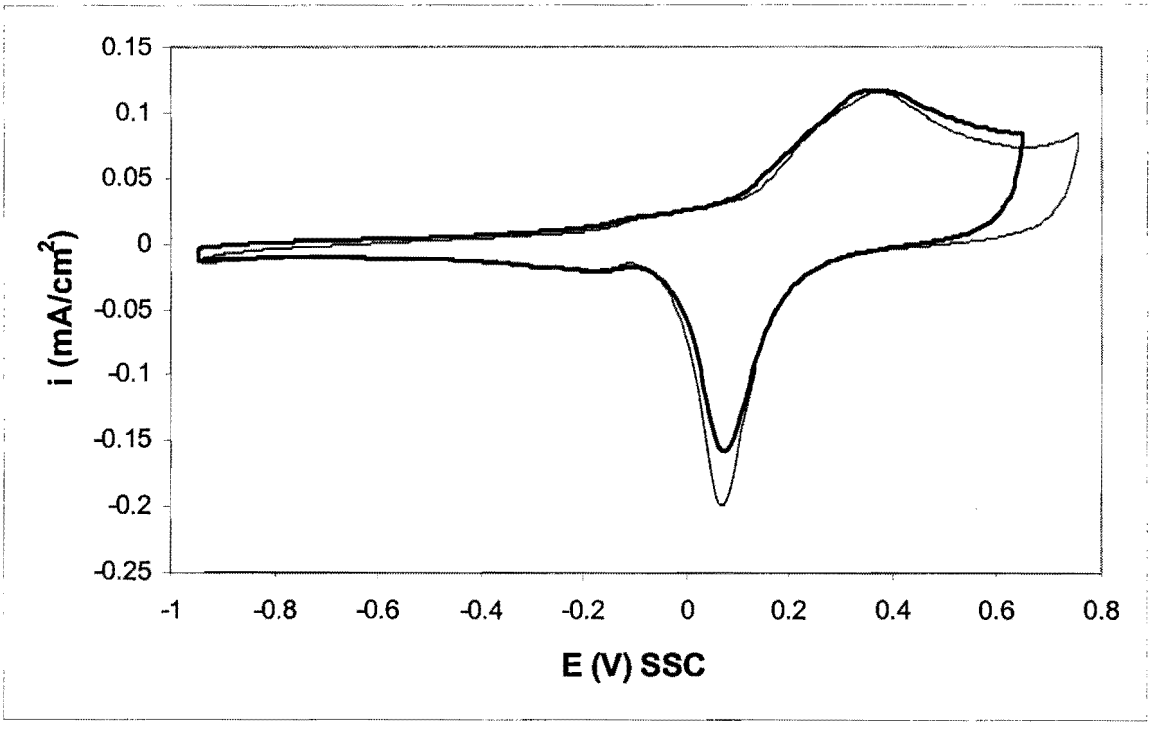

Figure 5.18. Cyclic voltammograms for the Gold 990 sample in the solid solution condition in 0.5 M NaOH. Scan rate 50 mV/s, 25°C.

5.3.5.2. The Gold 990 alloy in the precipitation-hardened condition

This sample is hardened by the presence of small Au_4Ti precipitates. The Vickers hardness of the sample in this condition is HV_5 = 150 kg/mm^2. Cyclic voltammograms

for this sample are shown in Figure 5.19. The behaviour of Gold 990 in the precipitation-hardened condition is also similar to pure gold (Fig. 5.1).

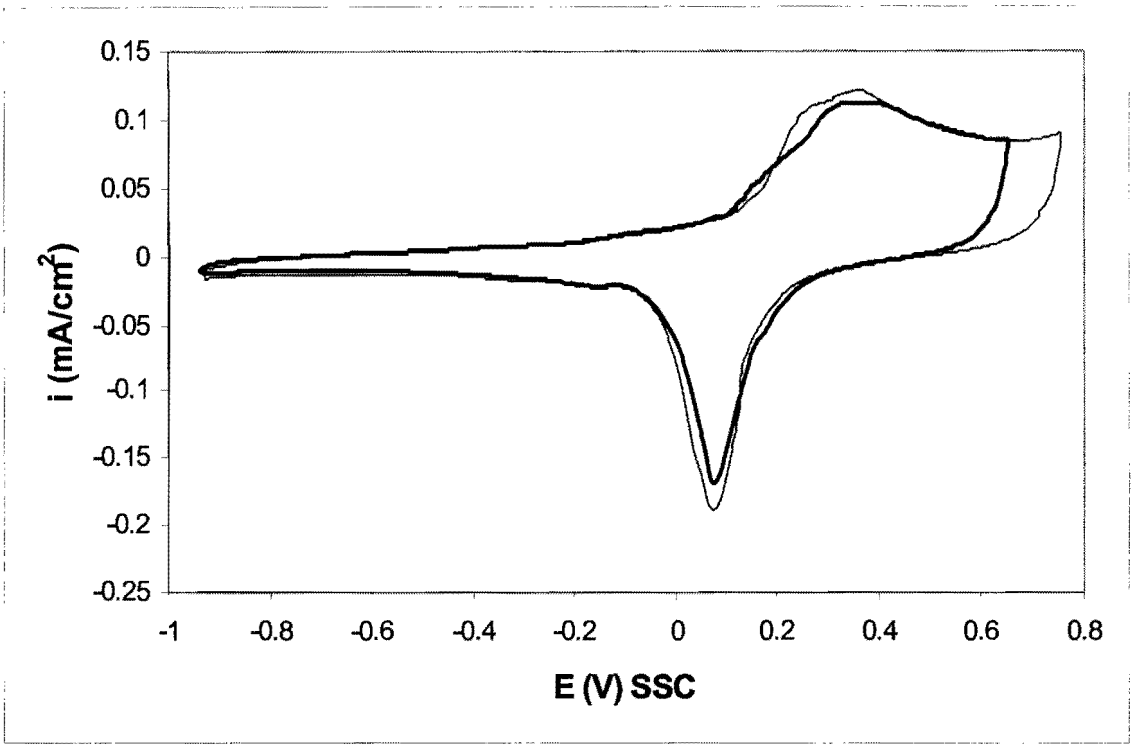

Figure 5.19. Cyclic voltammograms for the Gold 990 sample in the precipitation hardened condition in 0.5 M NaOH. Scan rate 50 mV/s, 25°C.

The cyclic voltammograms for the two Gold 990 electrodes and pure gold are compared in Figure 5.20. The cyclic voltammograms of the three electrodes are similar in alkaline solutions. This agrees with the result found in sulphuric acid (Fig. 4.20). The possible reasons for the similarities have already been discussed in Chapter 4 and are repeated below:

- The titanium content of 4 at% may be too low to have a significant influence on the electrochemical behaviour of gold.
- The titanium may be in the passive condition (Fig 2.21).
- The titanium may have dissolved selectively from the Gold 990 alloy resulting in a pure gold surface.

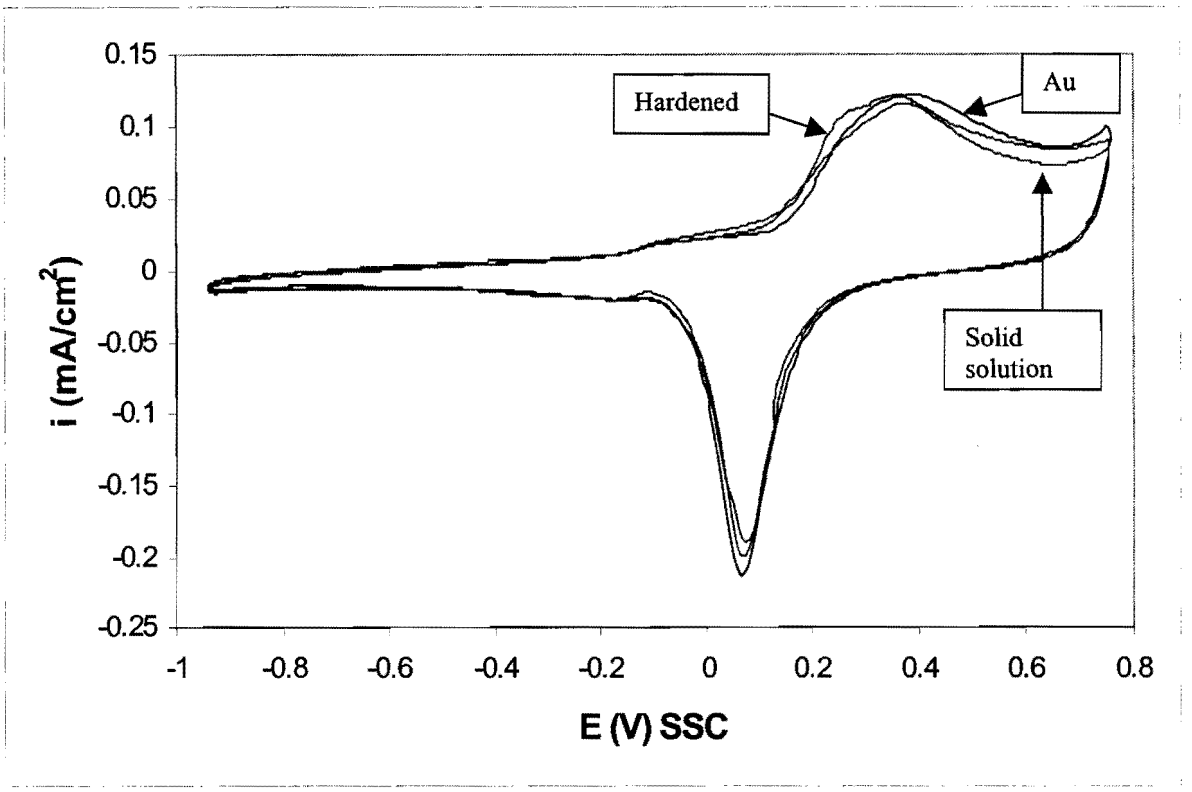

Figure 5.20. Cyclic voltammograms for gold and the Gold 990 samples in 0.5 M NaOH. Scan rate 50 mV/s, 25°C.

5.4. Conclusions

The electrochemical properties of the gold-based alloys in 0.5 M NaOH have been investigated. The most important results can be summarised as follows:

- All reactions occur at a lower potential in base than in acid.

Many of the results obtained in base are similar to what was observed in acid. These include:

- The cyclic voltammograms of the Au-Pt alloys have features corresponding to both pure gold and platinum.
- The Au-Pt alloys in the solid solution condition have two oxide reduction peaks. The one peak corresponds to oxide reduction of platinum and the other to oxide reduction of gold.

- The high surface areas of the porous electrodes result in higher currents. The current densities of these electrodes are therefore higher when the apparent surface area is considered.
- The surface areas of the 50Au-50Pt alloy electrode in the "ductile" condition and in the solid solution condition are similar. Kirkendall porosity is absent in the 50Au-50Pt solid solution alloy.
- The cyclic voltammograms of pure gold and the Gold 990 electrodes are similar.

The oxygen gas evolution reaction in alkaline solution is not inhibited on the 800°C heat treated sample compared to the 600°C heat treated sample (Fig. 5.13). This is in contrast to what was found in acid solution (Fig. 4.13).

The electrochemical properties of the gold-based alloys without organics in solution have been discussed in Chapters 4 and 5. The information gathered with these experiments will be useful to understand the electro-oxidation reactions of organic compounds at the electrodes. The objective of the next chapter is to investigate the electro-oxidation of ethylene glycol at the gold-based alloys.

Chapter 6

THE ELECTRO-OXIDATION OF ETHYLENE GLYCOL AT GOLD-BASED ALLOYS IN AN ALKALINE SOLUTION

6.1. Introduction

The heat treatments of the Au-Pt and Gold 990 samples were investigated in Chapter 3. This was followed by a discussion of the electrochemical properties of the Au-Pt and Gold 990 electrodes in acid (Chapter 4) and in alkaline solutions (Chapter 5) without ethylene glycol.

The purpose of this chapter is to study the electro-oxidation of ethylene glycol at the gold-based alloys in an alkaline solution. High current densities for ethylene glycol oxidation at gold (Kadirgan et al., 1990) and at platinum (Kadirgan et al., 1983) were found in solutions of high pH. By contrast, the electro-oxidation of ethylene glycol at gold (Beden et al., 1987) and at platinum (Hahn et al., 1987) in acid solutions occurs to a lesser extent. It has also been shown by Beden and co-workers (1982) that a synergistic effect is found when gold-platinum alloys are used for the electro-oxidation of ethylene glycol in alkaline solutions. If one considers the possible mechanisms for the synergistic effect observed for Au-Pt alloys (Section 2.6.5), it is expected that the distribution of the gold and platinum atoms at the surface of the electrode will influence the electro-oxidation properties of the alloy. The effect of the microstructure of the alloys on the electro-oxidation of ethylene glycol in alkaline solution was therefore studied and will be discussed in this chapter.

6.2. Experimental

The experimental work was performed with polycrystalline gold (99.99%), platinum (99.99%), 60Au-40Pt, 50Au-50Pt and Gold 990 electrodes. The electrodes were disc-shaped with 6mm diameter. All the electrodes were mounted in a resin by employing a black phenolic thermosetting powder. Electrical contact was achieved by drilling a hole through the rear of the mounting and tapping M6 thread. A Pine analytical rotator was

used as electrode rotator. The apparent surface area of 0.28 cm^2 was used in all cases to calculate current densities. The electrodes were polished before the experiments with diamond paste (down to 1 μm) and ultrasonically cleaned in 0.5 M NaOH.

A water-jacketed perspex electrochemical cell was used for all the experiments. The cell had an inside diameter of 90 mm and a height of 100 mm. Approximately 400 ml electrolyte was used. The distance between the working electrode and the bottom of the cell was about 60 mm. The temperature was controlled at 25°C. The cover of the perspex cell had six openings which allowed the insertion of two counter electrodes, the working electrode, the Luggin capillary, the tube for nitrogen purging and a thermometer.

"Proanalysi" ethylene glycol from Merck was used to prepare solutions containing 0.1 M ethylene glycol in 0.5 M NaOH. CP grade NaOH pellets from Associated Chemical Enterprises (Pty) Ltd were used, together with double distilled water.

A Solartron 1287 Electrochemical Interface was used for the cyclic voltammetry experiments. Platinum wire was used as counter electrode. All potentials quoted in this study are with respect to the silver/silver chloride reference electrode (SSC). The scan rate employed was 50 mV/s. Rotation of the electrodes produced an unacceptable high level of noise in the cyclic voltammograms and it was decided to rather stir the solution with a Heidolph MR 3001 K magnetic stirrer. A rotation speed of 500 revolutions per minute was used. The length of the magnet that was used is 40 mm and its diameter 8 mm (The water-jacketed perspex electrochemical cell has an inside diameter of 90 mm).

The cyclic voltammetry experiments of all the electrodes were performed by using the following procedure:

- The 0.5 M NaOH solution (without ethylene glycol) was purged with nitrogen for 30 minutes to remove dissolved oxygen.
- The electrode potential was cycled for fifteen cycles between the values for onset of O_2 and H_2 evolution until the I-E curves were reproducible. The cyclic voltammogram (15^{th} cycle) of the electrode was then compared to the cyclic voltammogram found in chapter 5. This was done to make certain that the solution did not contain impurities and that the behaviour of the electrode was similar to what was found in chapter 5.
- The ethylene glycol was added to the solution.

- The electrode was anodically activated at 1.2 V_{SSC} for 10 seconds (the solution was stirred during activation). Poisoning species and the electrode surface are oxidised at this potential. Oxygen gas evolution is also expected to occur at 1.2 V_{SSC}.
- The electrode potential was then cycled for 10 cycles between the values for onset of O_2 and H_2 evolution (the solution was stirred in one set of experiments and not stirred in the other set of experiments).
- The electrode was anodically reactivated at 1.2 V_{SSC} for 10 seconds (the solution was stirred during reactivation).
- The electrode potential was cycled once between the values for onset of O_2 and H_2 evolution to see if reactivation was successful (the solution was stirred in one set of experiments and not stirred in the other set of experiments).

6.3. Results and discussion

6.3.1. Gold

Cyclic voltammograms for gold in 0.5 M NaOH without ethylene glycol are shown in Figure 5.1. The cyclic voltammograms (1^{st} and 10^{th} cycles) with 0.1 M ethylene glycol in the solution are shown in Figure 6.1. The solution was not stirred in Figure 6.1(a) and stirred in Figure 6.1(b). The first cycles after anodic reactivation of the gold electrode are also shown in Figures 6.1(a) and (b).

The voltammograms in Figure 6.1 compare well with those found in the literature (Fig. 2.14). It is seen from Figure 6.1 that ethylene glycol electro-oxidation commences during the positive sweep at a potential of –0.3 V_{SSC}. This is in the potential region before the surface oxide forms on gold (Figure 5.1). It has been suggested (Vitt et al., 1990) that organic compounds are oxidised in the presence of AuOH formed in the premonolayer region (also see section 2.4.1).

During the first positive scan, a peak of 16 mA/cm^2 at 0.27 V_{SSC} (Fig. 6.1(a)) is found when the solution is not stirred and a peak of 10.5 mA/cm^2 at 0.25 V_{SSC} (Fig. 6.1(b)) is

found when the solution is stirred. Hauffe and Heitbaum (1978) also found that the peak currents were smaller when the solution was stirred with argon gas. They postulated that

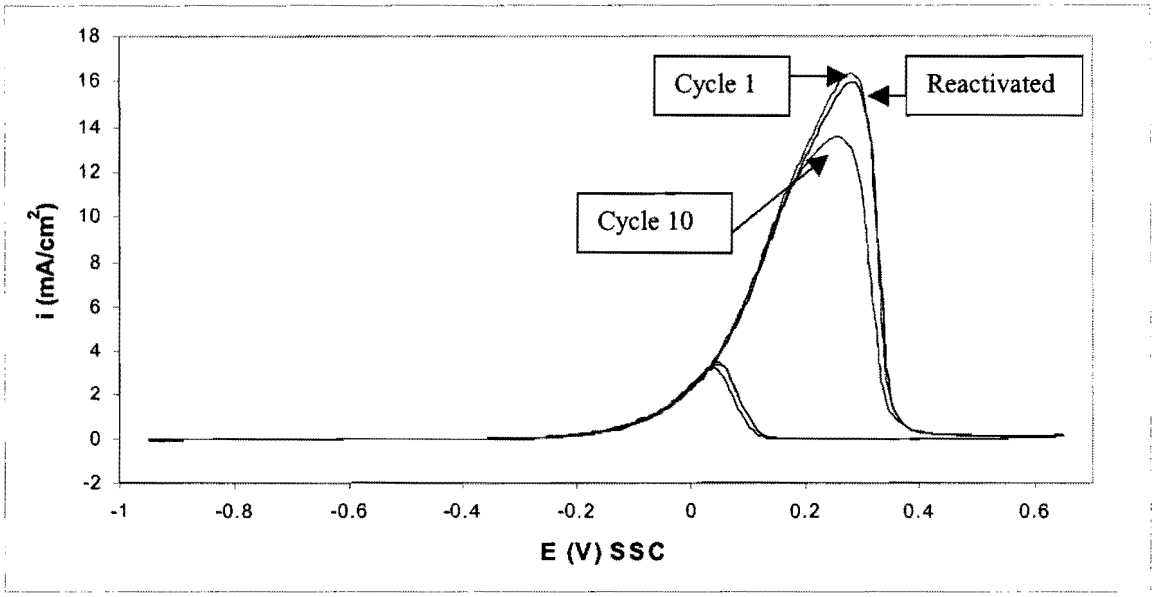

(a)

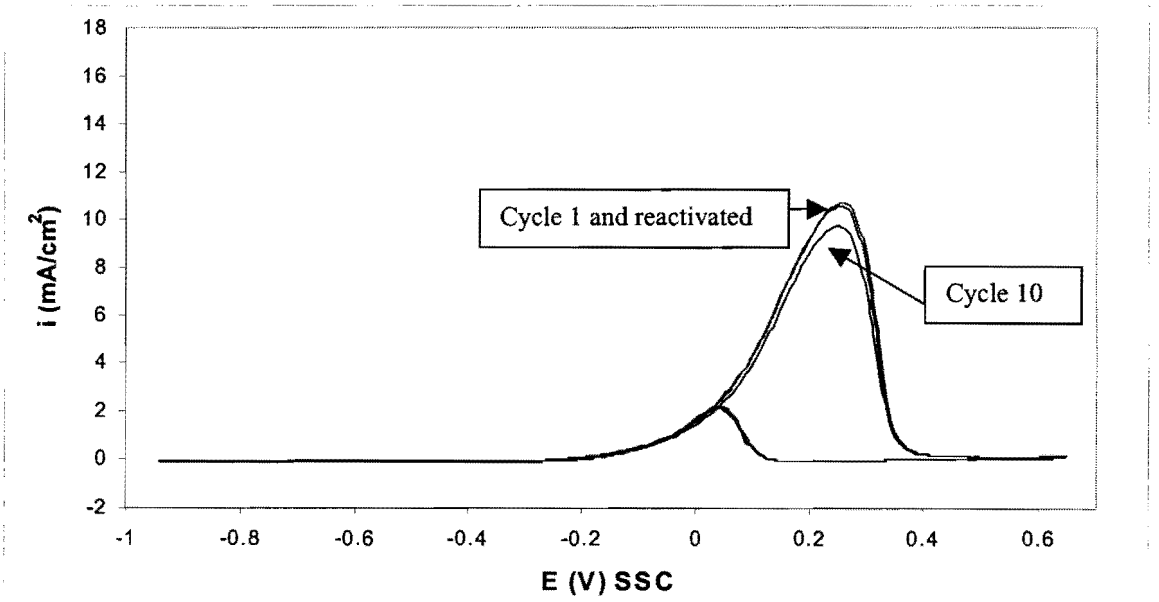

(b)

Figure 6.1. Cyclic voltammograms for the electro-oxidation of 0.1 M ethylene glycol in 0.5 M NaOH at a gold electrode (50mV/s, 25°C). (a) Solution not stirred; (b) Solution stirred.

stirring caused an accelerated transportation of partially oxidised intermediates into the solution. These intermediates cannot be oxidised at the electrode surface, resulting in lower current densities.

The electro-oxidation of ethylene glycol is inhibited by the surface oxide on the gold electrode from 0.25 to 0.65 V_{SSC} during the positive sweep (Fig 6.1). During the negative sweep, oxidation of ethylene glycol commences only after the surface gold oxide has been reduced (Figure 5.1), reaching a current density maximum of 3.5 mA/cm^2 (not stirred) and 2.2 mA/cm^2 (stirred) at 0.03 V_{SSC}.

The peak current densities of the 10^{th} cycles are lower than for the 1^{st} cycles (Fig. 6.1(a), (b)). This occurs due to electrode poisoning. CO poisons are expected to form by the rupture of the C-C bond during chemisorption at negative potentials. Kadirgan and co-workers (1990) used electromodulated infrared reflectance spectroscopy (EMIRS) to study poison formation at gold electrodes during ethylene glycol electro-oxidation. They found that the CO band was not present initially and that it grew during spectral accumulation performed to improve signal to noise ratio. However, the CO band was far from being the main infrared band observed. It was therefore suggested that ethylene glycol does not dissociate immediately on gold at low potentials and that the CO poisoning species are formed only progressively. Glycolaldehyde and glyoxalate were found to be the main adsorbed species.

During the anodic reactivation procedure at 1.2 V_{SSC}, the poisons (and the electrode surface) are oxidised. The cyclic voltammograms (Fig. 6.1 (a), (b)) show that the original peak current densities (before poisoning) can be obtained after reactivation of the electrode.

6.3.2. Platinum

Cyclic voltammograms for platinum in 0.5 M NaOH without ethylene glycol are shown in Figures 5.2 and 5.3.

The cyclic voltammograms (1st and 10th cycles) with 0.1 M ethylene glycol in the solution are shown in Figure 6.2. The solution was not stirred in Figure 6.2(a) and it was stirred in Figure 6.2(b). The first cycles after anodic reactivation of the platinum electrode are also shown in Figures 6.2(a) and (b).

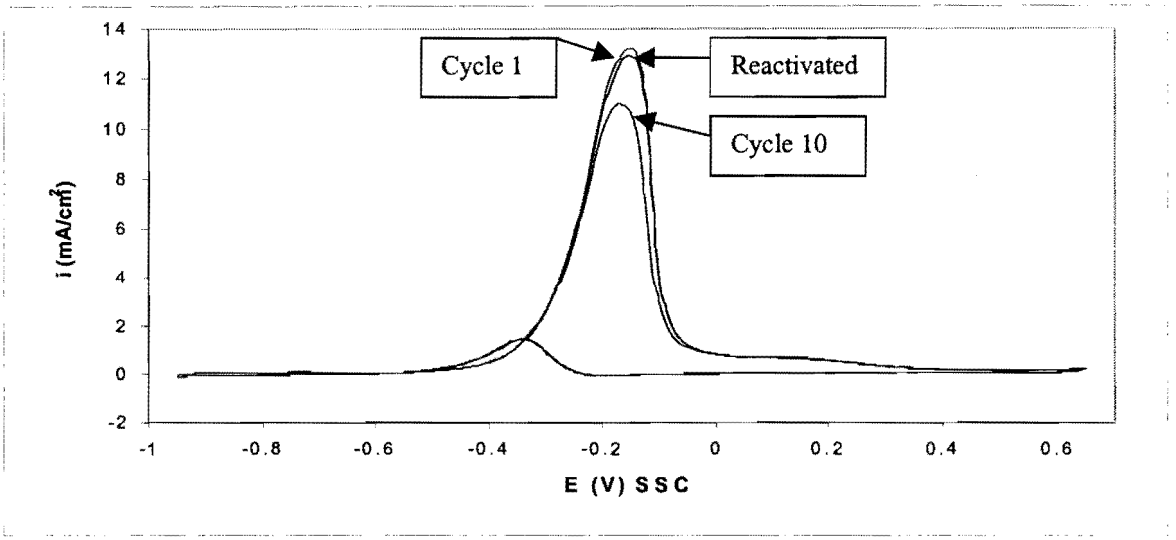

(a)

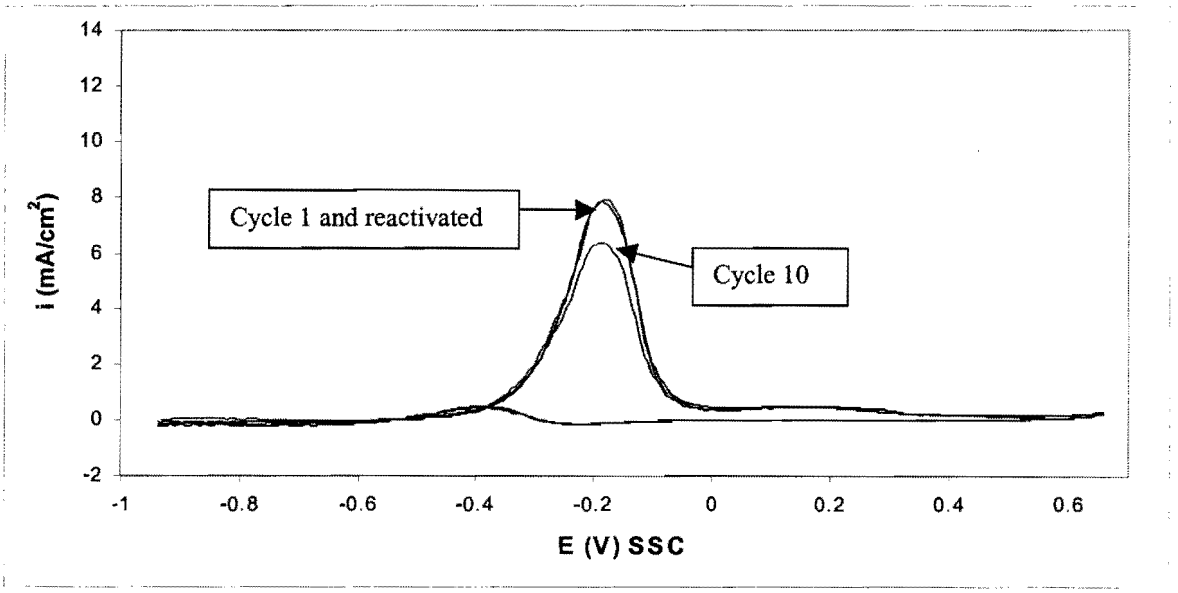

(b)

Figure 6.2. Cyclic voltammograms for the electro-oxidation of 0.1 M ethylene glycol in 0.5 M NaOH at a platinum electrode (50mV/s, 25°C). (a) Solution not stirred; (b) Solution stirred.

The voltammograms in Figure 6.2 compare well with those found in the literature (Fig. 2.16). It is seen from Figure 6.2 that ethylene glycol electro-oxidation commences during the positive sweep at a potential of –0.6 V_{SSC}. This is, as with gold, in the potential region before the surface oxide is formed (Fig.5.2). The electro-oxidation of ethylene glycol is apparently inhibited by the surface oxide on the platinum electrode. Xia and Birss (2000) postulated that hydroxide is adsorbed in the anodic sweep while hydrogen is desorbed over the potential region from –0.9 to –0.55 V_{SSC} (Fig. 2.6). It is generally accepted that the electro-oxidation of ethylene glycol at platinum occurs in the presence of OH_{ads} species. (Enea and Ango, 1989).

During the first positive scan, a peak of 13.5 mA/cm^2 at –0.15 V_{SSC} (Fig. 6.2(a)) is found when the solution is not stirred and a peak of 8 mA/cm^2 at –0.18 V_{SSC} (Fig. 6.2(b)) is found when the solution is stirred.
During the negative sweep, oxidation of ethylene glycol commences only after the surface platinum oxide has been reduced (Figure 5.2), reaching a current density maximum of 1.5 mA/cm^2 (not stirred) and 0.4 mA/cm^2 (stirred) at –0.35 V_{SSC}.

The peak current densities of the 10th cycles are lower than for the 1st cycles (Fig. 6.2(a), (b)). As was the case for gold, this is apparently due to electrode poisoning. Hahn and co-workers (1987) studied the adsorption of ethylene glycol at platinum in alkaline solutions. In contrast to gold, the adsorption at platinum was found to be dissociative. Almost equal amounts of bridge-bonded and linearly bonded CO species were found. The linearly-bonded CO is thought to be responsible for the poisoning of the electrode.
The cyclic voltammograms (Fig. 6.2 (a), (b)) show that the original peak current densities at platinum (before poisoning) can also be obtained after reactivation of the electrode.

Cyclic voltammograms for ethylene glycol oxidation at gold and platinum (1st cycles, stirred) are compared in Figure 6.3. It is seen that higher current densities are found with gold compared to platinum. However, the oxidation peaks for ethylene glycol oxidation are located at more negative potentials for platinum than for gold.

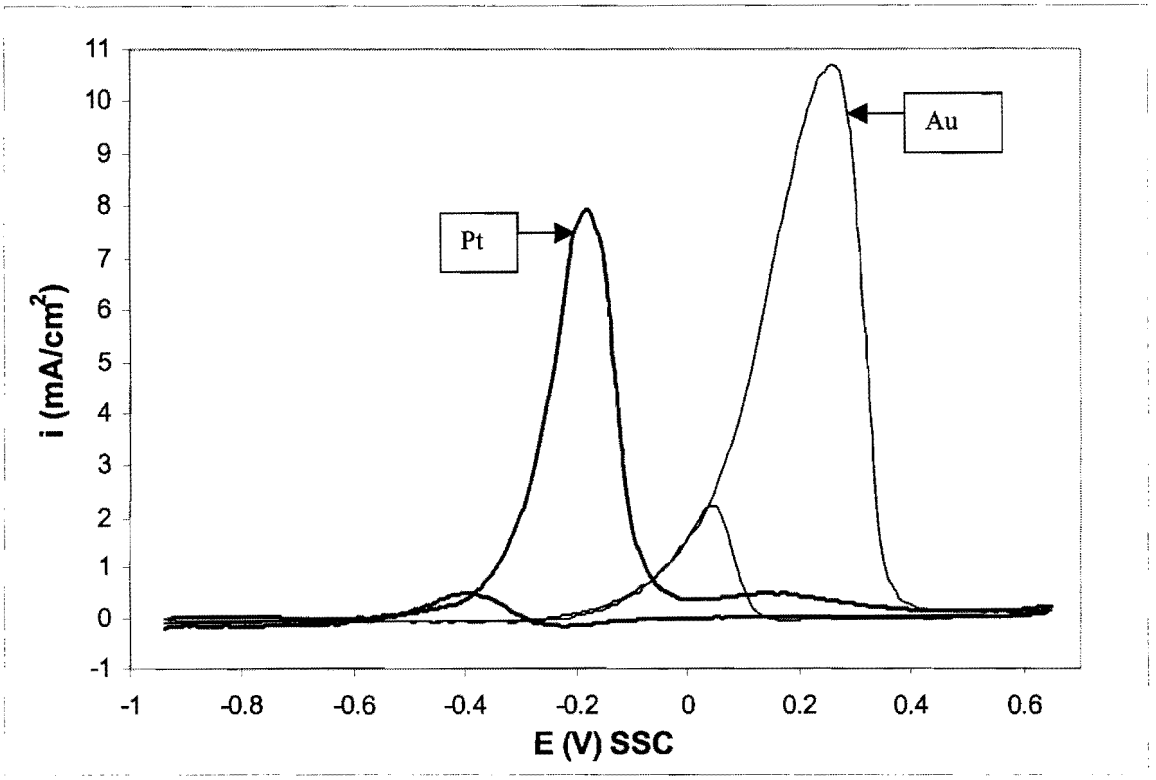

Figure 6.3. Cyclic voltammograms for the electro-oxidation of 0.1 M ethylene glycol in 0.5 M NaOH at gold and platinum electrodes (50mV/s, 25°C); 1st cycles, solution stirred.

Enea and Ango (1989) suggested that the adsorption of ethylene glycol at gold and platinum occur by different mechanisms. Gold is a weak chemisorber due to the absence of vacancies in its d-bands ($5d^{10}$ electron configuration). Platinum is a stronger chemisorber ($5d^{9}$ electron configuration) than gold. Dissociative adsorption of ethylene glycol on the surface of platinum is therefore significant and occurs even if at open circuit. This is presumably due to the interactions of the CH_2 groups with the metallic platinum sites. By contrast, such a dissociative adsorption does not take place at a gold surface: the applied potential must have positive values to allow adsorption of the OH groups at the surface and their subsequent dissociation (Enea and Ango, 1989). This may explain why the CO poisoning species are formed only progressively at gold, but are already present from the beginning at platinum (Kadirgan et al., 1990; Hahn et al., 1987).

6.3.3. The 60Au-40Pt alloy

6.3.3.1. The 60Au-40Pt alloy in the 1300°C heat treatment condition

The two-phased microstructure of this alloy can be seen in Figure 3.2. Cyclic voltammograms for the 1300°C treated electrode in 0.5 M NaOH without ethylene glycol are shown in Figure 5.5.

The cyclic voltammograms (1^{st} and 10^{th} cycles) with 0.1 M ethylene glycol in the solution are shown in Figure 6.4. The solution was not stirred in Figure 6.4(a) and stirred in Figure 6.4(b). The first cycles after anodic reactivation of this electrode are also shown in Figures 6.4(a) and (b). The electro-oxidation of ethylene glycol at the alloy electrode occurs in two regions: the first region is in the same potential range as pure platinum and the second in the same potential range as pure gold.

The peak current densities during the positive scan for this 60Au-40Pt electrode, pure gold and pure platinum are compared in Table 6.1.

Table 6.1. Peak current densities (in mA/cm^2) during the positive scans for Au, Pt and the 1300°C electrode

Scan no.	Stirred?	Pt	1300°C (Pt region)	Au	1300°C (Au region)
1	No	13.5	34	16	4.5
1	Yes	8	25	10.5	3
10	No	11	21	13.5	9
10	Yes	6.5	10	9.5	7

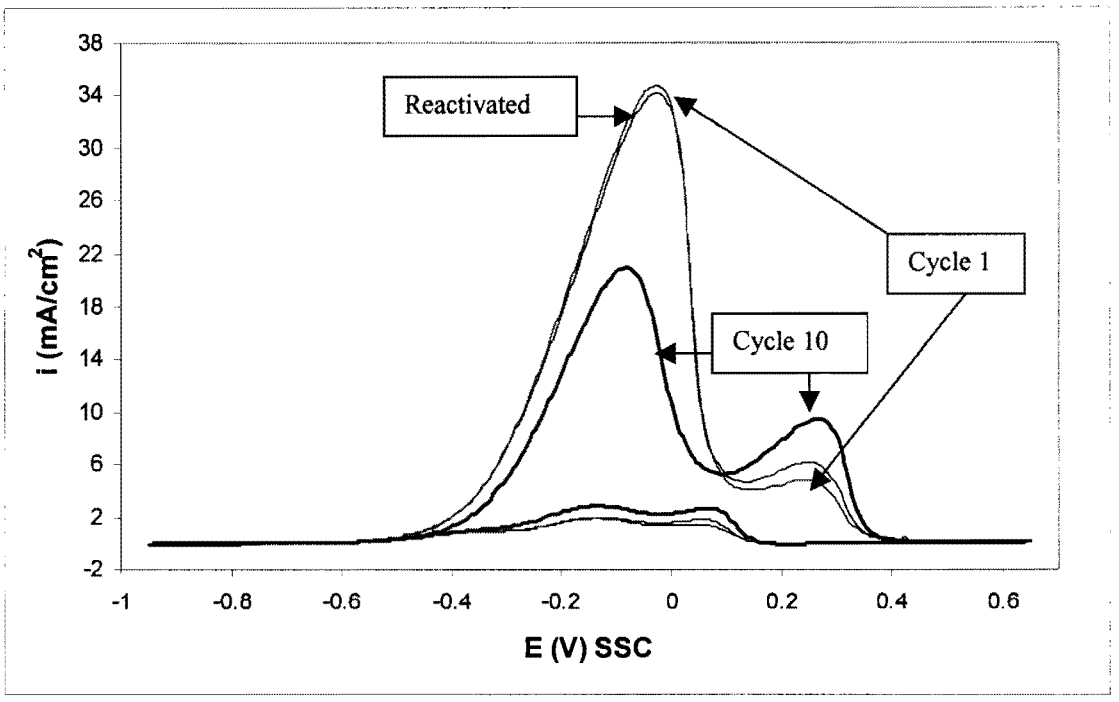

(a)

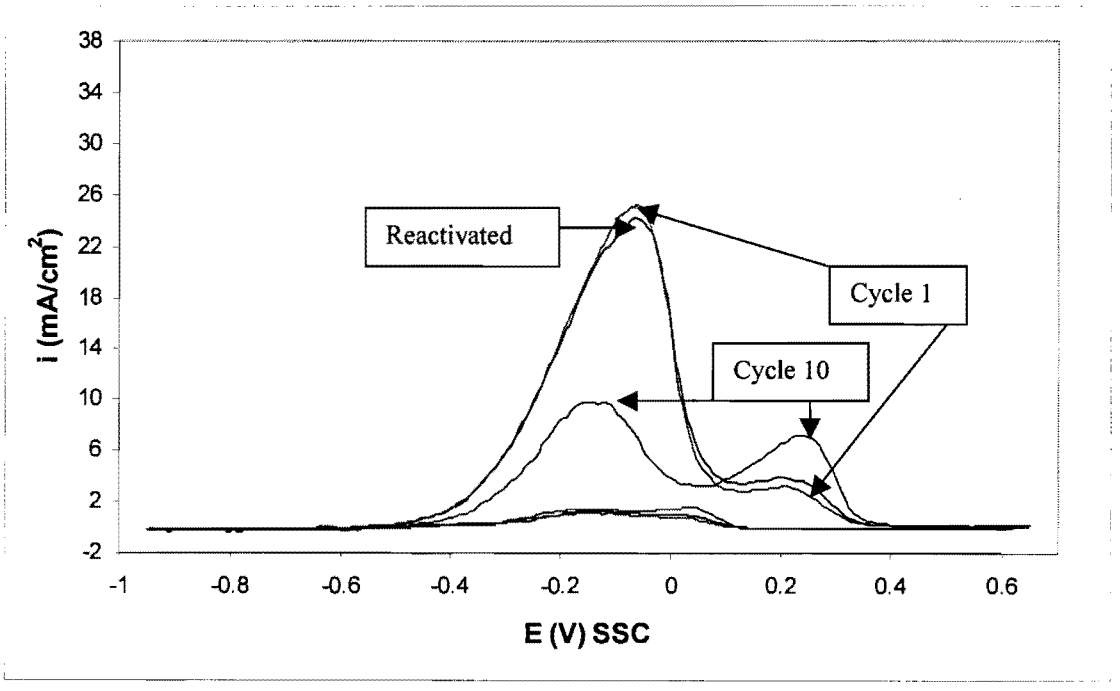

(b)

Figure 6.4. Cyclic voltammograms for the electro-oxidation of 0.1 M ethylene glycol in 0.5 M NaOH at the 1300°C (60Au-40Pt) electrode (50mV/s, 25°C). (a) Solution not stirred; (b) Solution stirred.

From Table 6.1, it is seen that the activity of the platinum region of the alloy is enhanced compared to pure platinum. The current densities of the platinum region of the alloy decrease from scan 1 to scan 10. Surprisingly, the current densities of the gold region increase as the number of scans increases. The activity of the gold region is decreased compared to pure gold. These results differ from those of Beden and co-workers (1982), who found that the activities of both the platinum and the gold regions for a 50Au-50Pt electrode were enhanced compared with the pure metals (Fig 2.17). As with pure gold and pure platinum, the current densities of the alloy electrode are lower when the solution is stirred (Table 6.1).

The anodic treatment at $1.2V_{SSC}$ after the 10^{th} cycle reactivates the platinum region of the alloy electrode, but deactivates the gold region again (Fig. 6.4). It therefore seems as if the activities of the two regions are linked – the activity of the one is high when the activity of the other is low and vice versa.

6.3.3.2. The 60Au-40Pt alloy in the 1200°C (24 hours) heat treatment condition

The microstructure of this alloy (single-phased, porous) can be seen in Figure 3.6. The sample was in the 1300°C heat treated condition prior to the heat treatment at 1200°C for 24 hours. Cyclic voltammograms for the 1200°C-24 h treated electrode in 0.5 M NaOH without ethylene glycol are shown in Figure 5.6.

The cyclic voltammograms (1^{st} and 10^{th} cycles) with 0.1 M ethylene glycol in the solution are shown in Figure 6.5. The solution was not stirred in Figure 6.5(a) and stirred in Figure 6.5(b). The first cycles after anodic reactivation of this electrode are also shown in Figures 6.5(a) and (b). The electro-oxidation of ethylene glycol at this solid solution electrode also occurs in two regions: the first region is in the same potential range as pure platinum and the second in the same potential range as pure gold.

The peak current densities during the positive scan for this 60Au-40Pt electrode, pure gold and pure platinum are compared in Table 6.2.

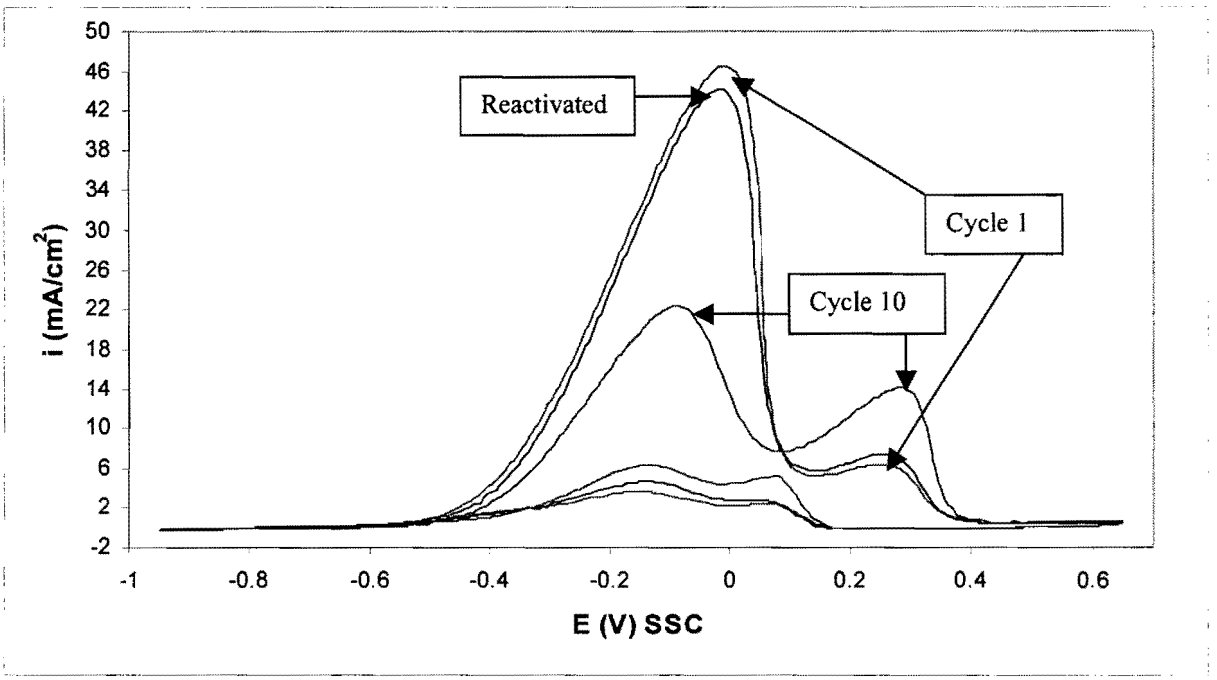

(a)

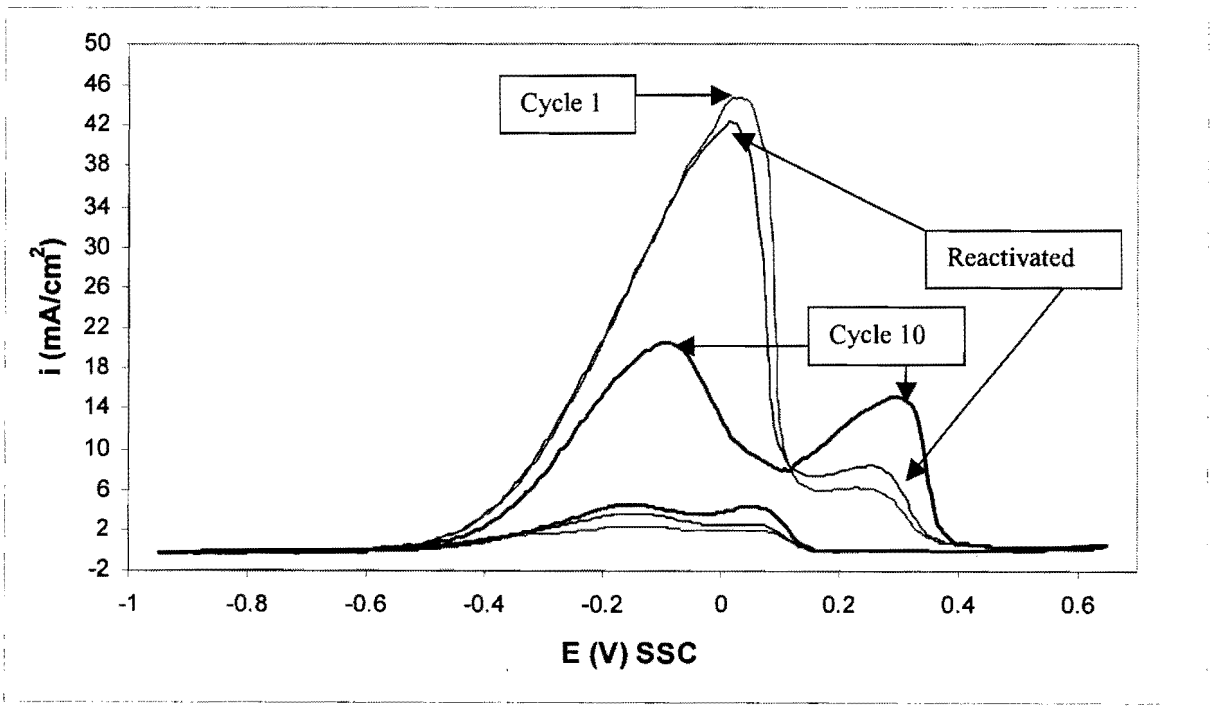

(b)

Figure 6.5. Cyclic voltammograms for the electro-oxidation of 0.1 M ethylene glycol in 0.5 M NaOH at the 1200°C-24h (60Au-40Pt) electrode (50mV/s, 25°C). (a) Solution not stirred; (b) Solution stirred.

Table 6.2. Peak current densities (in mA/cm^2) during the positive scans for Au, Pt and the 1200°C-24 h electrode

Scan no.	Stirred?	Pt	1200°C-24h (Pt region)	Au	1200°C-24h (Au region)
1	No	13.5	46	16	6
1	Yes	8	45	10.5	6
10	No	11	22	13.5	14
10	Yes	6.5	21	9.5	15

Comparing Tables 6.1 and 6.2, it is seen that the porous solid solution electrode produces higher apparent current densities than the non-porous, two-phased 1300°C electrode. The higher apparent current densities of the porous electrode may be due to one of the following reasons:

- The extra surface area of the porous electrode produces higher apparent current densities and the phase difference between the two electrodes is negligible.
- The solid solution of platinum in gold (single phase) is more effective for the electro-oxidation of ethylene glycol than the two-phased microstructure and the porosity does not play an important role.
- The combination of the extra surface area of the porous electrode and the solid solution leads to higher apparent current densities.
- The solid solution decreases the activity, but the extra surface area due to the porosity still leads to higher apparent current densities.

It is difficult to say at this point which of the above scenarios is the correct one. The 50Au-50Pt electrodes (single-phased and two-phased, but both non-porous) should give valuable information to indicate which scenario is correct (see paragraph 6.3.4.). The 60Au-40Pt electrode heat treated at 1200°C for 168 hours will also give valuable information (see paragraph 6.3.3.3.), because the porosity of this electrode appears to be less than that of the 1200°C-24h electrode (compare Figures 3.6 and 3.8).

From Table 6.2 it is evident that stirring does not have a great effect on the current densities obtained with this electrode - the solution inside the pores is probably not affected much by stirring.

The anodic treatment at $1.2V_{SSC}$ after the 10^{th} cycle once again reactivates the platinum region of the alloy electrode, but deactivates the gold region (Fig. 6.5).

6.3.3.3. The 60Au-40Pt alloy in the 1200°C (168 hours) heat treatment condition

The microstructure of this alloy (single-phased; porous, but with less porosity than after the 24 hour treatment at 1200°C) can be seen in Figure 3.8. The sample was in the 1300°C heat treated condition prior to the heat treatment at 1200°C for 168 hours. Cyclic voltammograms for the 1200°C-168 h treated electrode in 0.5 M NaOH without ethylene glycol are shown in Figure 5.8.

The cyclic voltammograms (1^{st} and 10^{th} cycles) with 0.1 M ethylene glycol in the solution are shown in Figure 6.6. The solution was not stirred in Figure 6.6(a) and stirred in Figure 6.6(b). The first cycles after anodic reactivation of this electrode are also shown in Figures 6.6(a) and (b). Once again, the electro-oxidation of ethylene glycol at this solid solution electrode occurs in two regions: the first region is in the same potential range as pure platinum and the second in the same potential range as pure gold.

The peak current densities during the positive scan for this 60Au-40Pt electrode, pure gold and pure platinum are compared in Table 6.3.

Table 6.3. Peak current densities (in mA/cm^2) during the positive scans for Au, Pt and the 1200°C-168 h electrode

Scan no.	Stirred?	Pt	1200°C-168h (Pt region)	Au	1200°C-168h (Au region)
1	No	13.5	42	16	3
1	Yes	8	41	10.5	3
10	No	11	24	13.5	8
10	Yes	6.5	20	9.5	10

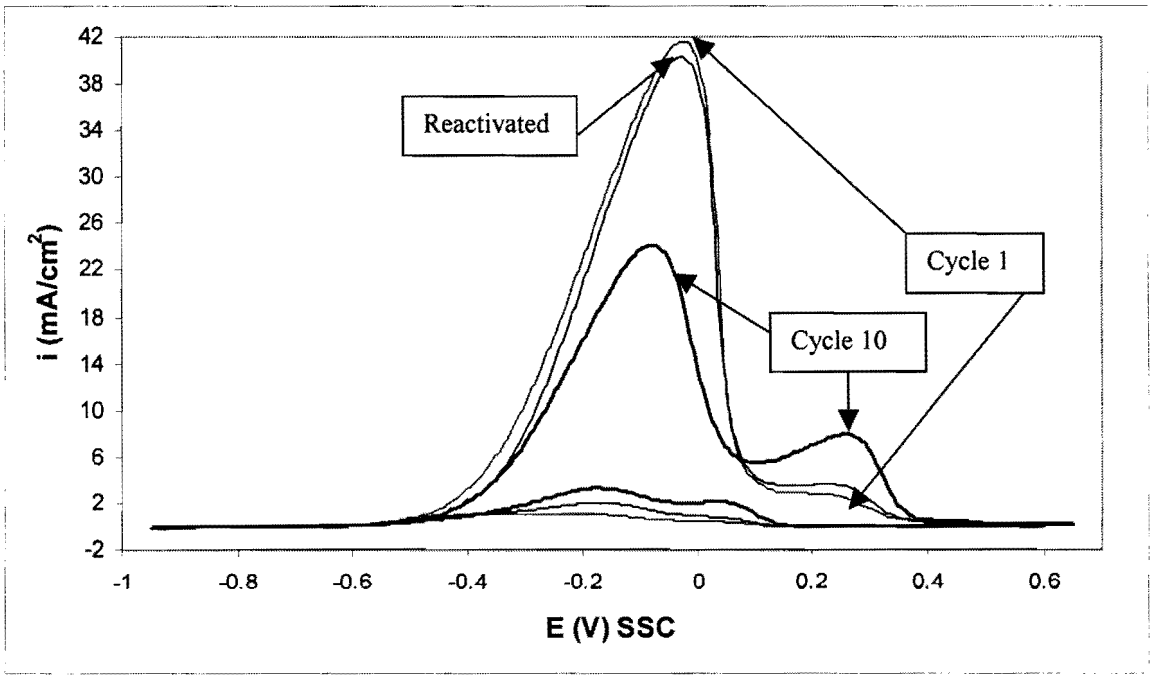

(a)

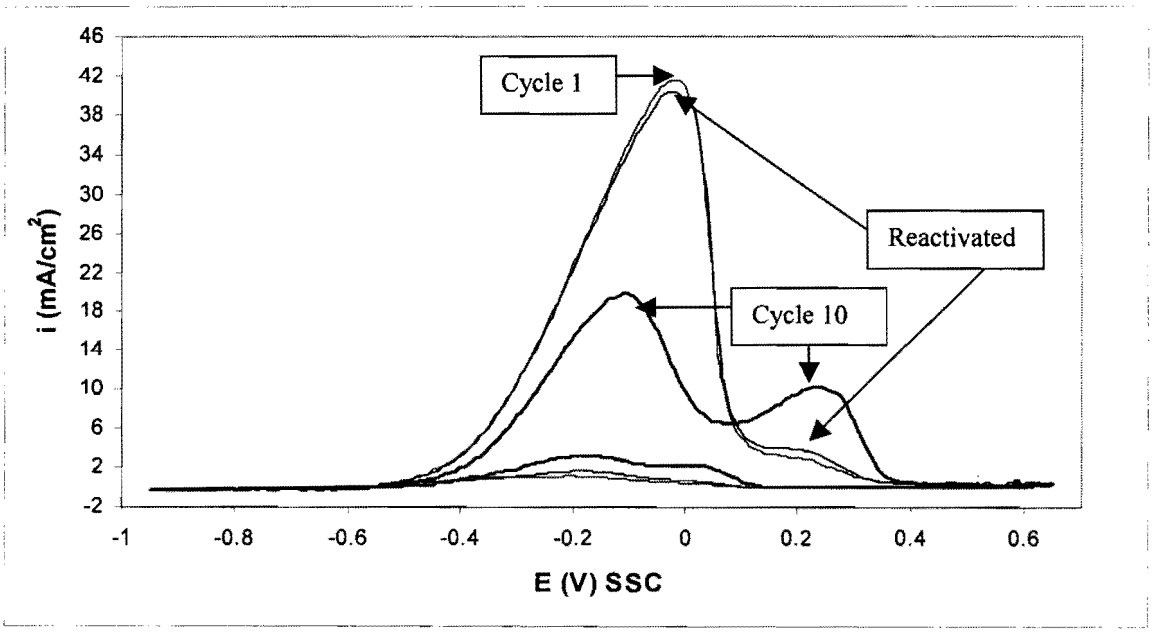

(b)

Figure 6.6. Cyclic voltammograms for the electro-oxidation of 0.1 M ethylene glycol in 0.5 M NaOH at the 1200°C-168h (60Au-40Pt) electrode (50mV/s, 25°C). (a) Solution not stirred; (b) Solution stirred.

Comparing Tables 6.2 and 6.3, it is seen that the two porous solid solution electrodes produce rather similar apparent current densities (especially the Pt-regions). This is surprising if one considers the large difference in apparent current densities between the two electrodes without ethylene glycol in solution (Fig. 5.9). It therefore appears as if the extra surface area due to the porosity does not significantly increase the maximum apparent current densities for ethylene glycol electro-oxidation.

From Table 6.3 it is evident that stirring also does not have a great effect on the current densities obtained with this electrode.

The anodic treatment at $1.2V_{SSC}$ after the 10^{th} cycle once again reactivates the platinum region of the alloy electrode, but deactivates the gold region (Fig. 6.6).

6.3.3.4. The 60Au-40Pt alloy in the 800°C heat treatment condition

The microstructure of this alloy (two-phased, porous) can be seen in Figure 3.12. The sample was in the 1200°C-24h (single-phased, porous) heat treatment condition prior to the heat treatment at 800°C for 50 hours. Cyclic voltammograms for the 800°C treated electrode in 0.5 M NaOH without ethylene glycol are shown in Figure 5.11.

The cyclic voltammograms (1^{st} and 10^{th} cycles) with 0.1 M ethylene glycol in the solution are shown in Figure 6.7. The solution was not stirred in Figure 6.7(a) and stirred in Figure 6.7(b).

The first cycles after anodic reactivation of this electrode are also shown in Figures 6.7(a) and (b).

The peak current densities during the positive scan for this 60Au-40Pt electrode, pure gold and pure platinum are compared in Table 6.4.

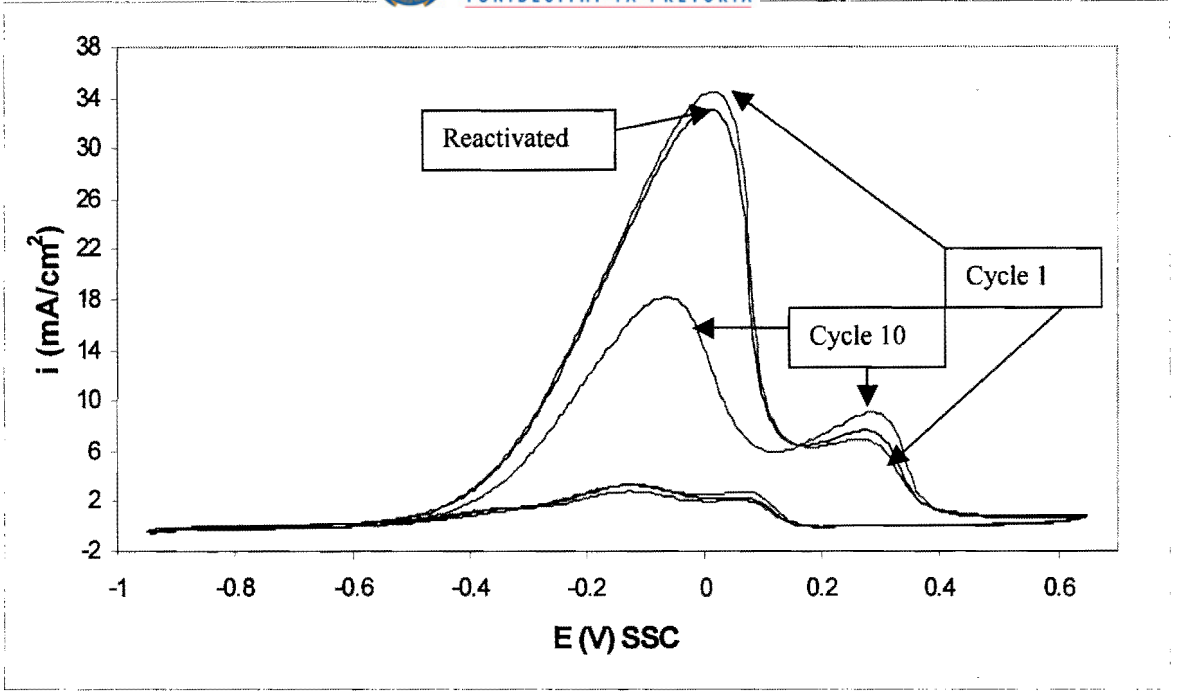

(a)

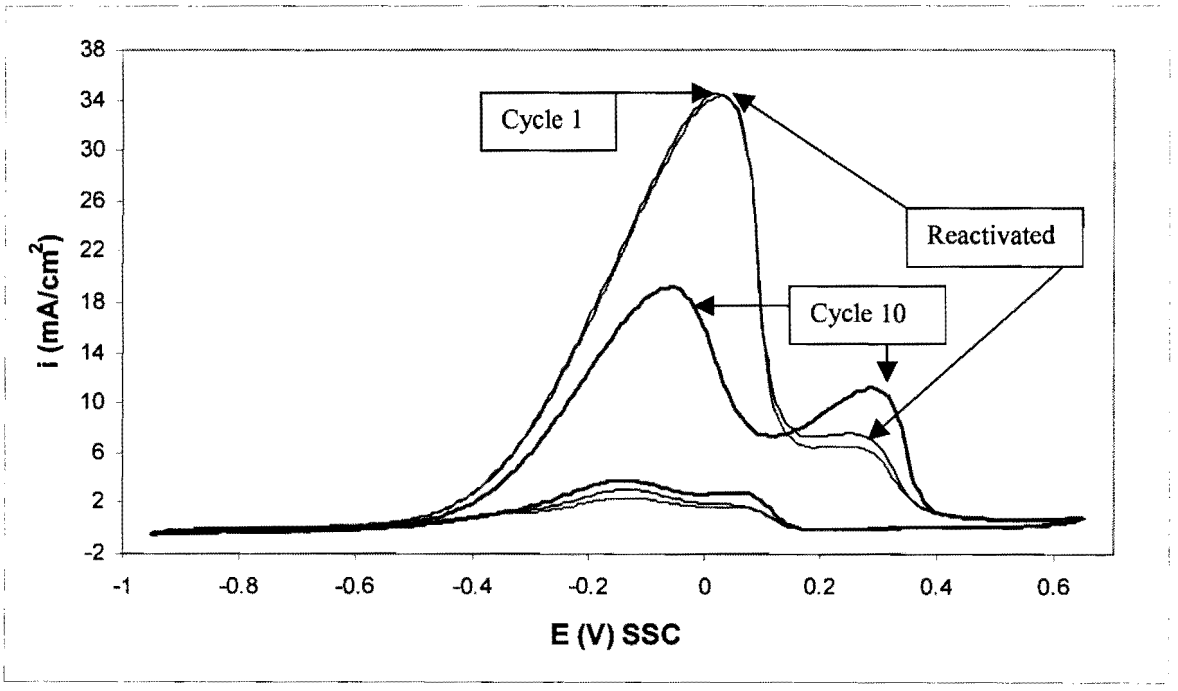

(b)

Figure 6.7. Cyclic voltammograms for the electro-oxidation of 0.1 M ethylene glycol in 0.5 M NaOH at the 800°C (60Au-40Pt) electrode (50mV/s, 25°C). (a) Solution not stirred; (b) Solution stirred.

Table 6.4. Peak current densities (in mA/cm^2) during the positive scans for Au, Pt and the 800°C electrode

Scan no.	Stirred?	Pt	800°C (Pt region)	Au	800°C (Au region)
1	No	13.5	34	16	7
1	Yes	8	34	10.5	6
10	No	11	18	13.5	9
10	Yes	6.5	19	9.5	11

Comparing Tables 6.2 and 6.4, it is seen that the solid solution electrode produces higher apparent current densities than the two-phased 800°C heat treated electrode (especially the Pt-regions, 1st scans). It therefore seems as if a solid solution is more effective for the electro-oxidation than a two-phased microstructure. This can perhaps be explained by the "third-body effect" (see section 2.6.5.3.). The formation of poisonous species adsorbed on more than one surface site is suppressed. A platinum atom cannot be "poisoned" by a strongly bound intermediate when it is surrounded by gold atoms. Adsorption sites that are only available on larger platinum clusters are needed (Rach and Heitbaum, 1987). Fewer platinum atoms are surrounded by gold atoms in the two-phased electrode (the equilibrium gold content of the platinum-rich areas of the 800°C treated alloy is shown in Table 3.1) than with the solid solution electrode. The two-phased electrode is therefore more likely to be poisoned and the current densities are lower.

From Table 6.4 it is evident again that stirring does not have a great effect on the current densities obtained with this porous electrode.

The anodic treatment at 1.2 V_{SSC} after the 10th cycle once again reactivates the platinum region of the alloy electrode, but deactivates the gold region (Fig. 6.7).

6.3.3.5. The 60Au-40Pt alloy in the 600°C heat treatment condition

The microstructure of this alloy (two-phased, porous) can be seen in Figure 3.15. The sample was in the 1200°C-24h (single-phased, porous) heat treatment condition prior to the heat treatment at 600°C for 100 hours. Cyclic voltammograms for the 600°C treated electrode in 0.5 M NaOH without ethylene glycol are shown in Figure 5.12.

The cyclic voltammograms (1^{st} and 10^{th} cycles) with 0.1 M ethylene glycol in the solution are shown in Figure 6.8. The solution was not stirred in Figure 6.8(a) and stirred in Figure 6.8(b). The first cycles after anodic reactivation of this electrode are also shown in Figures 6.8(a) and (b).

The peak current densities during the positive scan for this 60Au-40Pt electrode, pure gold and pure platinum are compared in Table 6.5.

Table 6.5. Peak current densities (in mA/cm^2)during the positive scans for Au, Pt and the 600°C electrode

Scan no.	Stirred?	Pt	600°C (Pt region)	Au	600°C (Au region)
1	No	13.5	28	16	5
1	Yes	8	25	10.5	4
10	No	11	17	13.5	7
10	Yes	6.5	16	9.5	7

Comparing Tables 6.4 and 6.5, it is seen that the 800°C electrode produces slightly higher apparent current densities than the 600°C heat treated electrode. The higher equilibrium gold content of the platinum-rich areas of the 800°C treated sample compared to the 600°C treated sample (Table 3.1) is probably responsible for this result.

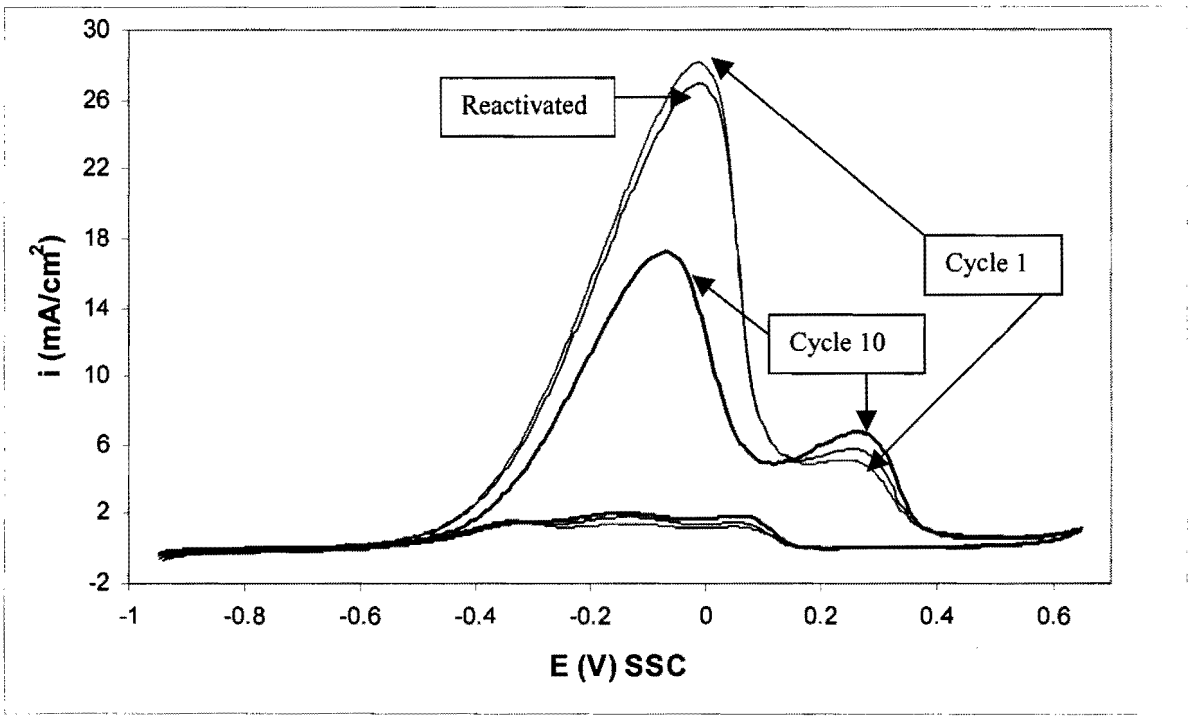

(a)

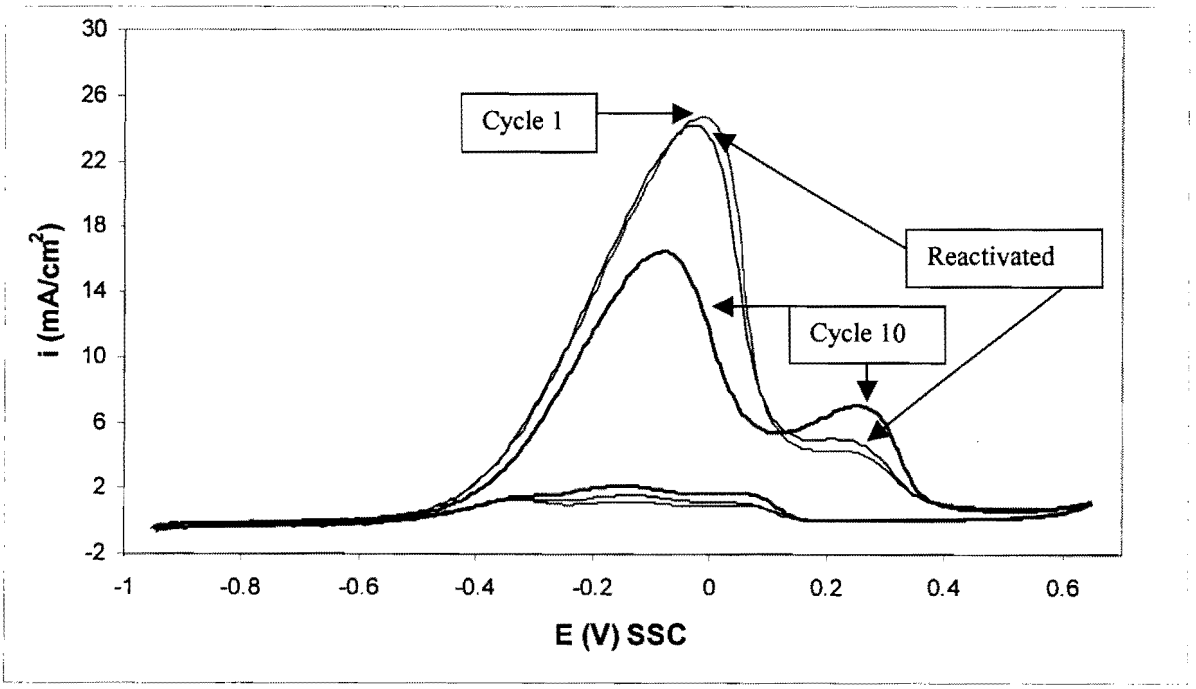

(b)

Figure 6.8. Cyclic voltammograms for the electro-oxidation of 0.1 M ethylene glycol in 0.5 M NaOH at the 600°C (60Au-40Pt) electrode (50mV/s, 25°C). (a) Solution not stirred; (b) Solution stirred.

From Table 6.5 it is evident again that stirring does not have a great effect on the current densities obtained with porous electrodes.

As before, the anodic treatment at 1.2 V_{SSC} after the 10th cycle reactivates the platinum region of the alloy electrode, but deactivates the gold region (Fig. 6.7).

6.3.4. The 50Au-50Pt alloy

6.3.4.1. The 50Au-50Pt alloy in the "ductile" heat treatment condition

The microstructure of this sample (two-phased, fine microstructure, not porous) can be seen in Figure 3.17. Cyclic voltammograms for the "ductile" electrode in 0.5 M NaOH without ethylene glycol are shown in Figure 5.14.
The cyclic Figure 6.9. The solution was not stirred in Figure 6.9(a) and stirred in Figure 6.9(b). The first cycles voltammograms (1st and 10th cycles) with 0.1 M ethylene glycol in the solution are shown in after anodic reactivation of this electrode are also shown in Figures 6.9(a) and (b).
The peak current densities during the positive scan for this 50Au-50Pt electrode, pure gold and pure platinum are compared in Table 6.6.

Table 6.6. Peak current densities (in mA/cm^2) during the positive scans for Au, Pt and the "ductile" 50Au-50Pt electrode

Scan no.	Stirred?	Pt	Ductile (Pt region)	Au	Ductile (Au region)
1	No	13.5	38	16	3
1	Yes	8	27	10.5	3
10	No	11	20	13.5	6
10	Yes	6.5	8	9.5	6

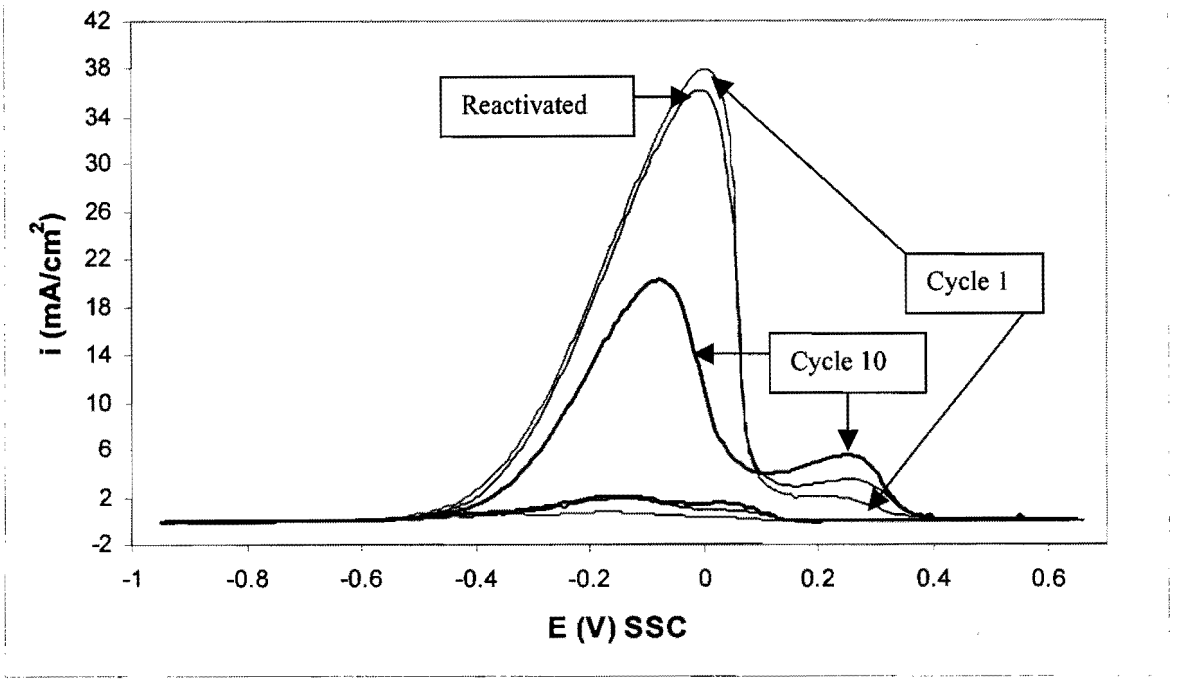

(a)

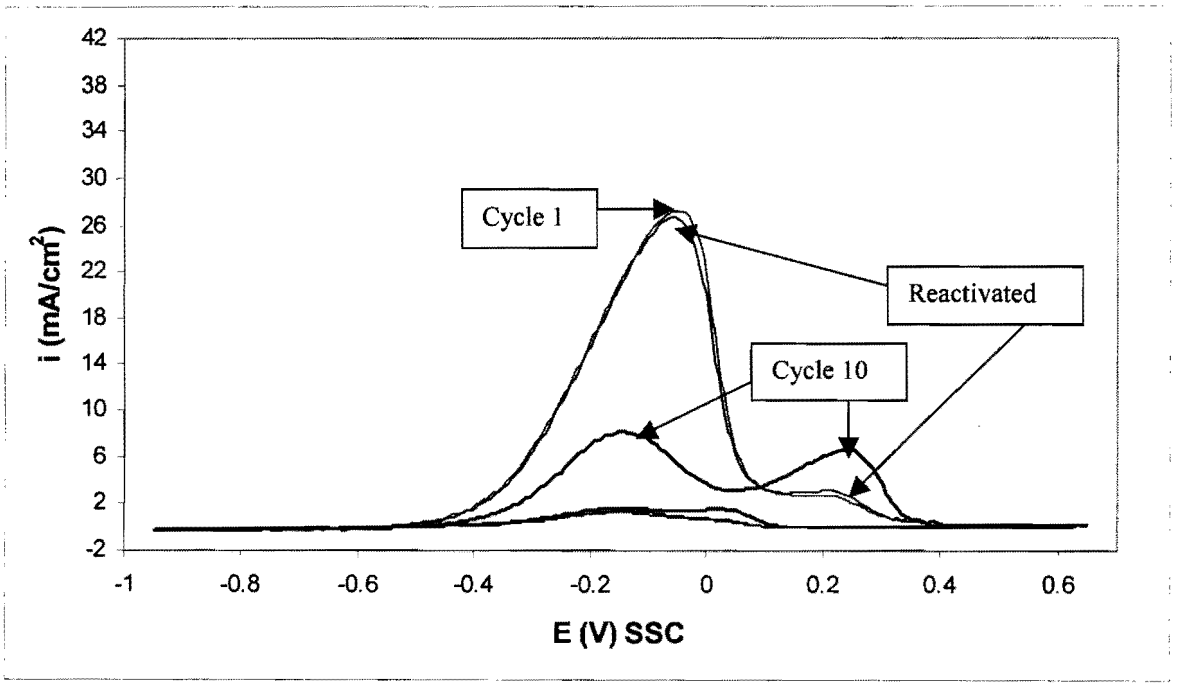

(b)

Figure 6.9. Cyclic voltammograms for the electro-oxidation of 0.1 M ethylene glycol in 0.5 M NaOH at the "ductile" (50Au-50Pt) electrode (50mV/s, 25°C). (a) Solution not stirred; (b) Solution stirred.

Comparing Tables 6.1 and 6.6, it is seen that the two-phased, non-porous 60Au-40Pt electrode and the two-phased, non-porous 50Au-50Pt electrode produce similar apparent current densities, despite differences in the compositions of the phases for the two electrodes (Figures 3.1 and 3.16). Solution stirring in both cases reduces the current densities significantly. This confirms that the non-porous electrodes are negatively affected by stirring.

The anodic treatment at 1.2 V_{SSC} after the 10^{th} cycle once again reactivates the platinum region of the alloy electrode, but deactivates the gold region (Fig. 6.9).

6.3.4.2. The 50Au-50Pt alloy in the solid solution heat treatment condition

The microstructure of this sample (single-phased, not porous) can be seen in Figure 3.19. The sample was in the "ductile" heat treatment condition prior to solutionising at 1250°C for 24 hours. Cyclic voltammograms for the solid solution electrode in 0.5 M NaOH without ethylene glycol are shown in Figure 5.15.

The cyclic voltammograms (1^{st} and 10^{th} cycles) with 0.1 M ethylene glycol in the solution are shown in Figure 6.10. The solution was not stirred in Figure 6.10(a) and stirred in Figure 6.10(b). The first cycles after anodic reactivation of this electrode are also shown in Figures 6.10(a) and (b). The peak current densities during the positive scan for this 50Au-50Pt electrode, pure gold and pure platinum are compared in Table 6.7.

Table 6.7. Peak current densities (in mA/cm^2) during the positive scans for Au, Pt and the solid solution 50Au-50Pt electrode

Scan no.	Stirred?	Pt	Solid solution (Pt region)	Au	Solid solution (Au region)
1	No	13.5	45	16	3
1	Yes	8	38	10.5	2
10	No	11	24	13.5	11
10	Yes	6.5	13	9.5	9

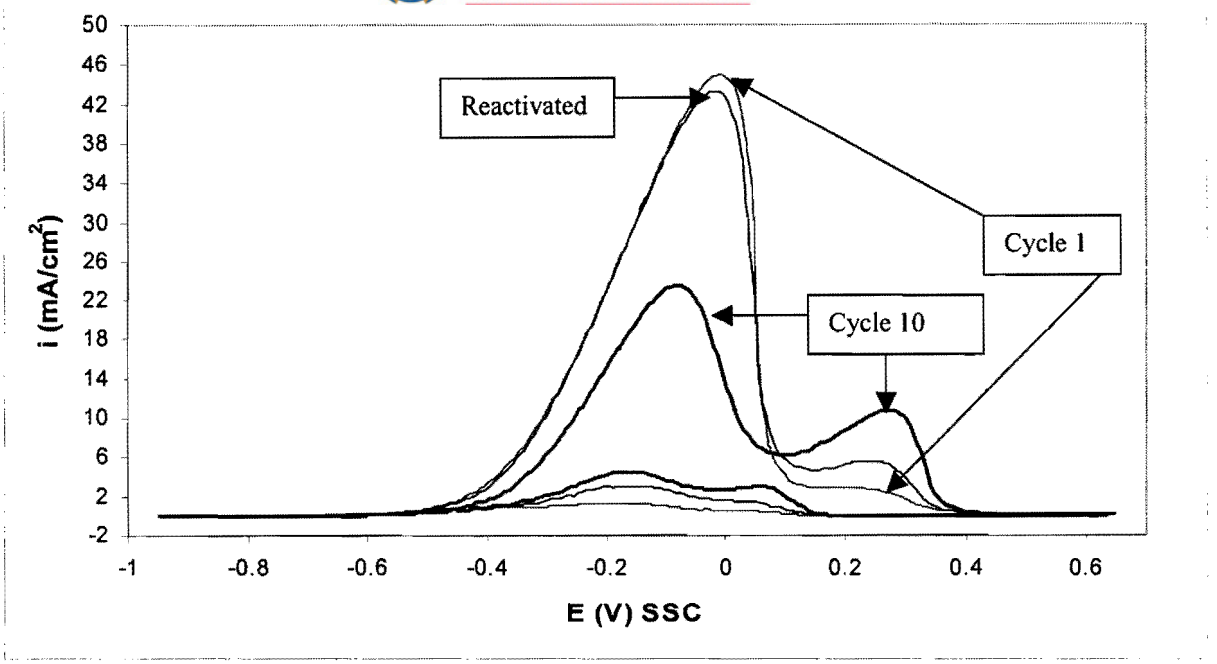

(a)

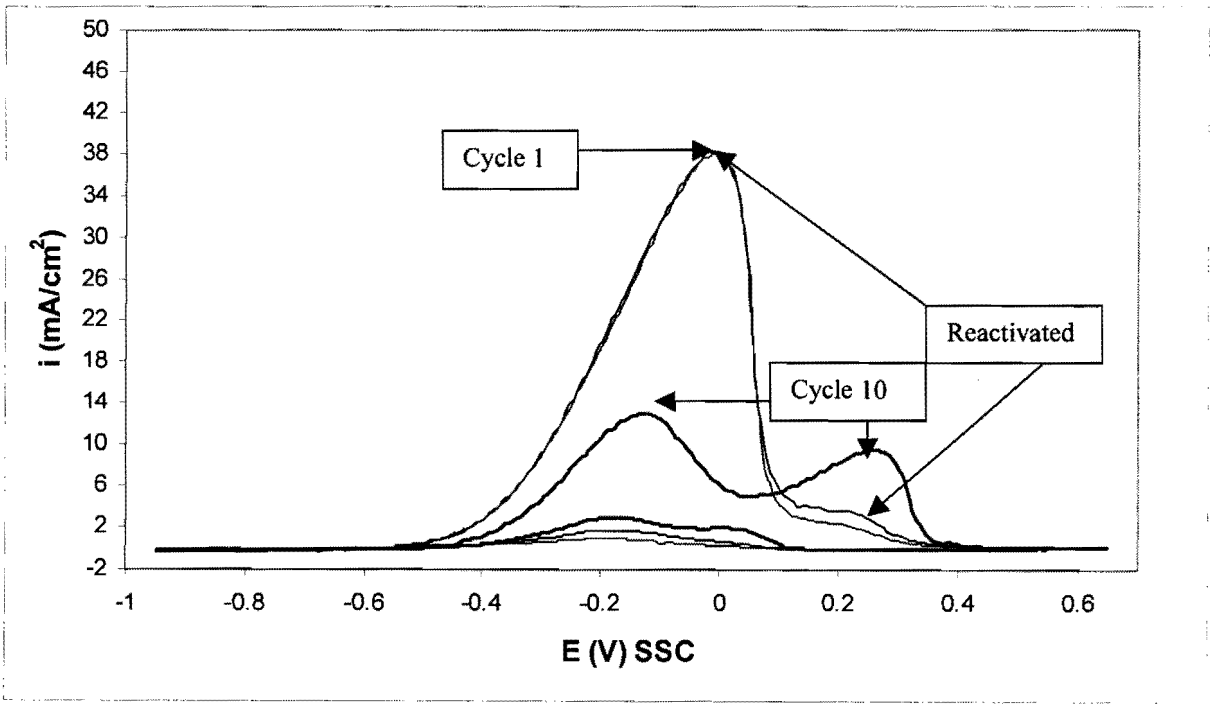

(b)

Figure 6.10. Cyclic voltammograms for the electro-oxidation of 0.1 M ethylene glycol in 0.5 M NaOH at the solid solution (50Au-50Pt) electrode (50mV/s, 25°C). (a) Solution not stirred; (b) Solution stirred.

Comparing Tables 6.6 and 6.7, it is seen that the solid solution 50Au-50Pt electrode produces higher apparent current densities than the "ductile" (two-phased) 50Au-50Pt electrode. These two electrodes are both not porous. The difference in current densities can therefore only be due to the difference in phase compositions.

If one compares the 60Au-40Pt solid solution electrode (porous, Table 6.2) with the 50Au-50Pt solid solution electrode (not porous, Table 6.7), it is seen that the apparent current densities of the two electrodes are similar when the solution is not stirred. Solution stirring with the non-porous electrode reduces the current densities. The advantage of the porosity is therefore not to increase the maximum peak current densities, but rather to maintain a higher current density when the solution is stirred. The solution inside the pores is probably not affected much by stirring. The intermediates that are formed inside the pores during the electro-oxidation of ethylene glycol are therefore not transported away from the electrode as with the non-porous electrodes when the solution is stirred. The intermediates are oxidised further inside the pores, resulting in higher current densities.

The anodic treatment at 1.2 V_{SSC} after the 10^{th} cycle once again reactivates the platinum region of the alloy electrode, but deactivates the gold region (Fig. 6.10).

6.3.5. The Gold 990 alloy

6.3.5.1. The Gold 990 alloy in the solid solution condition

This sample has 1 wt% (4 at%) titanium in solid solution with the gold. The Vickers hardness of the sample in this condition is HV_5 = 50 kg/mm^2. Cyclic voltammograms for this sample in 0.5 M NaOH without ethylene glycol are shown in Figure 5.18.
The cyclic voltammograms (1^{st} and 10^{th} cycles) with 0.1 M ethylene glycol in the solution are shown in Figure 6.11. The solution was not stirred in Figure 6.11(a) and stirred in Figure 6.11(b). The first cycles after anodic reactivation of this electrode are also shown in Figures 6.11(a) and (b).

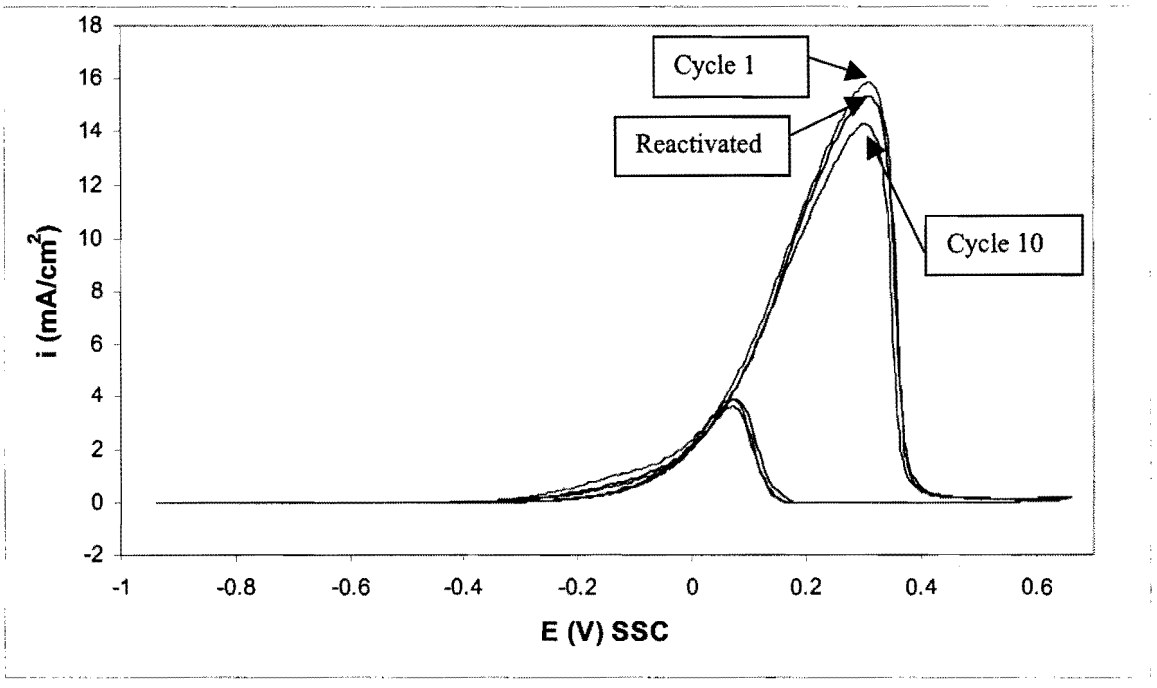

(a)

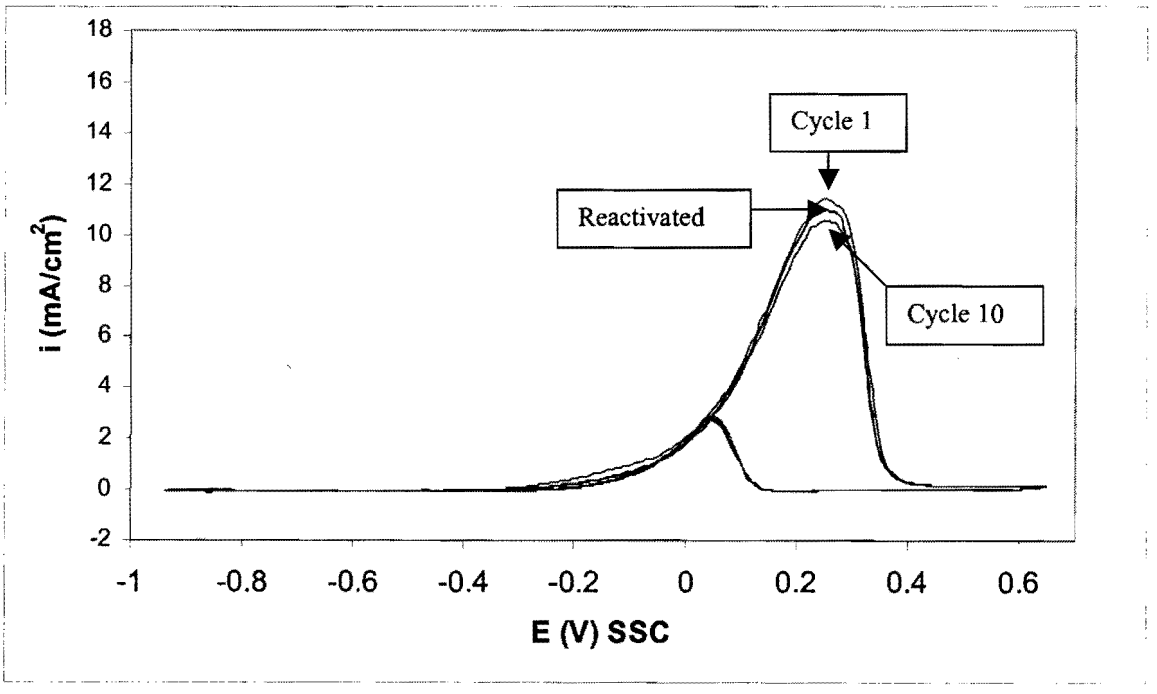

(b)

Figure 6.11. Cyclic voltammograms for the electro-oxidation of 0.1 M ethylene glycol in 0.5 M NaOH at the solid solution Gold 990 electrode (50mV/s, 25°C). (a) Solution not stirred; (b) Solution stirred.

The peak current densities during the positive scan for this Gold 990 electrode and pure gold are compared in Table 6.8.

Table 6.8. Peak current densities (in mA/cm^2) during the positive scans for Au and the solid solution Gold 990 electrode

Scan no.	Stirred?	Au	Solid solution (Gold 990)
1	No	16	16
1	Yes	10.5	11
10	No	13.5	14
10	Yes	9.5	10.5

The behaviour of Gold 990 in the solid solution condition is similar to pure gold (Table 6.8).

The anodic treatment at 1.2 V_{SSC} after the 10th cycle reactivates the electrode (Fig. 6.11).

6.3.5.2. The Gold 990 alloy in the precipitation-hardened condition

This sample is hardened by the presence of small Au_4Ti precipitates. The Vickers hardness of the sample in this condition is HV_5 = 150 kg/mm^2. Cyclic voltammograms for this sample in 0.5 M NaOH without ethylene glycol are shown in Figure 5.19.

The cyclic voltammograms (1st and 10th cycles) with 0.1 M ethylene glycol in the solution are shown in Figure 6.12. The solution was not stirred in Figure 6.12(a) and stirred in Figure 6.12(b). The first cycles after anodic reactivation of this electrode are also shown in Figures 6.12(a) and (b).

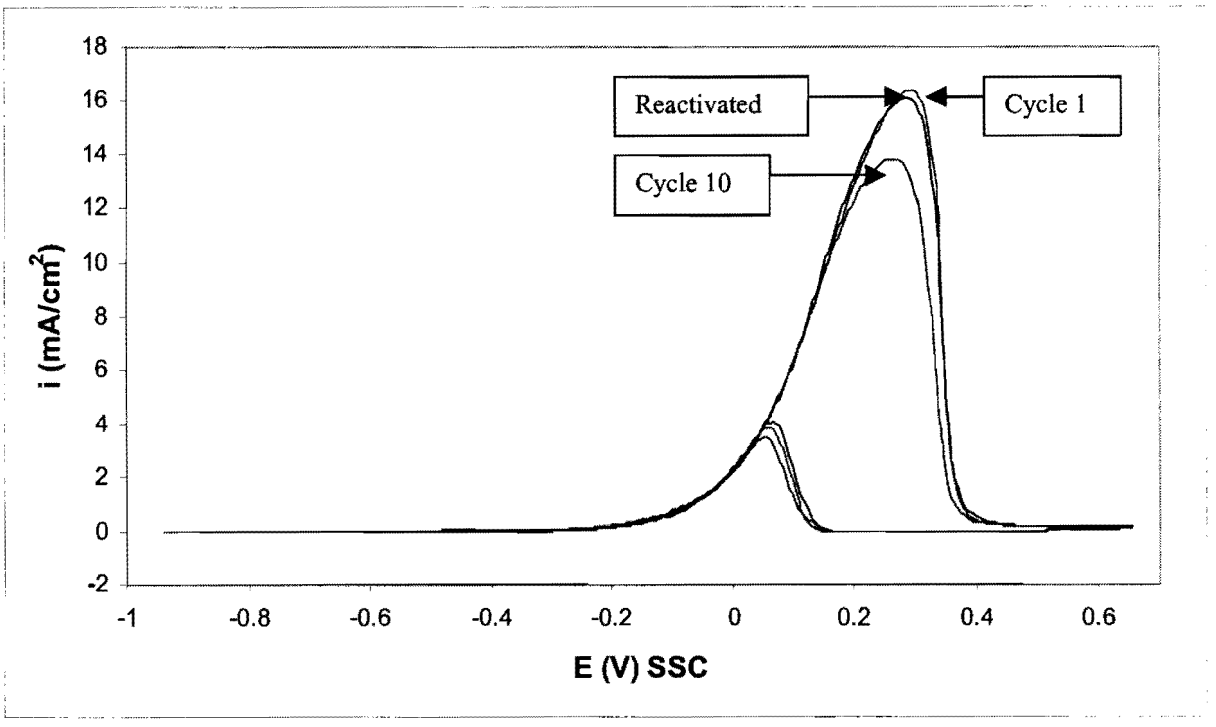

(a)

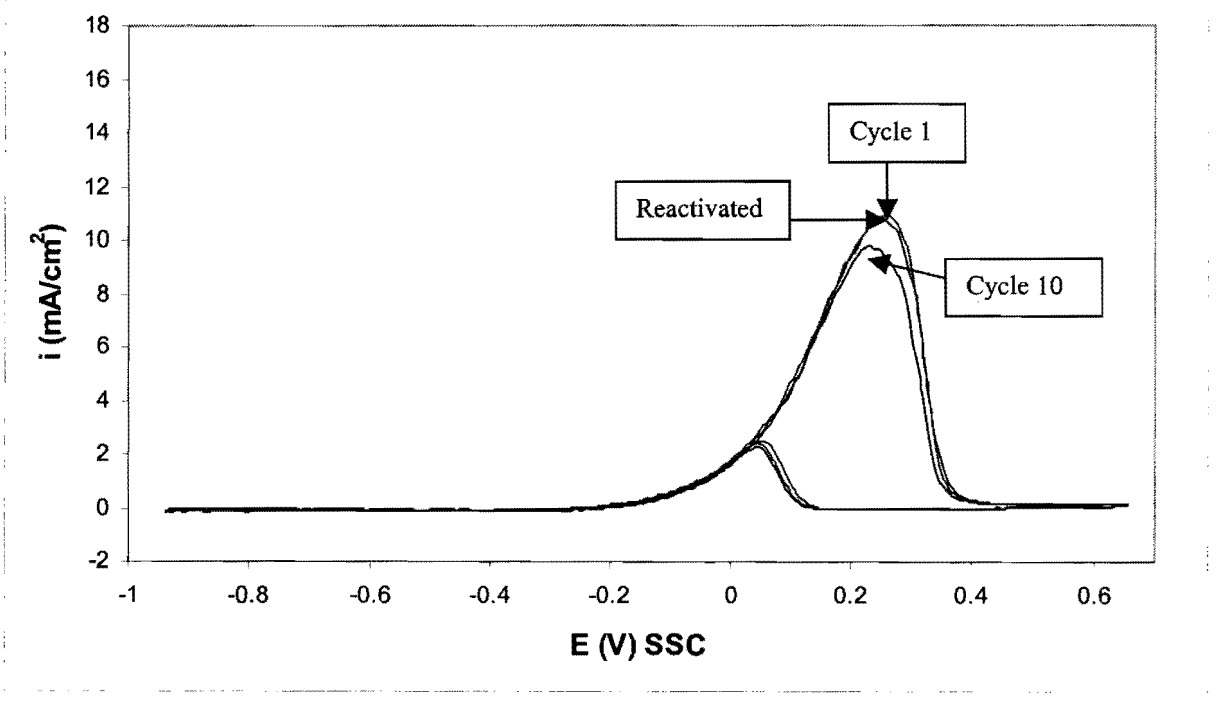

(b)

Figure 6.12. Cyclic voltammograms for the electro-oxidation of 0.1 M ethylene glycol in 0.5 M NaOH at the precipitation-hardened Gold 990 electrode (50mV/s, 25°C). (a) Solution not stirred; (b) Solution stirred.

The peak current densities during the positive scan for this Gold 990 electrode and pure gold are compared in Table 6.9.

Table 6.9. Peak current densities (in mA/cm^2) during the positive scans for Au and the precipitation-hardened Gold 990 electrode

Scan no.	Stirred?	Au	Hardened (Gold 990)
1	No	16	16
1	Yes	10.5	11
10	No	13.5	14
10	Yes	9.5	10.5

The behaviour of Gold 990 in the precipitation-hardened condition is also similar to pure gold (Table 6.9). The possible reasons for the similarities between pure gold and Gold 990 have been discussed before (5.3.5.2.).

To summarise this section, the maximum peak current densities obtained at the electrodes during the first scan (Fig. 6.13(a)) and the tenth scan (Fig. 6.13(b)) are shown together for better comparison. Table 6.10 describes the electrodes in Figure 6.13.

Table 6.10. Description of the electrodes in Figure 6.13.

Code	Composition	Phase composition	Heat treatment
Au	Pure gold	-	-
Au990soln	Au - 1wt% Ti	Single	Solution treated
Au990ppt	Au – 1wt% Ti	Dual (contains Au_4Ti)	Precipitation hardened
Pt	Pure platinum	-	-
1200short	60Au-40Pt	Single-phase, porous	1200°C, 24 h
1200long	60Au-40Pt	Single-phase, porous	1200°C, 168 h
50-50-soln	50Au-50Pt	Single-phase, non-porous	1250°C
1300	60Au-40Pt	Dual phase, non-porous	1300°C
800	60Au-40Pt	Dual-phase, porous	800°C
600	60Au-40Pt	Dual-phase, porous	600°C
50-50-dual	50Au-50Pt	Dual-phase, non-porous	"Ductile"-treatment

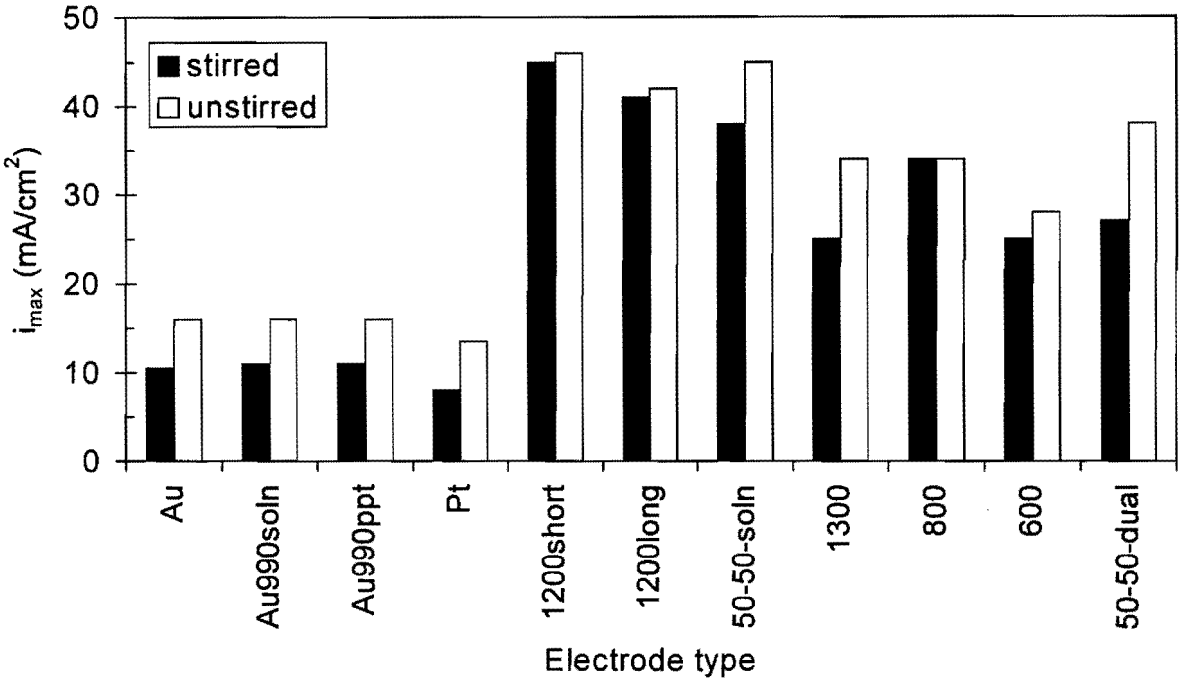

(a)

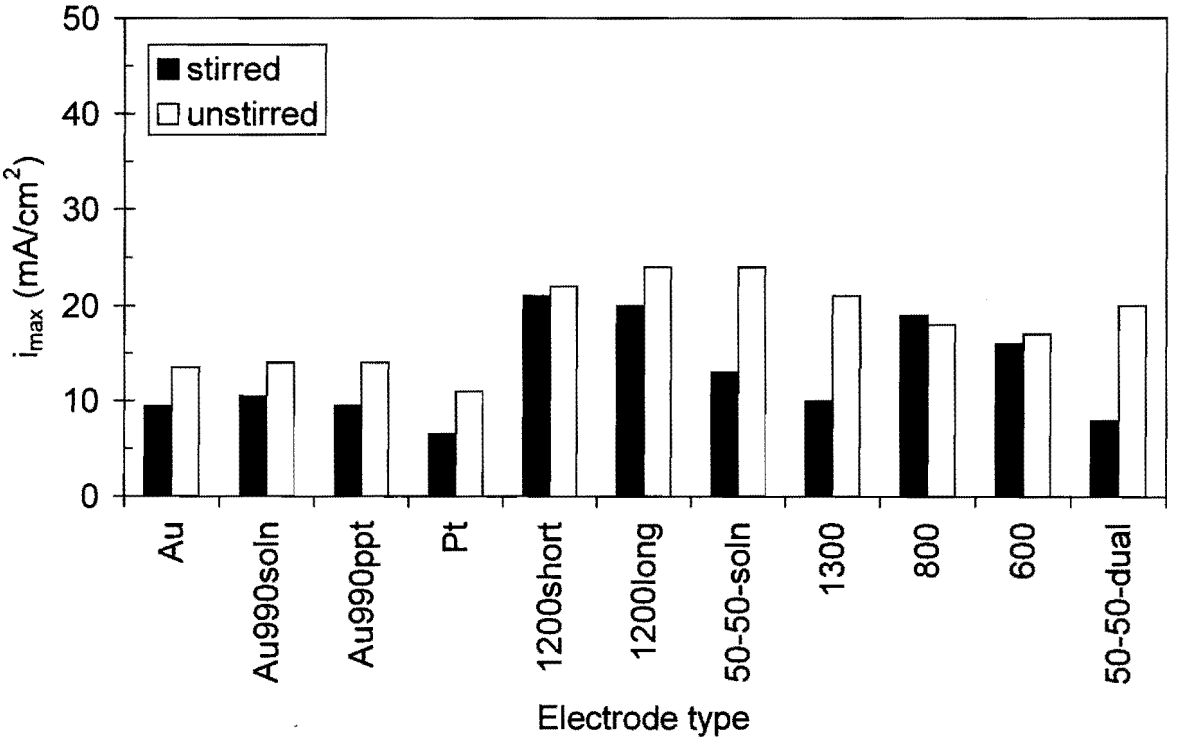

(b)

Figure 6.13. The maximum peak current densities obtained at the different electrodes. (a) the first scan, (b) the tenth scan.

6.3.6. Electrolysis of ethylene glycol at a fixed potential

It is known that it is not possible to sustain long electrolysis of ethylene glycol at a fixed potential because of poisoning phenomena that occur at the electrode surface (Kadirgan et al., 1990).

Poisoning of selected electrodes during the electrolysis of ethylene glycol at a fixed potential was studied. The following procedure was used:

- The 0.5 M NaOH solution (without ethylene glycol) was purged with nitrogen for 30 minutes to remove dissolved oxygen.
- The electrode potential was cycled for fifteen cycles between the values for onset of O_2 and H_2 evolution until the I-E curves were reproducible.
- The ethylene glycol was added to the solution.
- The electrode was anodically activated at 1.2 V_{SSC} for 10 seconds (the solution was stirred during activation).
- The surface oxides formed during anodic activation were removed at –0.6 V_{SSC} for 10 seconds (the solution was stirred during the cathodic reduction of the surface oxides)
- The electrolysis of ethylene glycol was performed at a fixed potential (Table 6.11). The potential was selected from the cyclic voltammograms with ethylene glycol in solution. The solution was stirred in one set of experiments and not stirred in the other set of experiments. The results of all the different electrodes are presented on the same time and current density scales for better comparison.

Table 6.11. The potential of ethylene glycol electrolysis at the various electrodes

Electrode	Potential (V_{SSC})
Au	0.23
Pt	-0.20
60Au-40Pt electrodes	-0.05
50Au-50Pt electrodes	-0.05
Gold990 electrodes	0.23

6.3.6.1. Gold

The electrolysis of ethylene glycol at gold was performed at 0.23 V_{SSC} (Table 6.11) and the results are shown in Figure 6.14. The apparent current density at the start of electrolysis is 21 mA/cm^2, but drops quickly due to electrode poisoning. The maximum apparent current density obtained with the cyclic voltammogram (Fig. 6.1) is 16 mA/cm^2. This indicates that the electrode is partially poisoned during the positive scan (from –0.2 V to 0.27 V_{SSC}) and the maximum apparent current density during cyclic voltammetry is therefore lower than at the start of potentiostatic electrolysis.
Stirring of the solution results in an even faster decay of current density, perhaps because the transportation of intermediates into the solution is accelerated. These intermediates cannot be oxidised at the surface of the electrode, resulting in lower current densities.

6.3.6.2. Platinum

The electrolysis of ethylene glycol at platinum was performed at -0.20 V_{SSC} (Table 6.11) and the results are shown in Figure 6.15. The apparent current density at the start of electrolysis is 14 mA/cm^2 (slightly higher than the peak value obtained with cyclic voltammetry in Fig. 6.2), but also drops quickly due to electrode poisoning. As with gold, stirring of the solution results in an even faster decay of current density.

6.3.6.3. The 60Au-40Pt alloy in the 1300°C heat treatment condition

The electrolysis of ethylene glycol at this non-porous, two-phased electrode was performed at –0.05 V_{SSC} (Table 6.11) and the results are shown in Figure 6.16. The apparent current density at the start of electrolysis is 40 mA/cm^2, but the alloy electrode unfortunately also poisons rapidly. As was the case with the pure metals, stirring of the solution also results in a faster decay of current density.

6.3.6.4. The 60Au-40Pt alloy in the 1200°C-24h heat treatment condition

The electrolysis of ethylene glycol at this porous, single-phased electrode was performed at –0.05 V_{SSC} (Table 6.11) and the results are shown in Figure 6.17. The apparent current density at the start of electrolysis at this electrode is a high 60 mA/cm^2. From Table 6.2 it is seen that stirring did not influence the current density much with the porous electrode. The results from Figure 6.17 show that stirring does produce lower current densities, but the effect is much smaller than with non-porous electrodes (Fig. 6.16).

6.3.6.5. The 50Au-50Pt alloy in the "ductile" heat treatment condition

The electrolysis of ethylene glycol at this non-porous, two-phased electrode was performed at –0.05 V_{SSC} (Table 6.11) and the results are shown in Figure 6.18. The apparent current density at the start of electrolysis at this electrode is 40 mA/cm^2. The electrolysis results from this sample are similar to that of the 1300°C heat treated 60Au-40Pt sample (Fig. 6.16, also compare Tables 6.1 and 6.6)

6.3.6.6. The 50Au-50Pt alloy in the solid solution heat treatment condition

The electrolysis of ethylene glycol at this non-porous, single-phased electrode was performed at –0.05 V_{SSC} (Table 6.11) and the results are shown in Figure 6.19. The apparent current density at the start of electrolysis at this electrode is a high 52 mA/cm^2. Higher apparent current densities are obtained with this single-phased 50Au-50Pt electrode than with the two-phased 50Au-50Pt electrode (Fig. 6.18). This confirms the cyclic voltammetry results (Tables 6.6 and 6.7).

6.3.6.7. The Gold 990 alloy in the solid solution heat treatment condition

The electrolysis of ethylene glycol at this electrode was performed at 0.23 V_{SSC} (Table 6.11) and the results are shown in Figure 6.20. The apparent current density at the start of

electrolysis at this electrode is 20.5 mA/cm^2. Once again, the results obtained with this Gold 990 electrode are similar to that of pure gold (Fig. 6.14, Table 6.8).

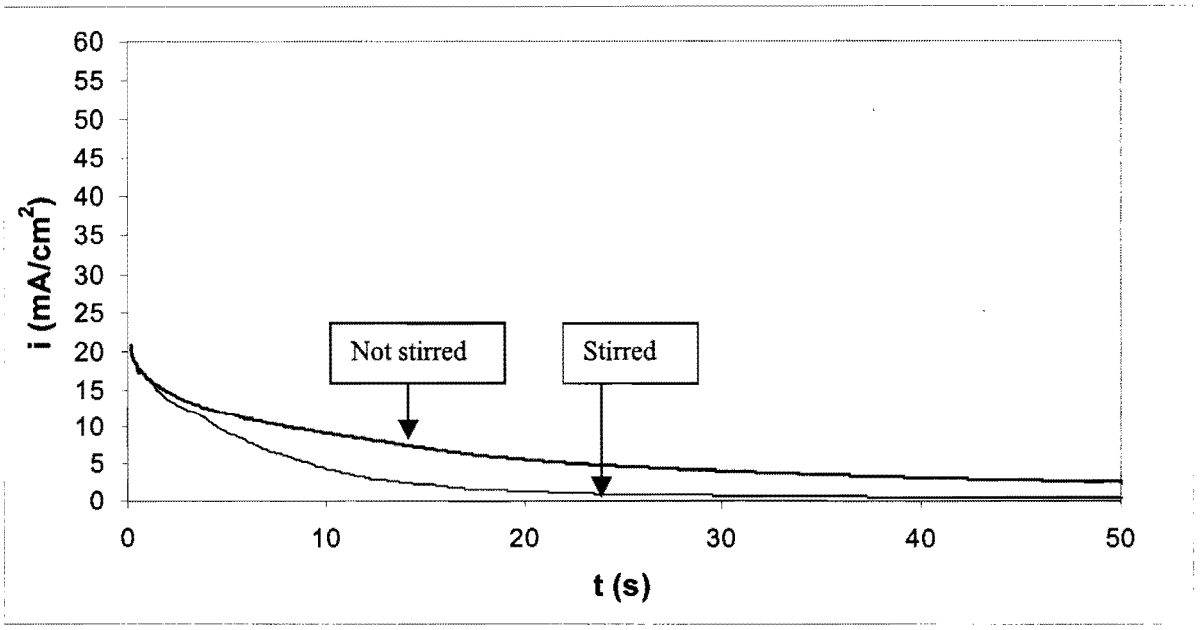

Figure 6.14. Electrolysis of ethylene glycol at gold at a fixed potential of 0.23 V_{SSC}.

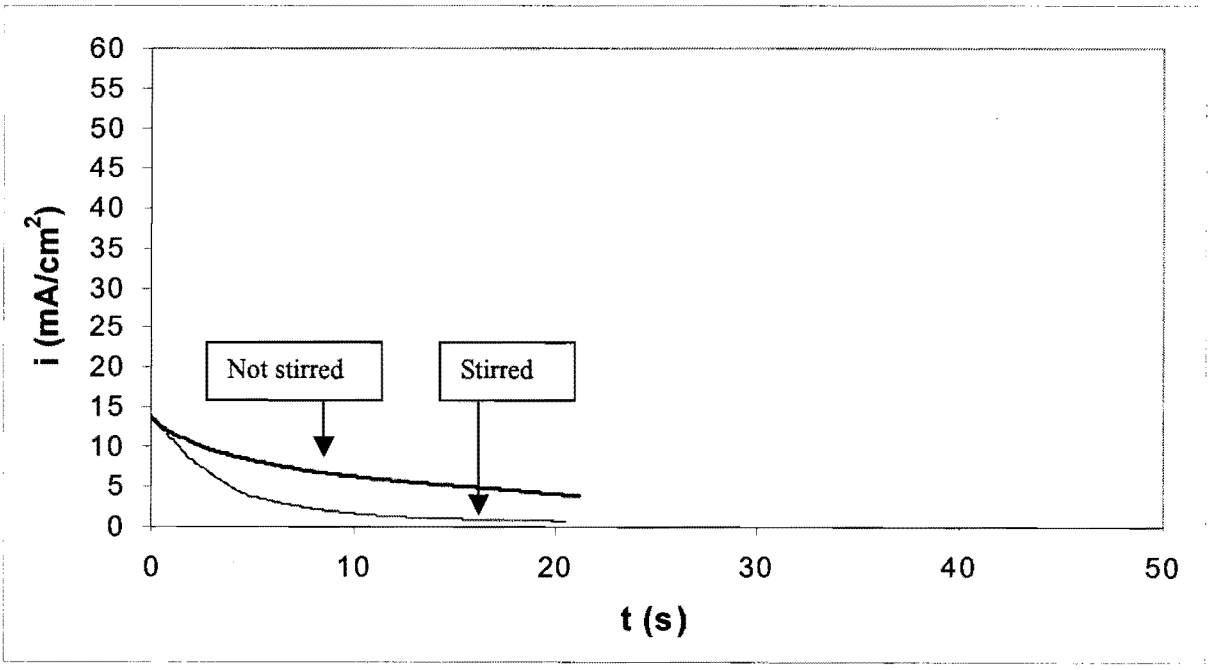

Figure 6.15. Electrolysis of ethylene glycol at platinum at a fixed potential of -0.20 V_{SSC}.

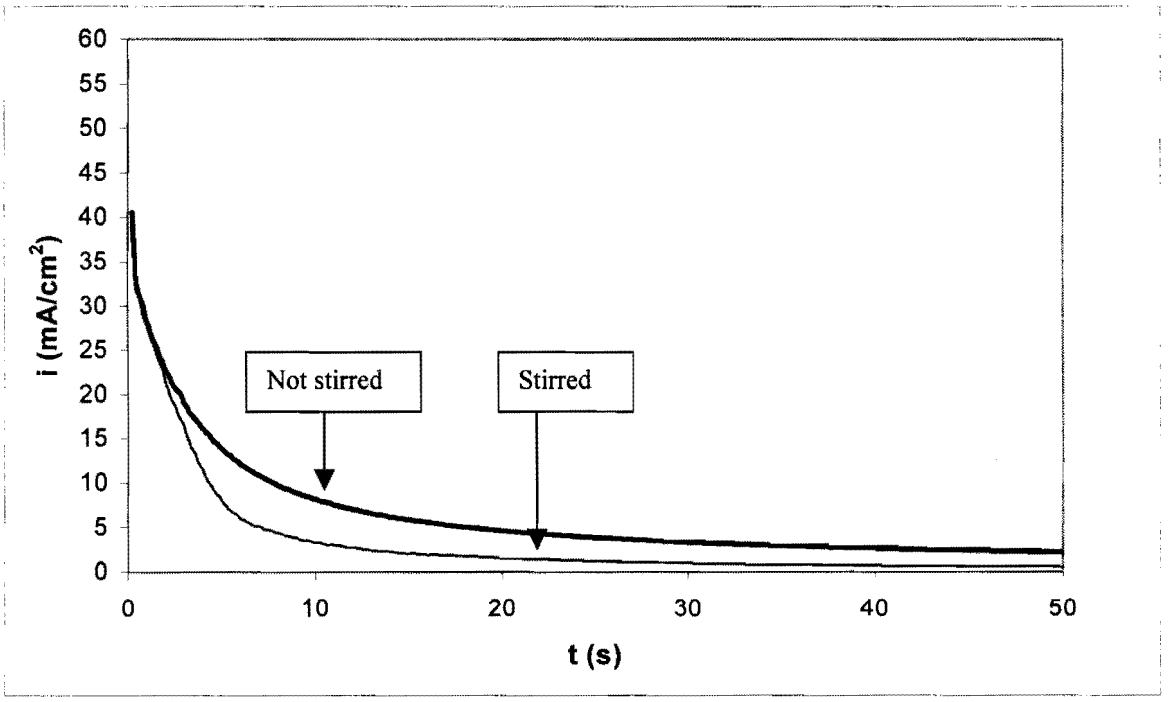

Figure 6.16. Electrolysis of ethylene glycol at the 1300°C (60Au-40Pt) electrode at a fixed potential of -0.05 V_{SSC}.

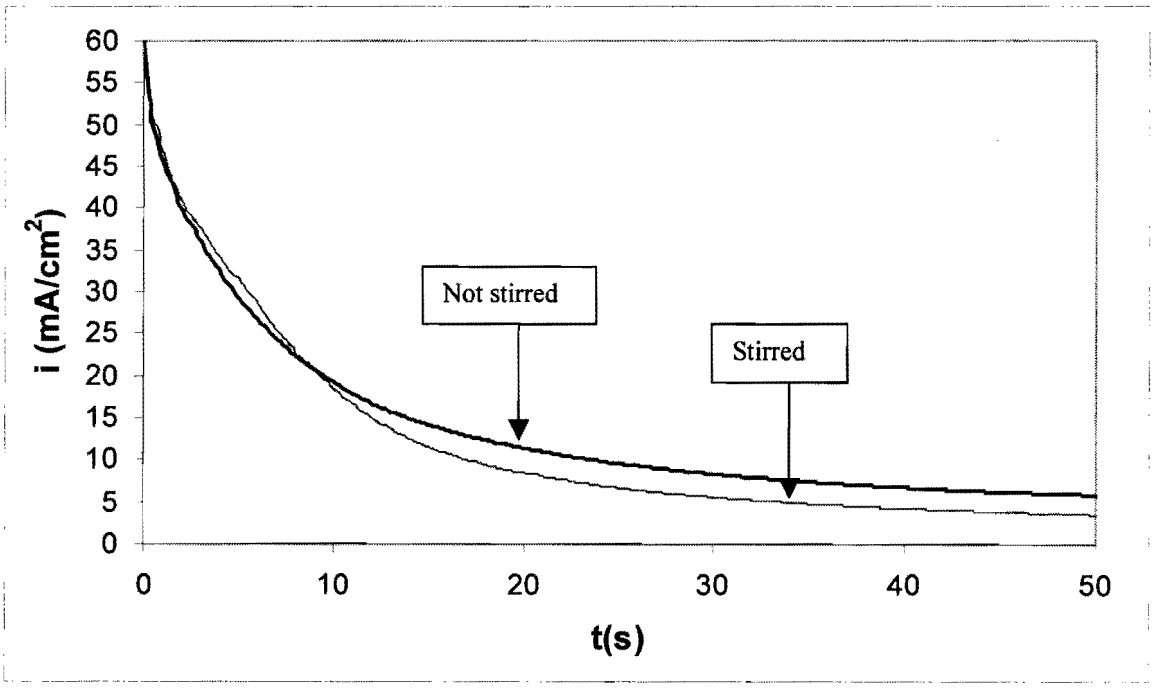

Figure 6.17. Electrolysis of ethylene glycol at the 1200°C-24h (60Au-40Pt) electrode at a fixed potential of -0.05 V_{SSC}.

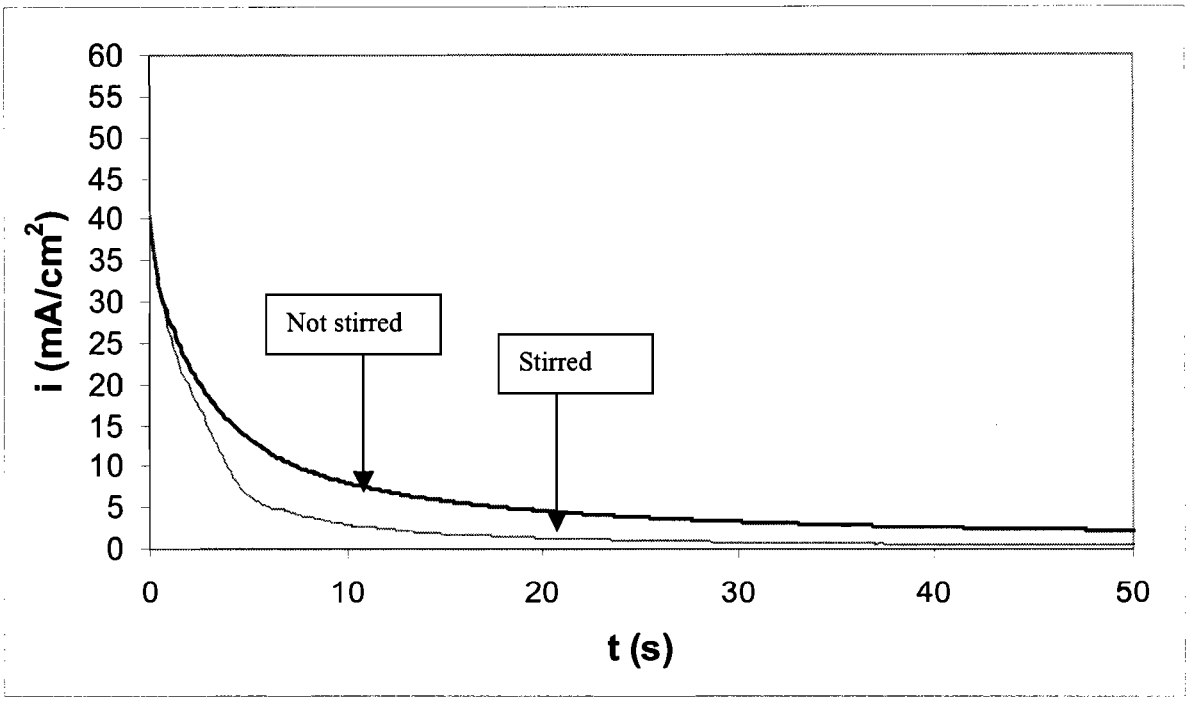

Figure 6.18. Electrolysis of ethylene glycol at the "ductile" (50Au-50Pt) electrode at a fixed potential of -0.05 V_{SSC}.

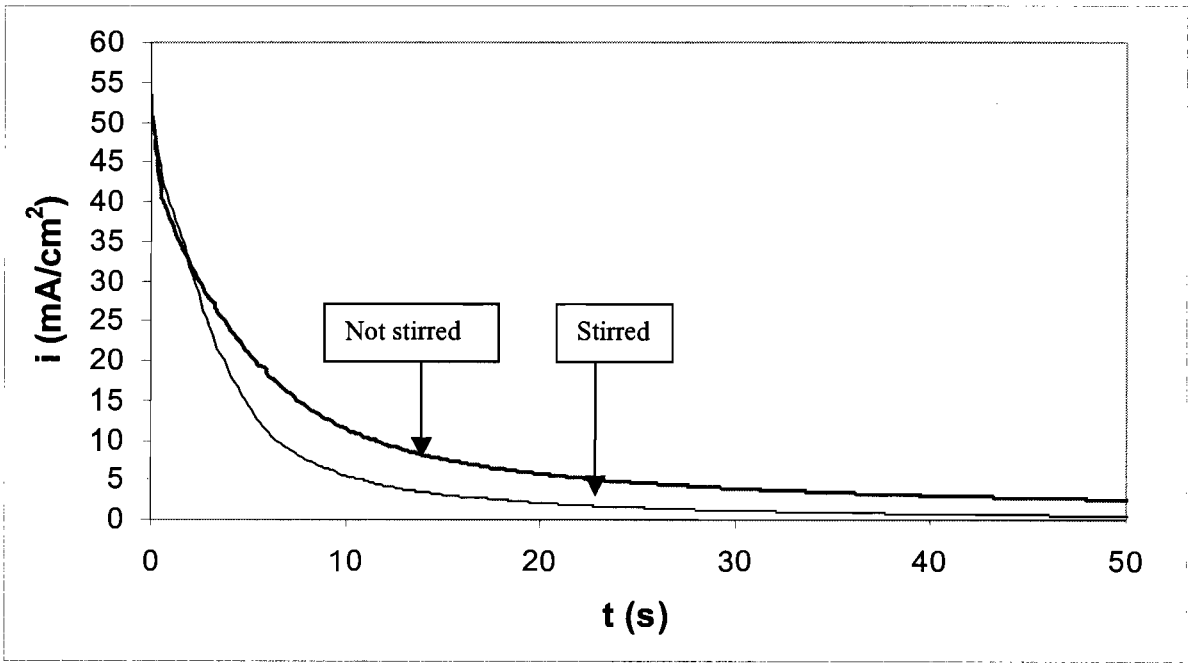

Figure 6.19. Electrolysis of ethylene glycol at the solid solution (50Au-50Pt) electrode at a fixed potential of -0.05 V_{SSC}.

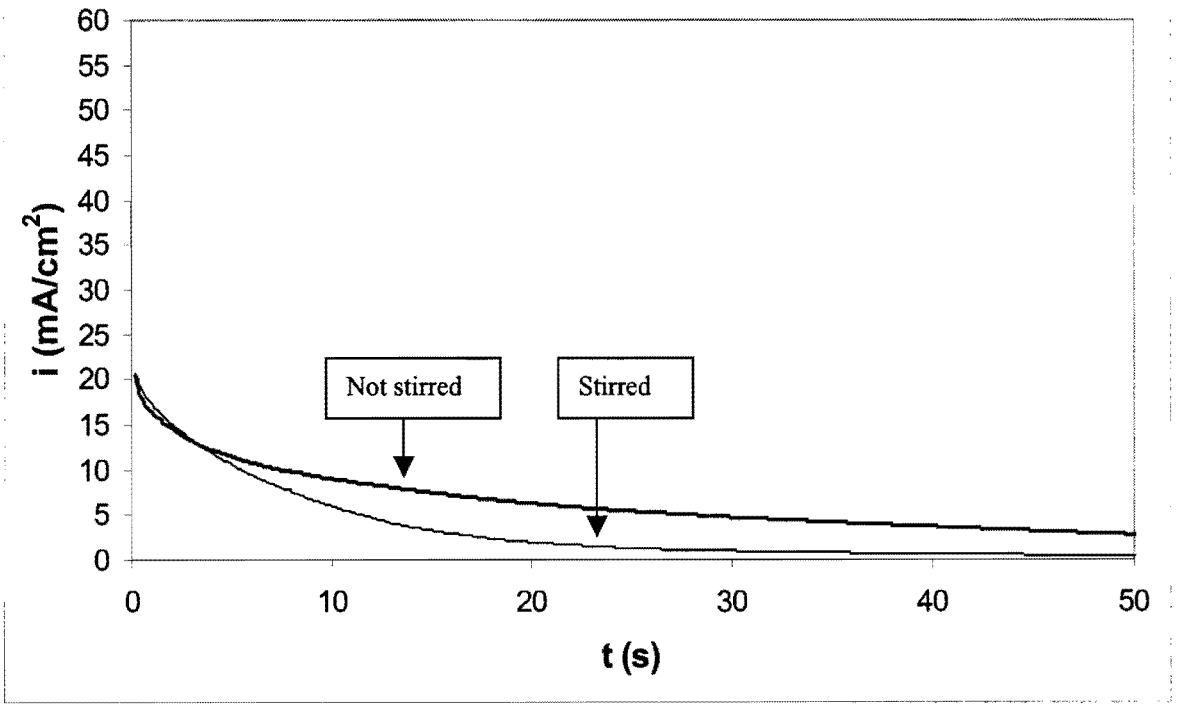

Figure 6.20. Electrolysis of ethylene glycol at the solid solution Gold 990 electrode at a fixed potential of 0.23 V_{SSC}.

The following conclusions can be made based on Figures 6.14 to 6.20:

- All the electrodes are poisoned, resulting in a decrease in the apparent current densities with time.
- Stirring of the solution causes a decrease in the apparent current densities of all the electrodes, although the effect is smaller with the porous electrode.
- The current densities obtained at time t = 0 during potentiostatic electrolysis follow the same ranking as for the maximum peak current densities during cyclic voltammetry.
- The rate at which poisoning occurs at the electrodes differs. The time necessary for a 50% decrease in the initial current densities during electrolysis are shown in Table 6.12.

Table 6.12. The time (in seconds) necessary for a 50% decrease in the initial current densities during potentiostatic electrolysis

	Solution not stirred	Solution stirred
Au	7.5	4
Pt	7.5	3
1300°C (60Au-40Pt)	3	2
1200°C-24h (60Au-40Pt)	5	5
Ductile (50Au-50Pt)	2.5	2
Solid solution (50Au-50Pt)	3.5	3
Gold 990 (Solid solution)	7	5

The gold-platinum alloys poison at a faster rate than both pure gold and pure platinum (Table 6.12). The higher apparent current densities obtained at the alloy electrodes at the start of electrolysis probably lead to the formation of more poisoning species than at both pure gold and platinum.

6.3.7. Electrolysis of ethylene glycol using potential pulsing

The results of the electrolysis of ethylene glycol at a constant potential have shown that electrode poisoning occurs rapidly and that the current densities drop to low values in a matter of seconds. A cleaning procedure has to be used for sustainable electrolysis (Kadirgan et al., 1990).

Electrolysis of ethylene glycol at selected electrodes by employing the potential pulsing technique was studied. The following procedure was used:

- The 0.5 M NaOH solution (without ethylene glycol) was purged with nitrogen for 30 minutes to remove dissolved oxygen.
- The electrode potential was cycled for fifteen cycles between the values for onset of O_2 and H_2 evolution until the I-E curves were reproducible. The cyclic

voltammogram (15^{th} cycle) of the electrode was then compared to the cyclic voltammogram found in chapter 5. This was done to make certain that the solution did not contain impurities and that the behaviour of the electrode was similar to what was found in chapter 5.

- The ethylene glycol was added to the solution.
- The potential was pulsed. The electrode was first cleaned anodically at 1.2 V_{SSC} for 1.5 seconds. The surface oxides formed during anodic activation were then removed at –0.6 V_{SSC} for 1.5 seconds. The cleaning cycle was chosen to be only 3 seconds to maximise the fraction of the total time spent at the electrolysis potential. It was expected to be long enough to remove the poisoning species. The electrolysis of ethylene glycol was performed for 10 seconds at the potentials shown in Table 6.11. The apparent current densities for ethylene glycol electro-oxidation decline to low levels after 10 seconds (Figures 6.14 to 6.20) and the electrode has to be cleaned again. The potential pulsing was performed for 100 cycles. The solution was stirred during the cleaning procedure and during electrolysis.

6.3.7.1. Gold

The electrolysis of ethylene glycol at gold was performed at 0.23 V_{SSC}. The first cycle (cleaning and electrolysis) is shown in Figure 6.21. In Figure 6.22(a), the current densities during cycles 1 – 10 are shown. Figure 6.22(b) shows the current densities for cycles 91 – 100. The current densities of the cleaning procedure have been omitted in Figure 6.22. From Figure 6.22(a) it is seen the initial current density after potential pulsing (cycle 1) was approximately 20 mA/cm^2, falling to 3.5 mA/cm^2 after 10 seconds. The time necessary for a 50% decrease of the initial current density is 3.5 seconds, which agrees well with Table 6.12 (remember that the solution was stirred during potential pulsing).

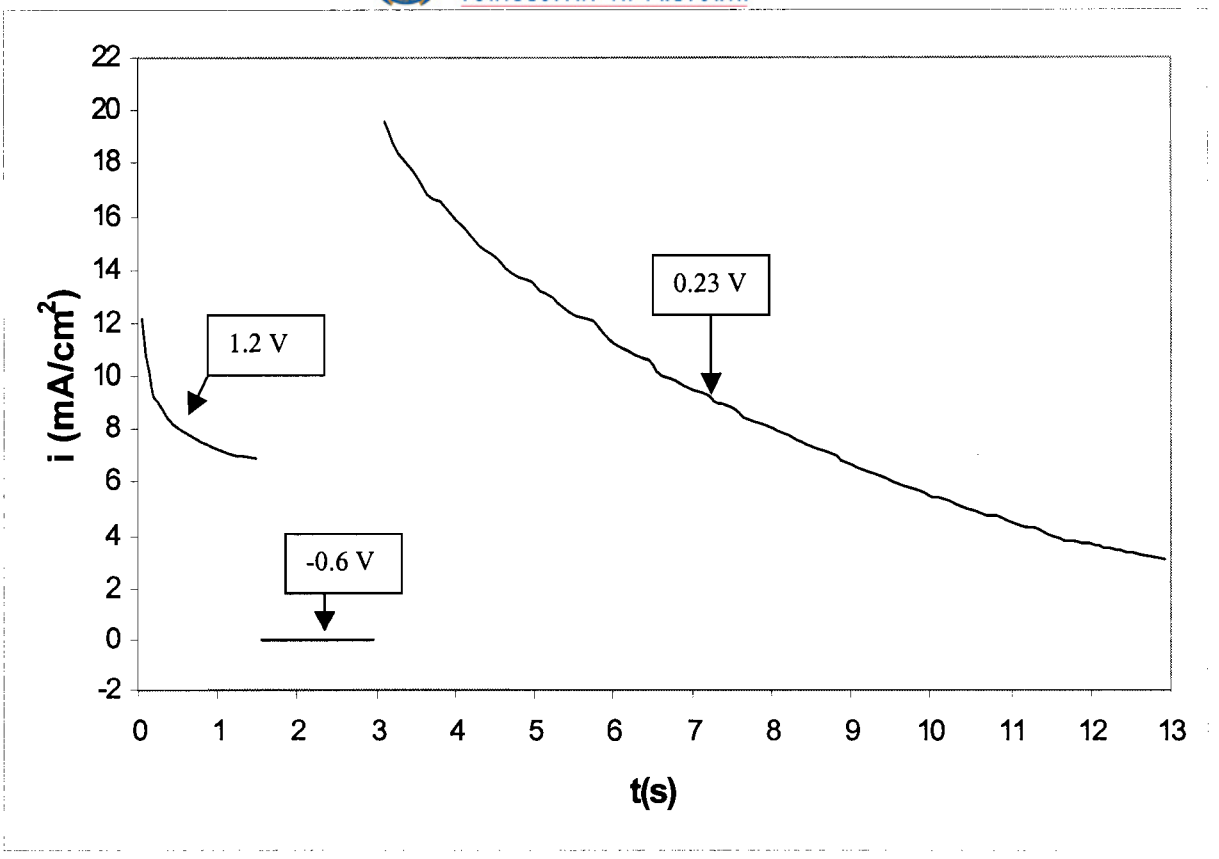

Figure 6. 21. The first cycle at a gold electrode during potential pulsing

The electrode was cleaned by the potential pulsing technique and it is seen that the 20 mA/cm^2 current density at the start of cycle 2 is once again achieved. The electrode poisons are therefore successfully removed by the potential pulsing technique. The current densities obtained during cycles 91 – 100 (Fig. 6.22(b)) are only slightly lower than those of cycles 1 – 10. Sustainable electrolysis of ethylene glycol at a gold electrode is therefore possible by potential pulsing. The initial current density for ethylene glycol oxidation obtained after each cleaning cycle is shown in Figure 6.23. This figure clearly illustrates how effective the potential pulsing technique is in cleaning the gold electrode of poisons to restore its activity.

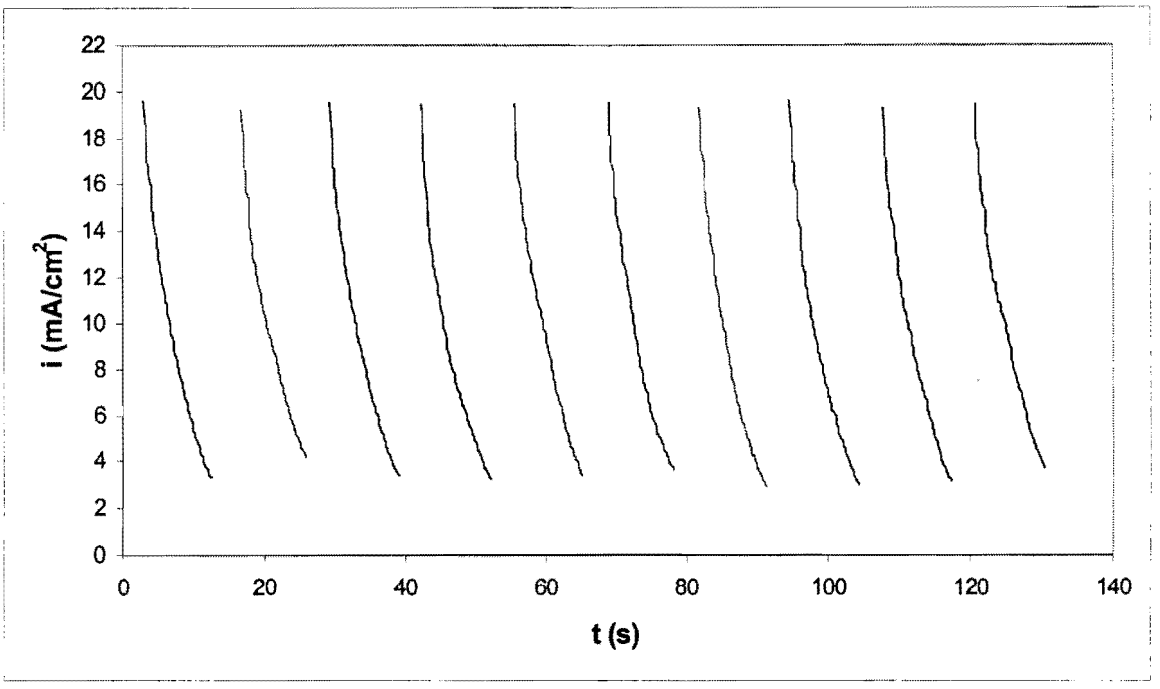

(a)

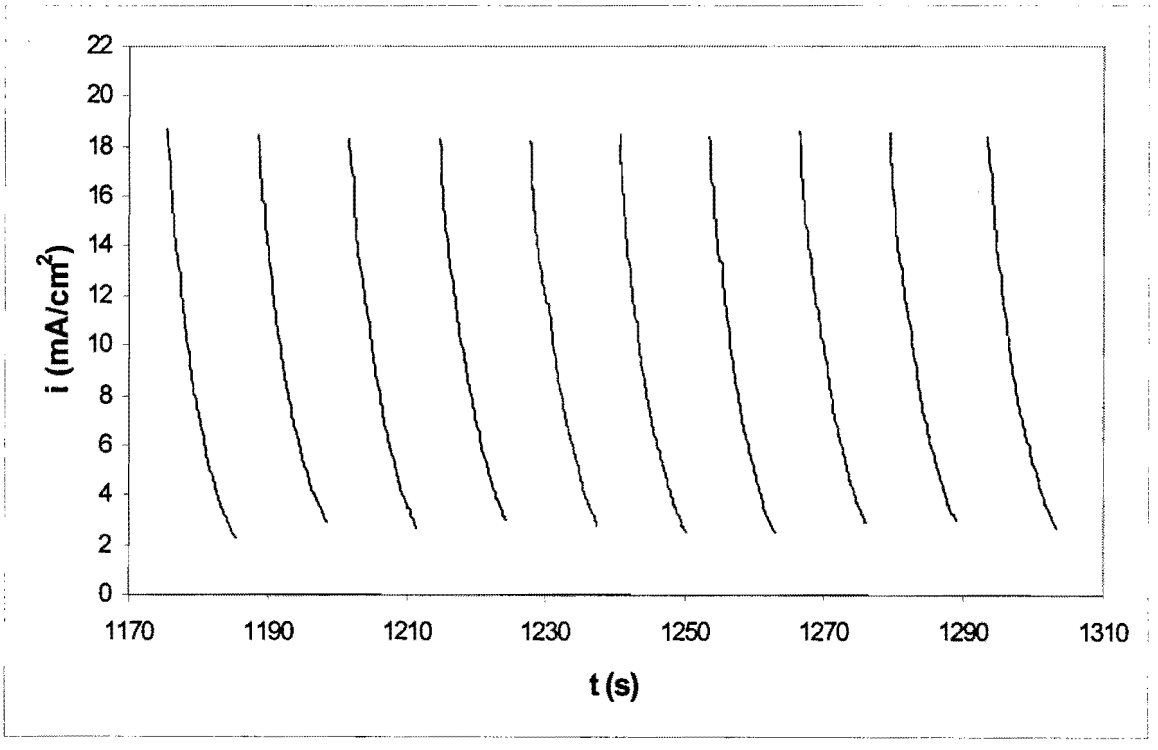

(b)

Figure 6.22. Electrolysis of ethylene glycol by potential pulsing at a gold electrode; (a) Cycles 1-10; (b) Cycles 91-100 (Solution stirred during potential pulsing).

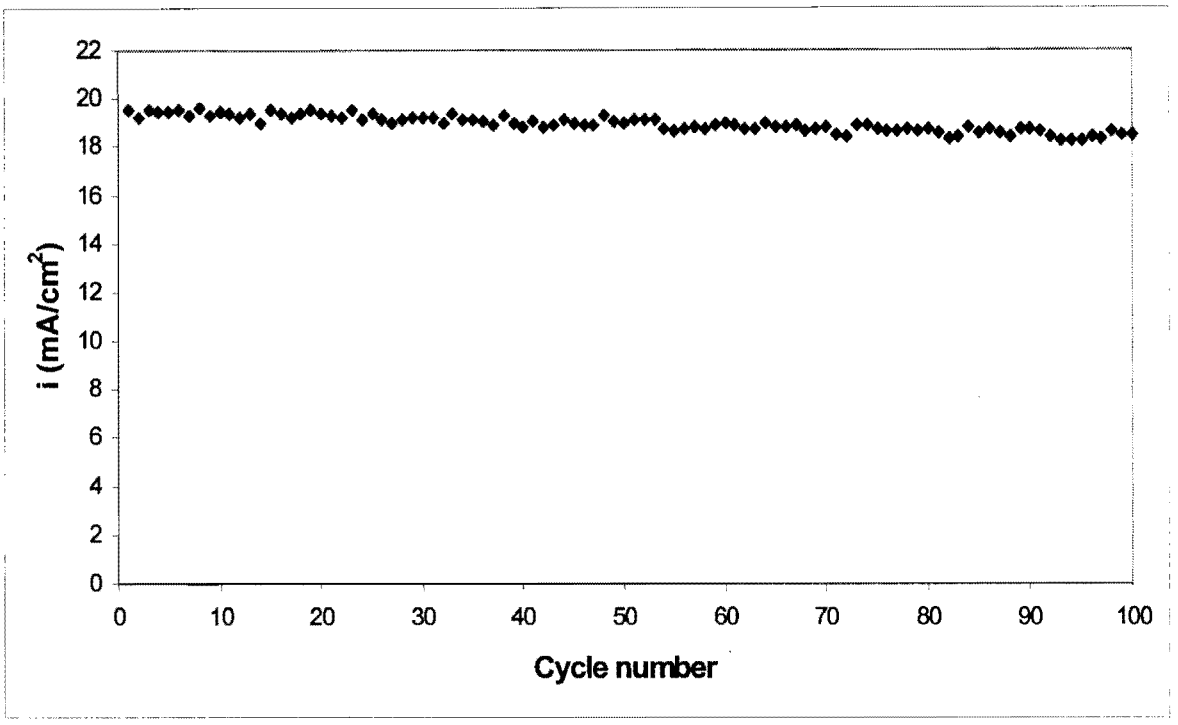

Figure 6.23. The initial current density for ethylene glycol oxidation at a gold electrode obtained after each cleaning cycle.

Numerical integration was used to calculate the charge passed during the electro-oxidation of ethylene glycol at the gold electrode over the time period of the 100 cycles. The results are summarised in Table 6.13.

Table 6.13. The charge passed during oxidation of ethylene glycol at a gold electrode during cycles 1-10, 91-100 and 1-100

Cycles 1-10	Cycles 91-100	Cycles 1-100
0.242 C	0.225 C	2.37 C

When ethylene glycol is oxidised up to oxalate, 8 electrons per molecule are delivered within the overall process (Hauffe and Heitbaum, 1978). The charge of 1 mol of electrons is 96472 C/mol (Faraday's constant) (Fishbane et al., 1996). The quantity of electrons for the oxidation of ethylene glycol at gold over 100 cycles equal (2.37)/(96472) = 2.46 x 10^{-5} mol electrons. The quantity of ethylene glycol molecules oxidised is (2.46 x 10^{-5})/8 = 3.07 x 10^{-6} mol.

The original quantity of ethylene glycol prior to the hundred cycles was (0.4)(0.1) = 0.04 mol, where the volume of the solution was 0.4 dm^3 and the concentration of ethylene glycol was 0.1 mol/dm^3.

Only (3.07 x 10^{-6})/0.04) = 0.008 % of the original ethylene glycol content was oxidised during the hundred cycles at gold. The above calculations are summarised in Table 6.14.

Table 6.14. The estimated amount of ethylene glycol oxidised at gold during the hundred cycles.

Original number of moles ethylene glycol	Number of moles oxidised	% ethylene glycol oxidised
0.04	3.07 x 10^{-6}	0.008

Even though the percentage of ethylene glycol that was oxidised is only an estimate, it still shows that its concentration did not change much during the hundred cycles. This is also true even if partial oxidation (less than 8 electrons/molecule) is assumed. Despite this, the charge passed during the final ten cycles is slightly lower than the first ten cycles (Table 6.13). The poisons are possibly more difficult to remove during the final cycles resulting in slightly less ethylene oxidation.

6.3.7.2. Platinum

The electrolysis of ethylene glycol was performed at –0.20 V_{SSC}. In Figure 6.24 (a), the current densities obtained during cycles 1 – 10 are shown. Figure 6.24(b) shows the current densities for cycles 91 – 100. The current densities for the electro-oxidation of ethylene glycol are lower than at gold (Fig. 6.22). The time needed to decrease the initial current density of the first cycle by 50% is 2.5 seconds (also see Table 6.12).

The electrode poisons are successfully removed by the potential pulsing technique at platinum. The current densities obtained during cycles 91 – 100 (Fig. 6.24(b)) are only slightly lower than those of cycles 1 – 10.

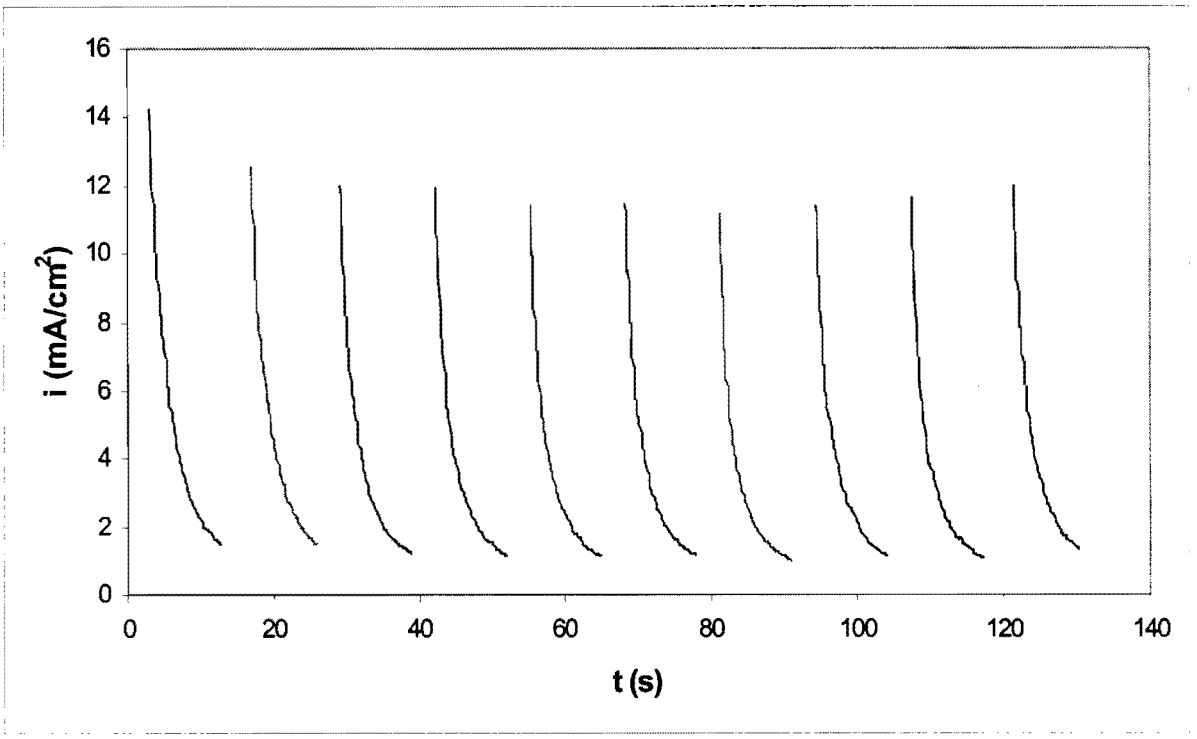

(a)

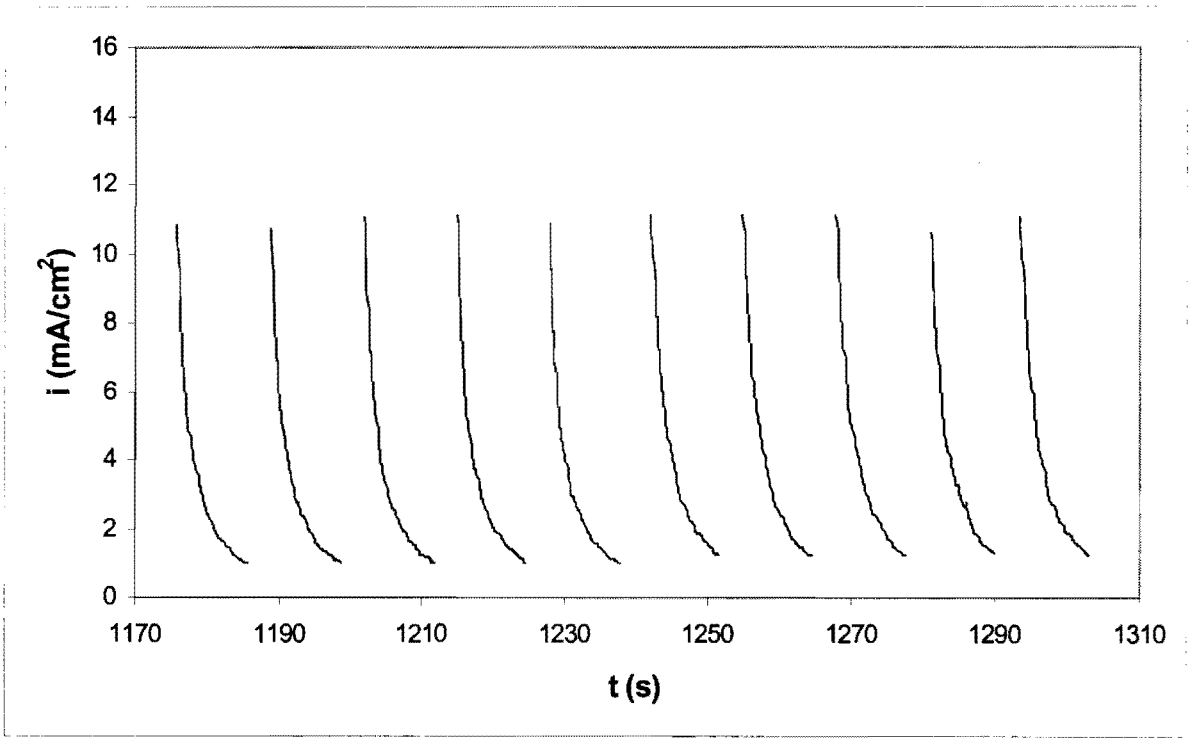

(b)

Figure 6.24. Electrolysis of ethylene glycol by potential pulsing at a platinum electrode; (a) Cycles 1-10; (b) Cycles 91-100 (Solution stirred during potential pulsing)

The initial current density for ethylene glycol oxidation obtained after each cleaning cycle is shown in Figure 6.25. This figure illustrates that the potential pulsing technique cleans the platinum electrode of poisons and restores its activity.

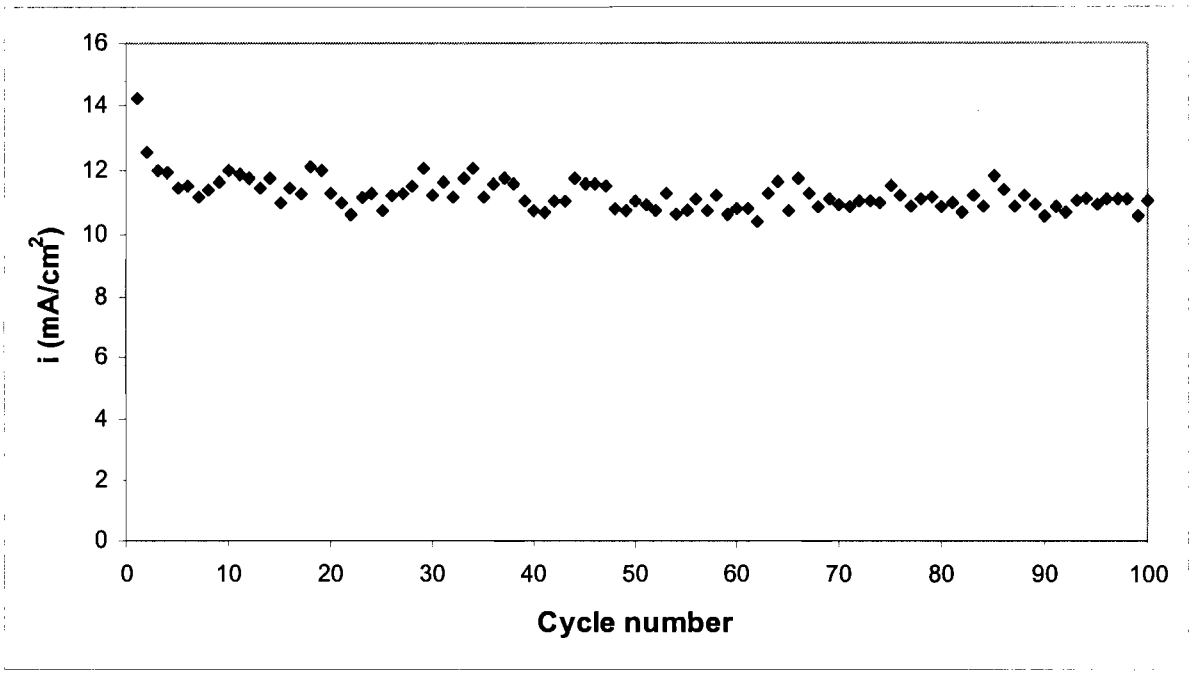

Figure 6.25. The initial current density for ethylene glycol oxidation at a platinum electrode obtained after each cleaning cycle.

Numerical integration was also used to calculate the charge passed during the electro-oxidation of ethylene glycol at the platinum electrode over the time period of the 100 cycles. The results are summarised in Table 6.15.

Table 6.15. The charge passed during oxidation of ethylene glycol at a platinum electrode during cycles 1-10, 91-100 and 1-100

Cycles 1-10	Cycles 91-100	Cycles 1-100
0.095 C	0.089 C	0.902 C

The same procedure to calculate the amount of ethylene glycol oxidised during the hundred cycles at gold was followed for platinum. The calculations are summarised in Table 6.16.

Table 6.16. The estimated amount of ethylene glycol oxidised at platinum during the hundred cycles.

Original number of moles ethylene glycol	Number of moles oxidised	% ethylene glycol oxidised
0.04	1.17×10^{-6}	0.003

Approximately 2.5 times more ethylene glycol was oxidised during the hundred cycles at gold than at platinum (Tables 6.14 and 6.16).

For platinum, the charge passed during the final ten cycles is also slightly lower than for the first ten cycles (Table 6.15). This cannot be due to a drop in ethylene glycol concentration (Table 6.16). As with gold, the poisons are possibly more difficult to remove during the final cycles resulting in slightly less ethylene oxidation.

6.3.7.3. The 60Au-40Pt alloy electrode in the 1200°C-24h condition

The electrolysis of ethylene glycol was performed at –0.05 V_{SSC}. In Figure 6.26 (a), the current densities during cycles 1 – 10 are shown. Figure 6.26(b) shows the current densities for cycles 91 – 100. The time needed to decrease the initial current density of the first cycle by 50% is 5.5 seconds (also see Table 6.12).

The initial apparent current density for first cycle is very high. However, the current density of each subsequent cycle is lower than that of the previous cycle. The current densities during cycles 91 – 100 (Fig. 6.26(b)) are much lower than those of cycles 1 – 10.

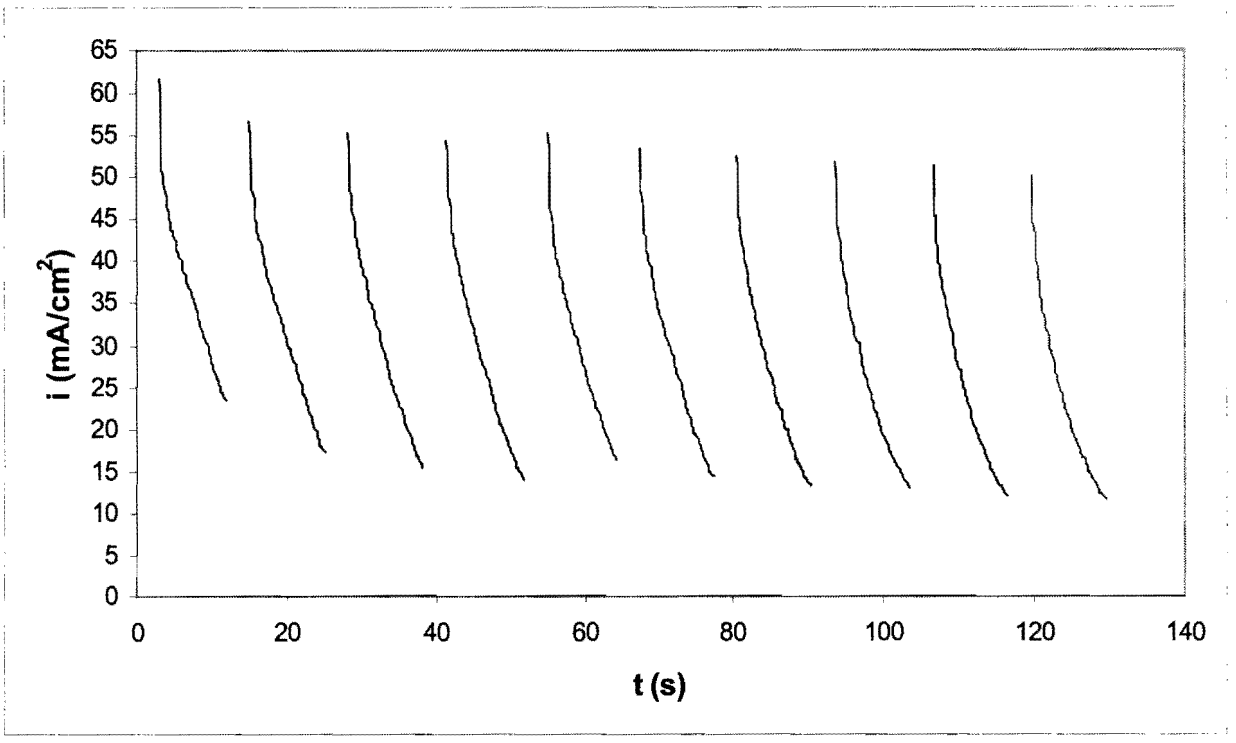

(a)

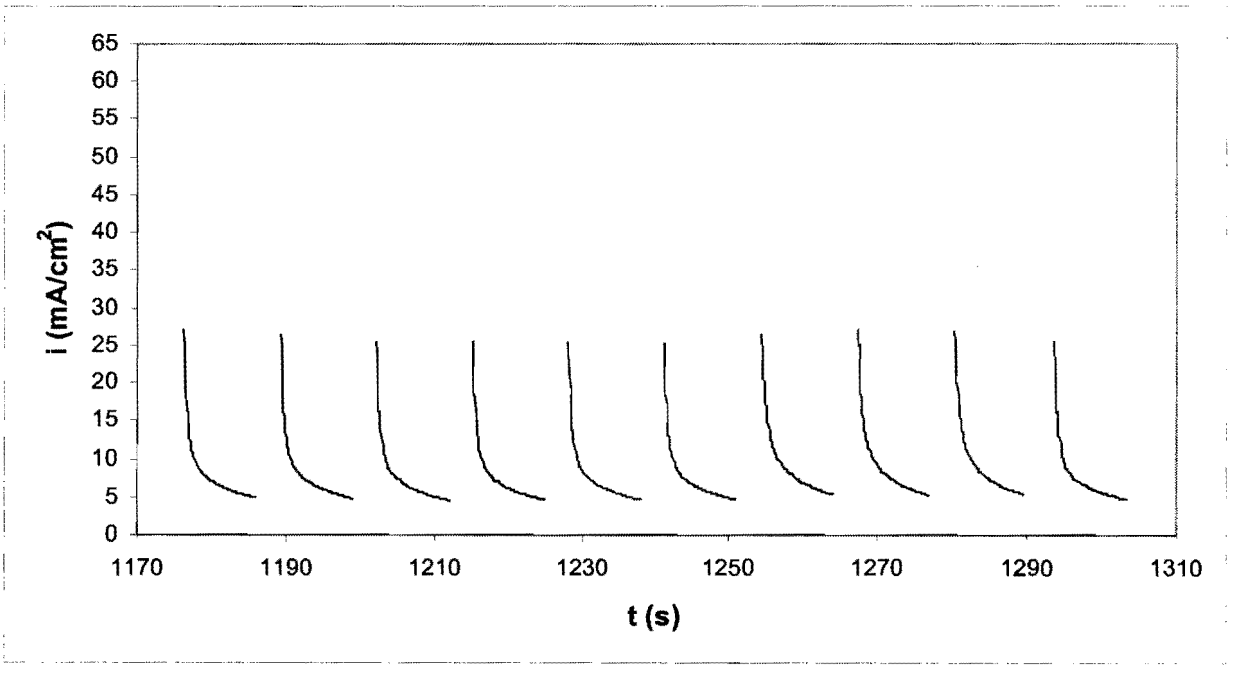

(b)

Figure 6.26. Electrolysis of ethylene glycol by potential pulsing at the 1200°C-24h (60Au-40Pt) electrode; (a) Cycles 1-10; (b) Cycles 91-100 (Solution stirred during potential pulsing)

The initial current density for ethylene glycol oxidation obtained after each cleaning cycle is shown in Figure 6.27. This figure illustrates that the potential pulsing technique is not able to restore the activity of the alloy completely. The very high current densities obtained during the first cycles presumably lead to the formation of more poisoning species than at both pure gold and platinum. It appears that the cleaning cycles are too short (or not aggressive enough) to remove all the poisons and the current densities decline.

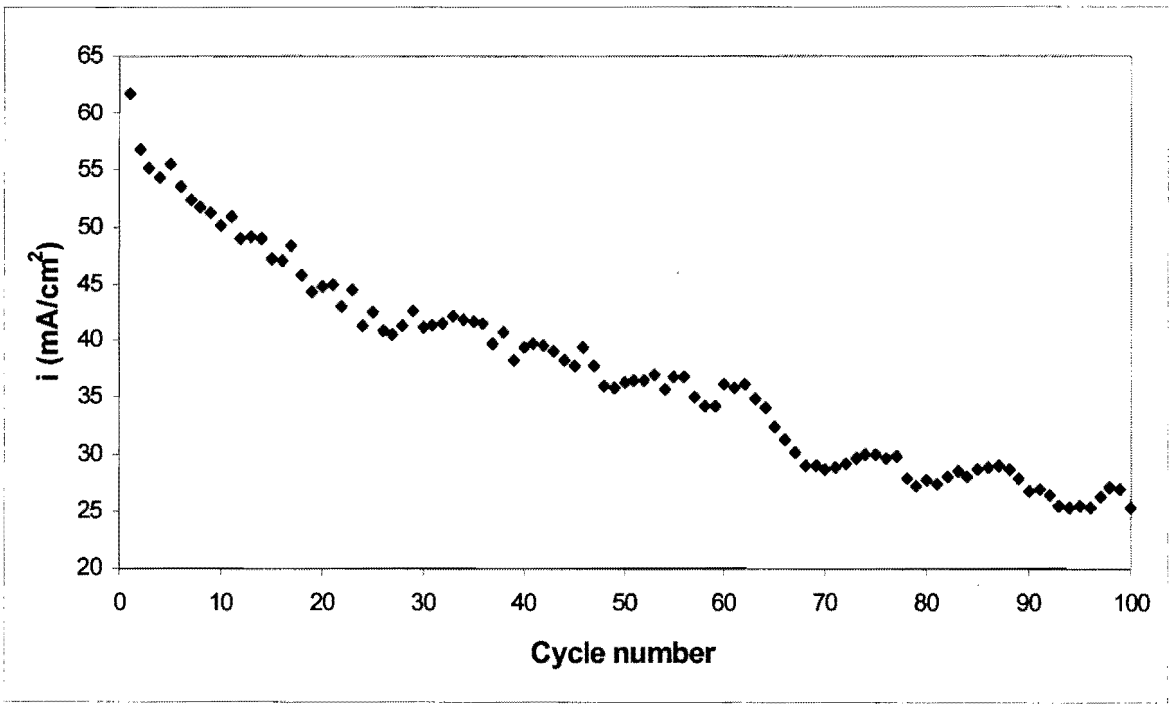

Figure 6.27. The initial current density for ethylene glycol oxidation at the 1200°C-24h (60Au-40Pt) electrode obtained after each cleaning cycle.

Numerical integration was also used to calculate the charge passed during the electro-oxidation of ethylene glycol at the 1200°C-24h (60Au-40Pt) electrode over the time period of the 100 cycles. The results are summarised in Table 6.17.

Table 6.17. The charge passed during oxidation of ethylene glycol at the porous 1200°C-24h electrode during cycles 1-10, 91-100 and 1-100

Cycles 1-10	Cycles 91-100	Cycles 1-100
0.768 C	0.220 C	3.67 C

Approximately three times more ethylene glycol is oxidised during the first ten cycles at the alloy electrode than at gold. Almost the same amount of ethylene glycol is oxidised during the final ten cycles. Over the period of the whole hundred cycles, only 1.5 times more ethylene glycol is oxidised at the alloy electrode than at gold (Tables 6.13 and 6.17).

The estimated amount of ethylene glycol oxidised during the hundred cycles at the 1200°C-24h electrode is shown in Table 6.18.

Table 6.18. The amount of ethylene glycol oxidised at the 1200°C-24h electrode during the hundred cycles.

Original number of moles ethylene glycol	Number of moles oxidised	% ethylene glycol oxidised
0.04	4.76×10^{-6}	0.012

Table 6.18 confirms that the decline in current densities cannot be due to a decrease in ethylene glycol concentration, but is rather a poisoning effect.

6.3.7.4. The 50Au-50Pt alloy electrode in the "ductile" condition

The electrolysis of ethylene glycol was performed at –0.05 V_{SSC}. In Figure 6.28 (a), the current densities during cycles 1 – 10 are shown. Figure 6.28(b) shows the current densities for cycles 91 – 100. The time needed to decrease the initial current density of the first cycle by 50% is 3 seconds (also see Table 6.12).

The apparent current densities for the first cycles are lower than for the porous 1200°C-24h electrode (60Au-40Pt) (Fig.6.26). The current densities decline more rapidly with each cycle than the 1200°C-24h electrode. The current densities during cycles 91 – 100 (Fig. 6.28(b)) are much lower than those of cycles 1 – 10.

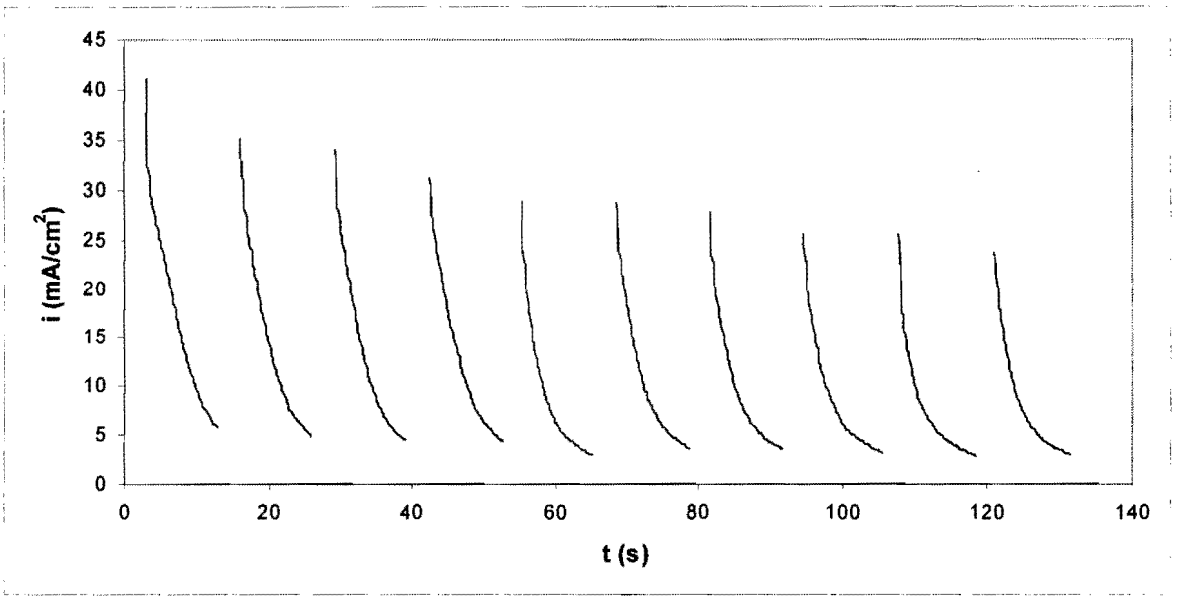

(a)

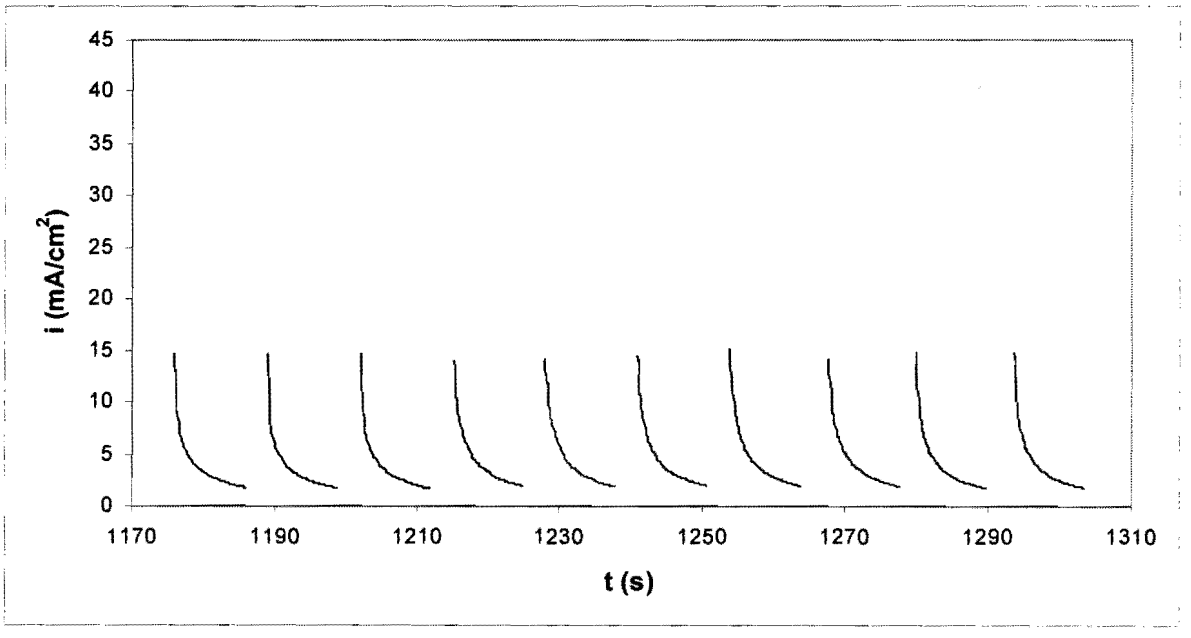

(b)

Figure 6.28. Electrolysis of ethylene glycol by potential pulsing at the "ductile" (50Au-50Pt) electrode; (a) Cycles 1-10; (b) Cycles 91-100 (Solution stirred during potential pulsing)

The initial current density for ethylene glycol oxidation obtained after each cleaning cycle is shown in Figure 6.29. This figure confirms that the potential pulsing technique is also not able to restore the activity of this alloy completely.

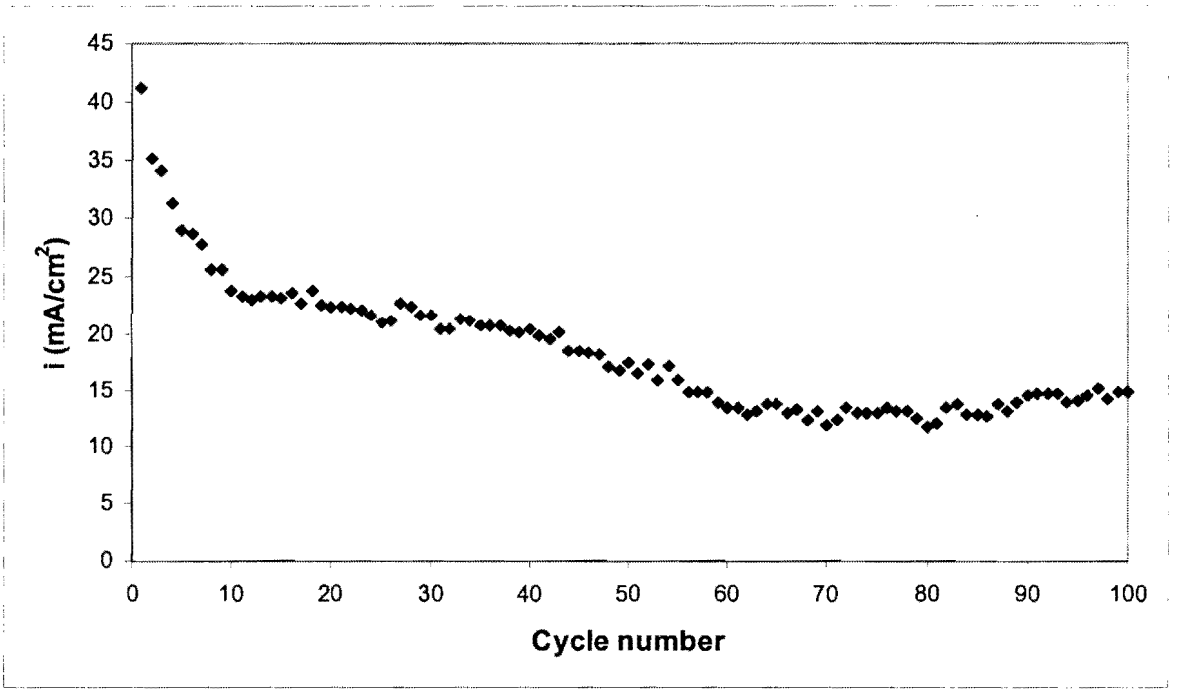

Figure 6.29. The initial current density for ethylene glycol oxidation at the "ductile" (50Au-50Pt) electrode obtained after each cleaning cycle.

Numerical integration was again used to calculate the charge passed during the electro-oxidation of ethylene glycol at the "Ductile" (50Au-50Pt) electrode over the time period of the 100 cycles. The results are summarised in Table 6.19.

Table 6.19. The charge passed during oxidation of ethylene glycol at the "ductile" electrode during cycles 1-10, 91-100 and 1-100

Cycles 1-10	Cycles 91-100	Cycles 1-100
0.306 C	0.109 C	1.52 C

Approximately 1.3 times more ethylene glycol is oxidised during the first ten cycles at this alloy electrode than at gold. Only half the amount of ethylene glycol is oxidised

during the final ten cycles Over the period of the whole hundred cycles, less ethylene glycol (1.5 times) is oxidised at the alloy electrode than at gold (Tables 6.13 and 6.19).

The estimated amount of ethylene glycol oxidised during the hundred cycles at the "ductile" electrode is shown in Table 6.20.

Table 6.20. The estimated amount of ethylene glycol oxidised at the "ductile" electrode during the hundred cycles.

Original number of moles ethylene glycol	Number of moles oxidised	% ethylene glycol oxidised
0.04	1.98×10^{-6}	0.0049

6.3.7.5. The 50Au-50Pt alloy electrode in the solid solution condition

The electrolysis of ethylene glycol was performed at –0.05 V_{SSC}. In Figure 6.30 (a), the current densities during cycles 1 – 10 are shown. Figure 6.30(b) shows the current densities for cycles 91 – 100. The time needed to decrease the initial current density of the first cycle by 50% is 3 seconds (also see Table 6.12).

The initial apparent current densities for the first cycles are higher than for the "ductile" electrode (Fig. 6.28). Unfortunately, the current densities also decline with each cycle. The current densities during cycles 91 – 100 (Fig. 6.30(b)) are much lower than those of cycles 1 – 10.

The initial current density for ethylene glycol oxidation obtained after each cleaning cycle is shown in Figure 6.31. This figure confirms that the potential pulsing technique is also not able to restore the activity of this alloy completely.

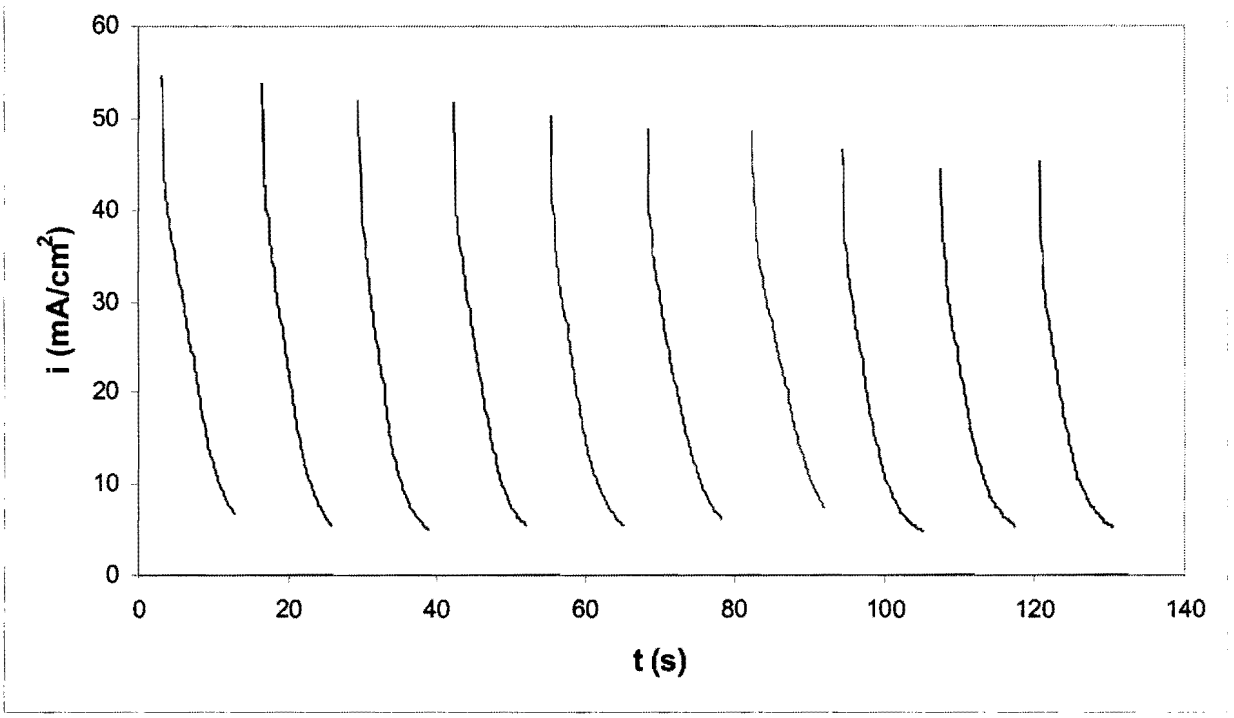

(a)

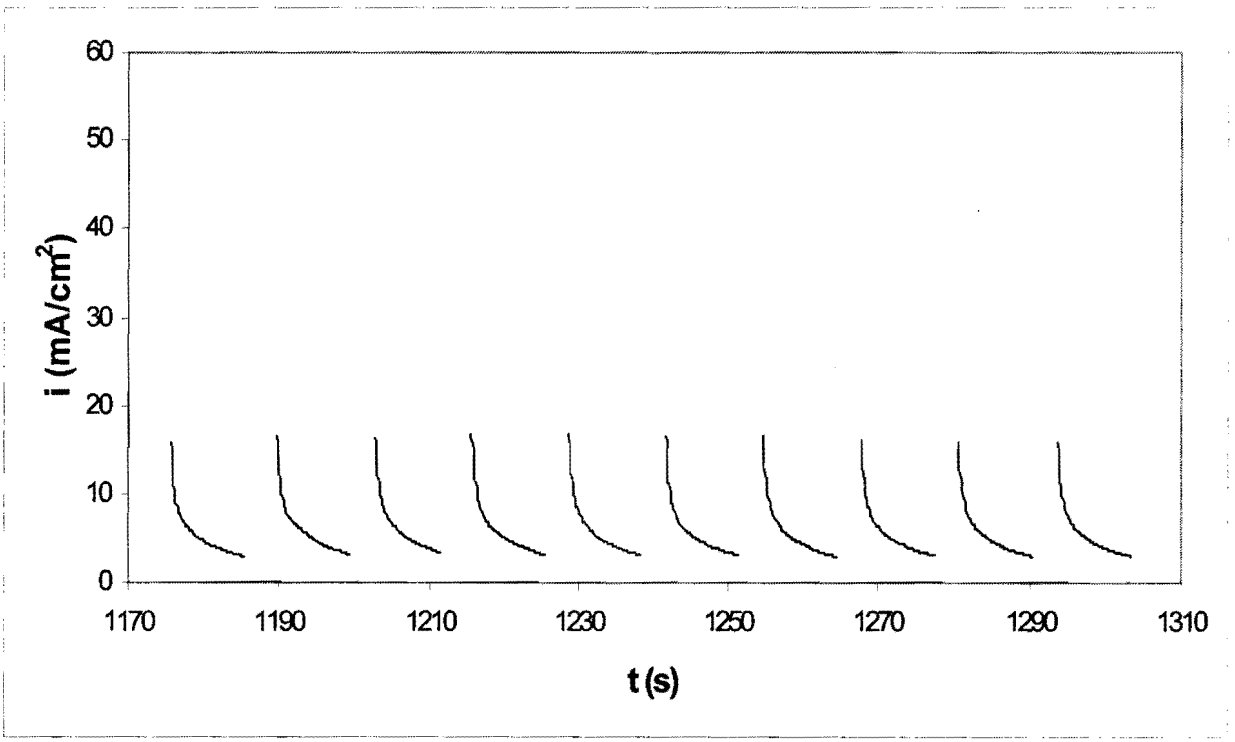

(b)

Figure 6.30. Electrolysis of ethylene glycol by potential pulsing at the solid solution (50Au-50Pt) electrode; (a) Cycles 1-10; (b) Cycles 91-100 (Solution stirred during potential pulsing).

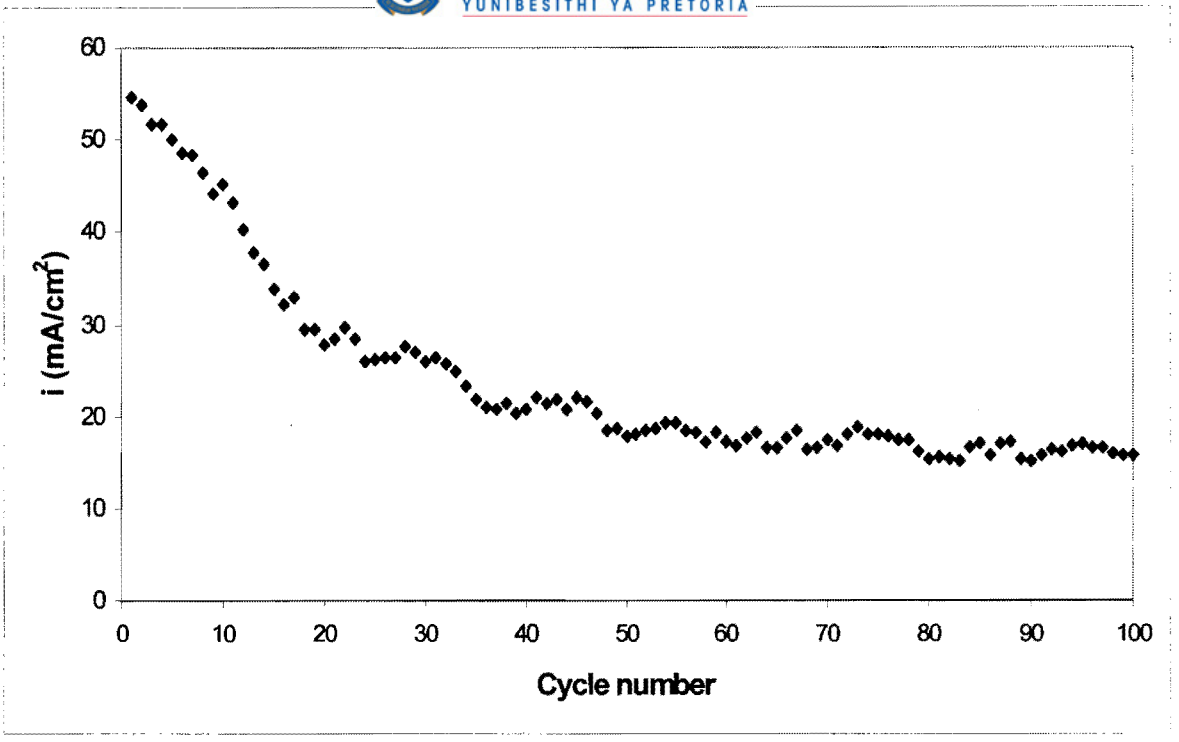

Figure 6.31. The initial current density for ethylene glycol oxidation at the solid solution (50Au-50Pt) electrode obtained after each cleaning cycle.

Numerical integration was again used to calculate the charge passed during the electro-oxidation of ethylene glycol at the solid solution (50Au-50Pt) electrode over the time period of the 100 cycles. The results are summarised in Table 6.21.

Table 6.21. The charge passed during oxidation of ethylene glycol at the solid solution 50Au-50Pt electrode during cycles 1-10, 91-100 and 1-100

Cycles 1-10	Cycles 91-100	Cycles 1-100
0.492 C	0.149 C	2.21 C

Approximately two times more ethylene glycol is oxidised during the first ten cycles at this alloy electrode than at gold. Less ethylene glycol is oxidised during the final ten cycles. Over the period of the whole hundred cycles, slightly less ethylene glycol is oxidised at the alloy electrode than at gold (Tables 6.13 and 6.21).

The estimated amount of ethylene glycol oxidised during the hundred cycles at the solid solution electrode is shown in Table 6.22.

Table 6.22. The estimated amount of ethylene glycol oxidised at the solid solution electrode during the hundred cycles.

Original number of moles ethylene glycol	Number of moles oxidised	% ethylene glycol oxidised
0.04	2.87×10^{-6}	0.0072

6.3.7.6. The Gold 990 alloy in the solid solution condition

The electrolysis of ethylene glycol was performed at 0.23 V_{SSC}. In Figure 6.32(a), the current densities during cycles 1 – 10 are shown. Figure 6.32(b) shows the current densities for cycles 91 – 100. The time needed to decrease the initial current density of the first cycle by 50% is 5 seconds (also see Table 6.12).

From Figure 6.32(a) it is seen the initial current density after potential pulsing (cycle 1) was approximately 20 mA/cm^2, falling to 5.5 mA/cm^2 after 10 seconds. The corresponding values for pure gold are 20 mA/cm^2 and 3.5 mA/cm^2 (Fig. 6.22). The decline in current density over the 10 seconds at the Gold 990 electrode is therefore slightly less than at pure gold.

The electrode poisons are successfully removed by the potential pulsing technique. The current densities during cycles 91 – 100 (Fig. 6.32(b)) are only slightly lower than those of cycles 1 – 10. Sustainable electrolysis of ethylene glycol at this electrode will therefore be possible by potential pulsing. The initial current density for ethylene glycol oxidation obtained after each cleaning cycle is shown in Figure 6.33. This figure illustrates how effective of the potential pulsing technique is to restore the activity of this electrode.

Numerical integration was used to calculate the charge passed during the electro-oxidation of ethylene glycol at the solid solution Gold 990 electrode over the time period of the 100 cycles. The results are summarised in Table 6.23.

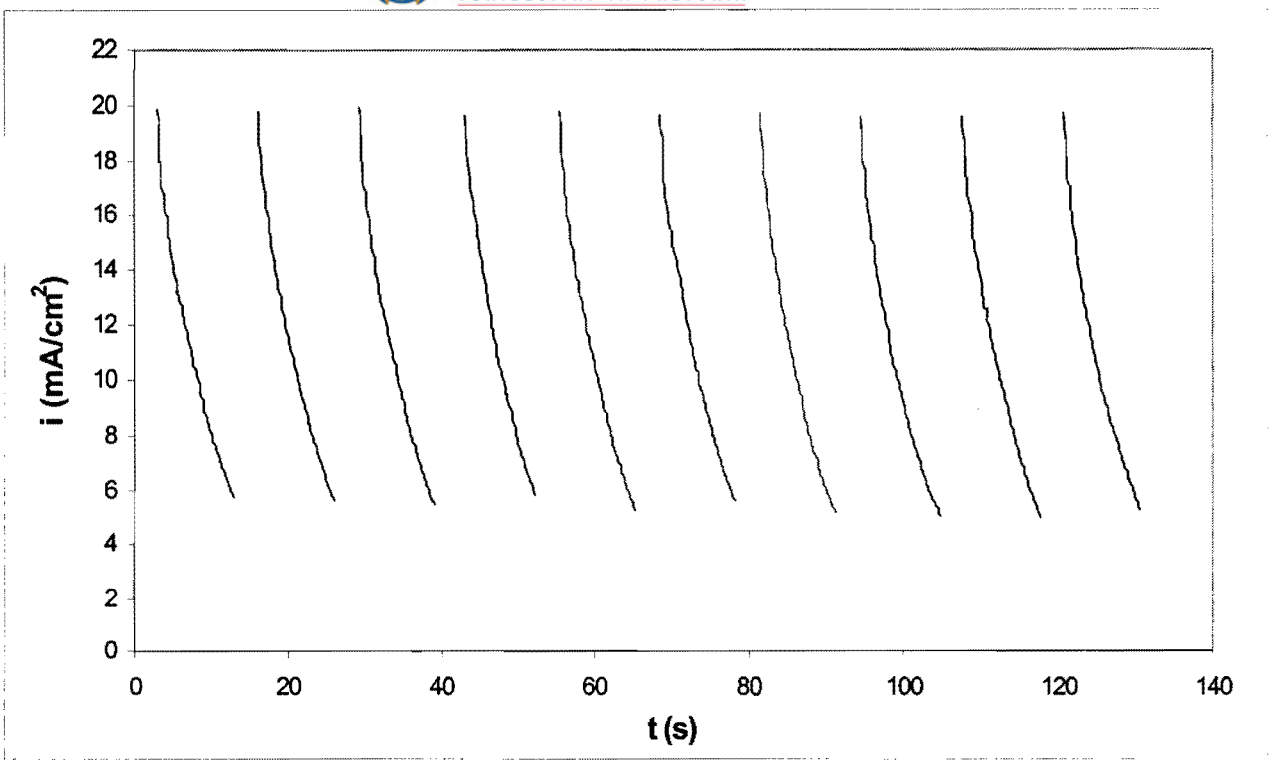

(a)

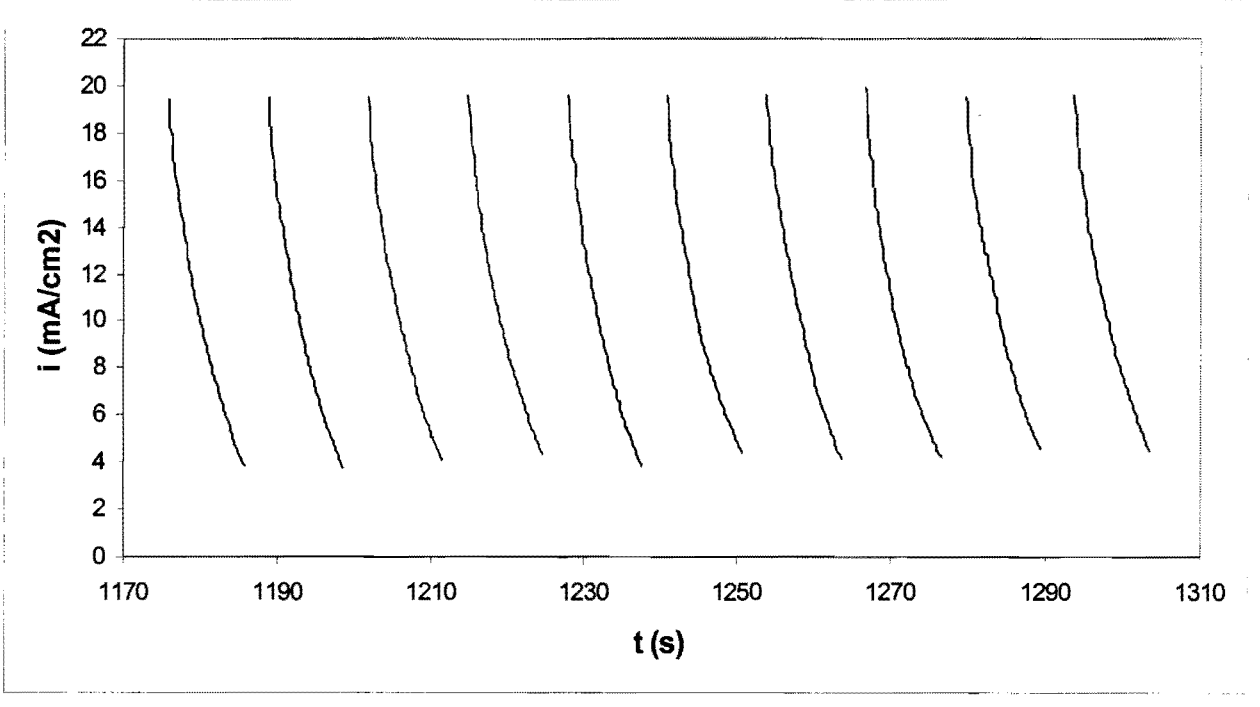

(b)

Figure 6.32. Electrolysis of ethylene glycol by potential pulsing at the solid solution Gold 990 electrode; (a) Cycles 1-10; (b) Cycles 91-100 (Solution stirred during potential pulsing).

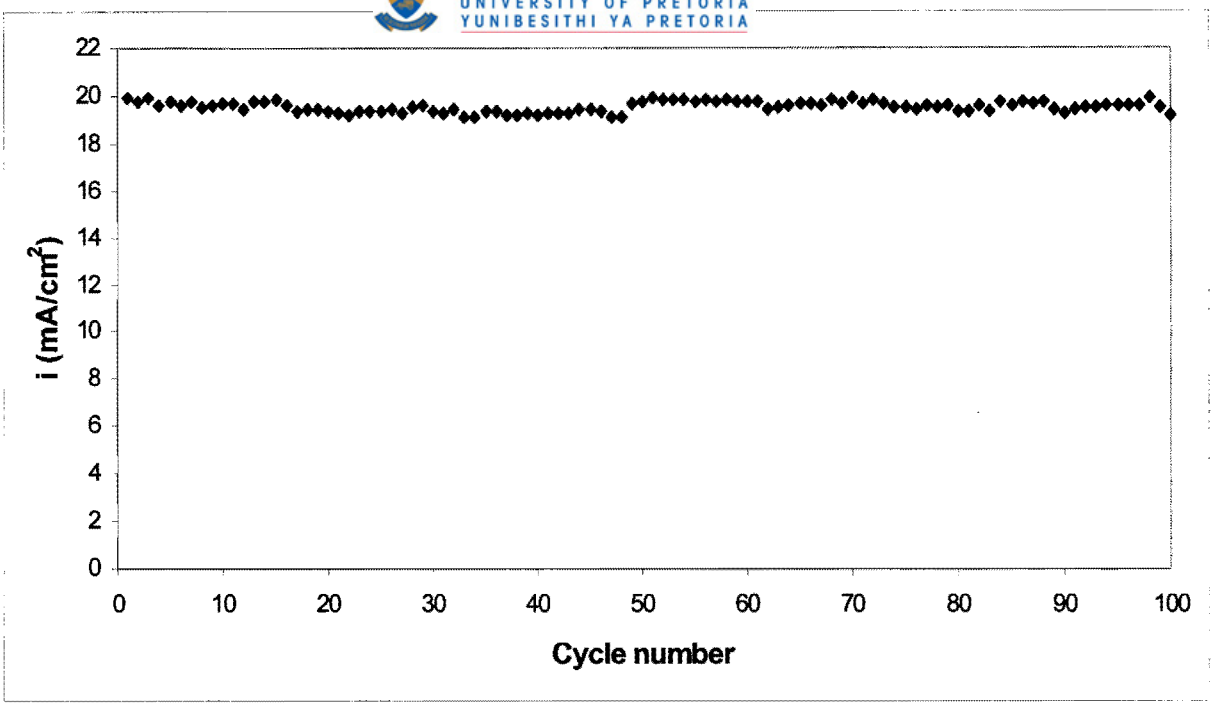

Figure 6.33. The initial current density for ethylene glycol oxidation at the solid solution Gold 990 electrode obtained after each cleaning cycle.

Table 6.23. The charge passed during oxidation of ethylene glycol at the solid solution Gold 990 electrode during cycles 1-10, 91-100 and 1-100

Cycles 1-10	Cycles 91-100	Cycles 1-100
0.293 C	0.268 C	2.76 C

Slightly more ethylene glycol is oxidised at this alloy electrode than at pure gold (Tables 6.13 and 6.23). This is probably due to the higher current densities obtained at the Gold 990 electrode at the end of the cycle prior to the cleaning procedure. Gold-titanium electrodes with a higher titanium content than Gold 990 have to be studied to indicate whether this observation is significant or not.

The estimated amount of ethylene glycol oxidised during the hundred cycles at the Gold 990 solid solution electrode is shown in Table 6.24.

Table 6.24. The estimated amount of ethylene glycol oxidised at the solid solution Gold 990 electrode during the hundred cycles

Original number of moles ethylene glycol	Number of moles oxidised	% ethylene glycol oxidised
0.04	3.59×10^{-6}	0.0089

The initial current densities for ethylene glycol oxidation at the different electrodes after each cleaning cycle are compared in Figure 6.34. This figure clearly illustrates that the initial current densities after each cleaning cycle remain fairly constant for gold and platinum (Gold 990 is similar to gold). The initial current densities for the Au-Pt alloy electrodes are high after the first few cycles, but then decline as the number of cycles increases.

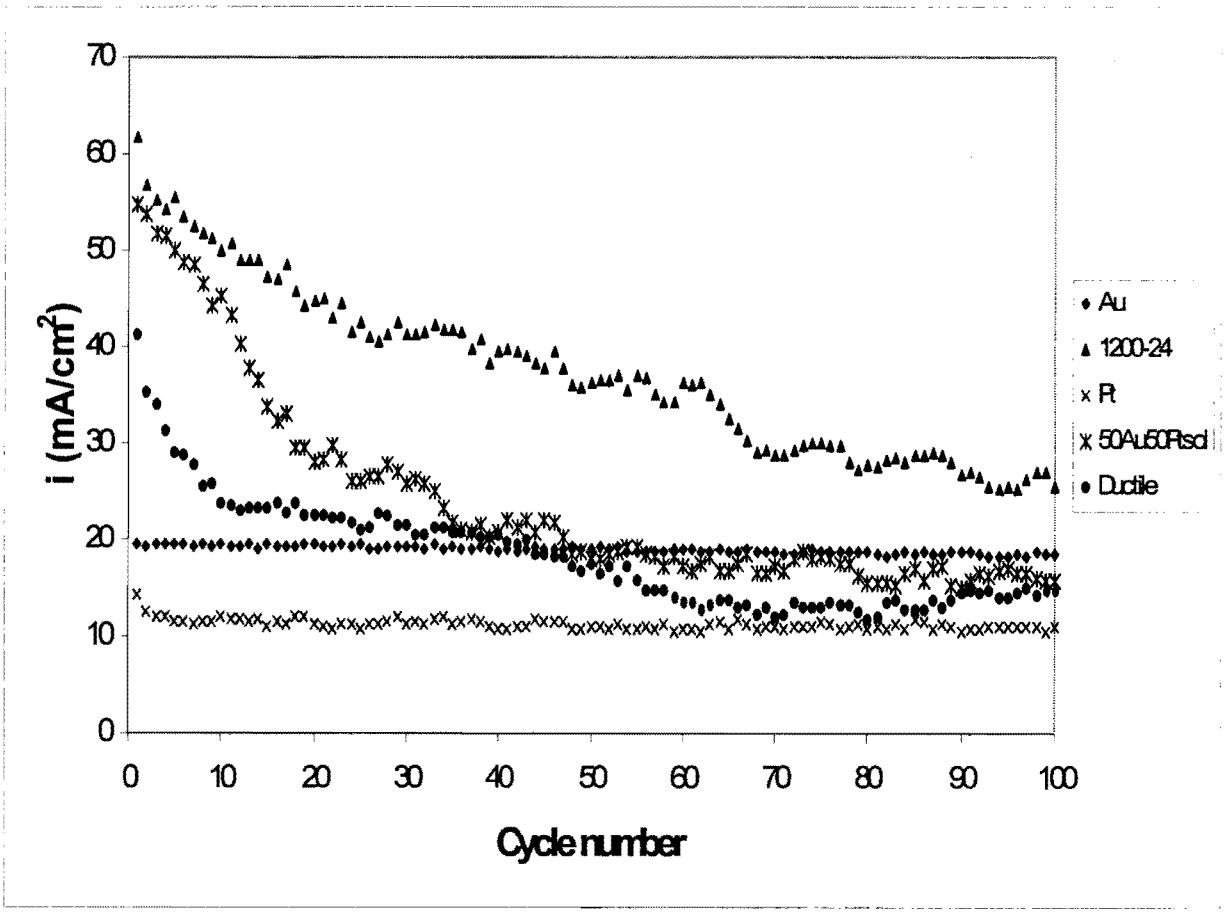

Figure 6.34. The initial current densities for ethylene glycol electro-oxidation at the different electrodes after each cleaning cycle.

This section is summarised by a graph of the charge density passed during electro-oxidation at the different electrodes against time (Fig. 6.35). The graphs of pure gold, pure platinum and the Gold 990 electrode are nearly linear, because the rate at which ethylene glycol is oxidised at these electrodes remained relatively constant over the 100 cycles period (Tables 6.13, 6.15 and 6.23). More ethylene glycol is oxidised during the first cycles at the Au-Pt alloys than during the final cycles (Tables 6.17, 6.19 and 6.21). The slopes of the graphs for these electrodes in Fig. 6.35 are therefore high at short times, but lower at longer times.

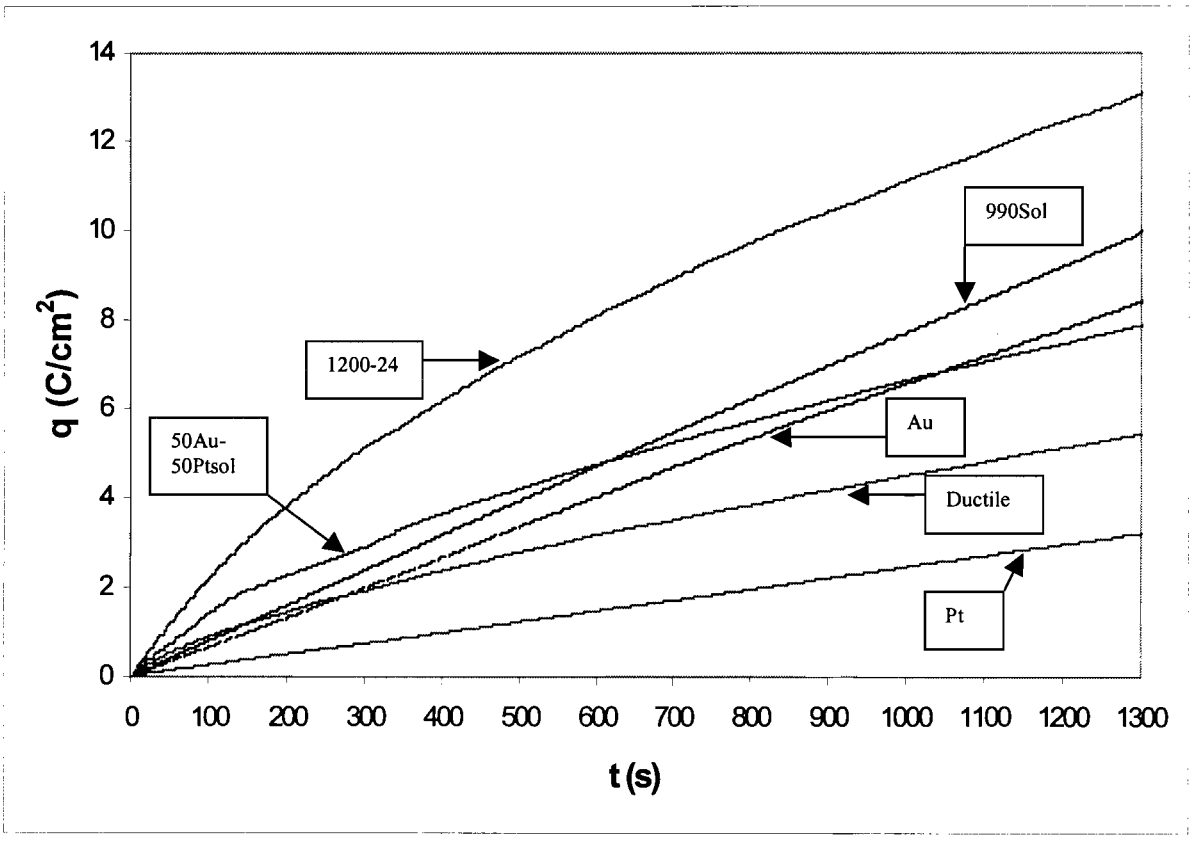

Figure 6.35. Charge density against time for the different electrodes

High apparent current densities are found during the first few cycles at the Au-Pt alloy electrodes (Fig. 6.34). Unfortunately, these high current densities lead to the formation of more poisoning species than at both pure gold and platinum. The cleaning cycles are too short (or not aggressive enough) to remove all the poisons and the current densities decline (Fig. 6.34). For this reason it was decided to increase the time of the cleaning

cycle for one of the Au-Pt alloys to see whether the poisoning species can be removed. The 50Au-50Pt alloy electrode was selected for this experiment (see paragraph 6.3.7.5.). The electrode was cycled for 100 cycles using the same procedure as before (1.5 s at 1.2 V_{SSC}, 1.5 s at –0.6 V_{SSC}, 10 seconds at –0.05 V_{SSC}). After the 100th cycle, the following procedure was used: 30 s at 1.2 V_{SSC}, 10 s at –0.6 V_{SSC}, 10 seconds at –0.05 V_{SSC}. The three cycles prior to the change in the cleaning procedure and the first three cycles after the change in the cleaning procedure are shown in Fig. 6.36 (The current densities for the cleaning cycles have been omitted). The longer cleaning procedure does indeed cause an increase in the current densities, because more of the poisoning species are removed from the surface of the electrode. The initial current densities of cycles 101-103 are much higher than those of cycles 98-100. Unfortunately, the current densities at the end of each cycle are not increased significantly by the longer cleaning procedure (Fig. 6.36).

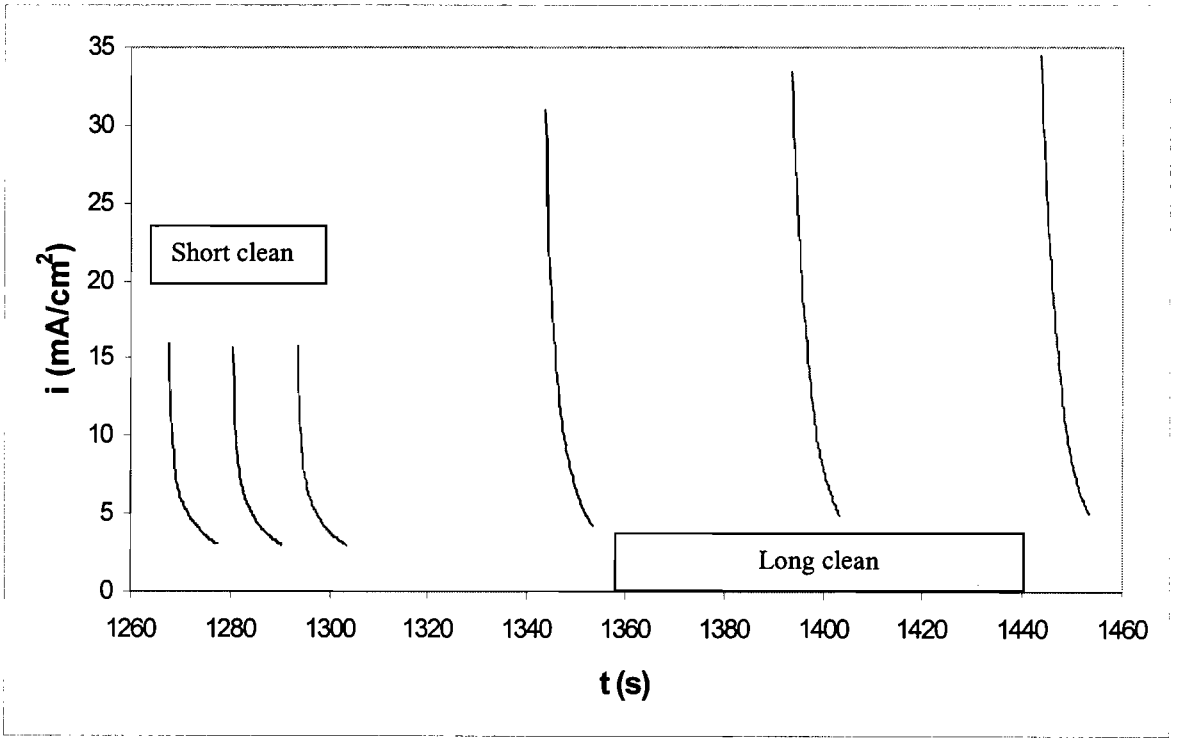

Figure 6.36. The three cycles prior to the change in the cleaning procedure and the first three cycles after the change in the cleaning procedure for the 50Au-50Pt electrode in the solid solution condition.

The initial current density after the longer cleaning procedure increases with each cycle. This effect is seen more clearly in Figure 6.37, where the initial current density for this electrode is shown after each cleaning cycle. The initial current densities after the longer cleaning cycles are still not as high as during the first few cycles with the short cleaning procedure (Fig. 6.31). This suggests that the poisoning species are not completely removed by the longer cleaning procedure.

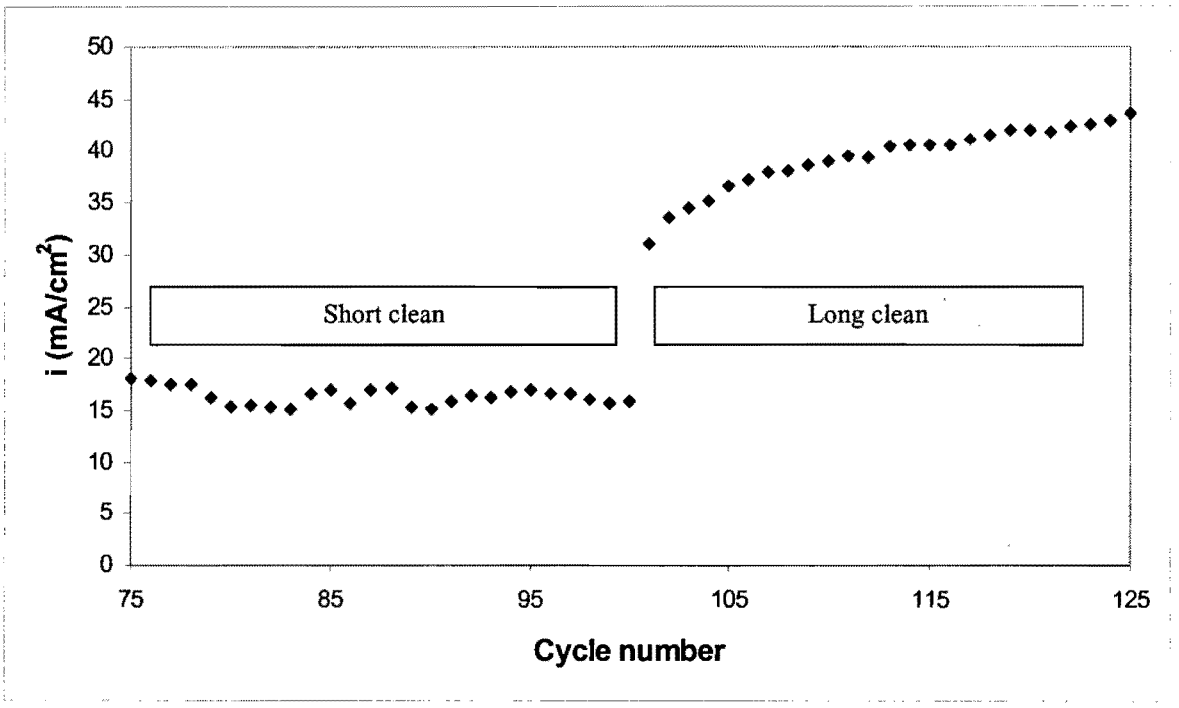

Figure 6.37. The initial current densities for ethylene glycol electro-oxidation at the 50Au-50Pt solid solution electrode.

6.4. Conclusions

The following conclusions on the electro-oxidation of ethylene glycol can be made based on the cyclic voltammetry experiments:

- The platinum region of the Au-Pt alloys is more active for ethylene glycol electro-oxidation than pure platinum after anodic activation. The gold region of the alloys is less active than pure gold after anodic activation.

- The solid solution Au-Pt electrodes are more active for the electro-oxidation of ethylene glycol than the two-phased electrodes. This can perhaps be explained by the "third-body effect".
- Poisoning of all electrodes occurs. Poisoning is thought to occur by linearly bonded CO.
- The anodic treatment at 1.2 V_{SSC} after the 10^{th} cycle (poisoned surface) reactivates the platinum region of the Au-Pt alloy electrodes, but deactivates the gold region. It therefore seems as if the activities of the two regions are linked – the activity of the one is high when the activity of the other is low and vice versa.
- Stirring of the solution reduces the current densities at non-porous electrodes. Stirring presumably causes an accelerated transportation of intermediates into the solution, resulting in lower current densities.
- Stirring does not have a great effect on the current densities at porous electrodes. The solution inside the pores is probably not affected much by stirring.
- The porosity does not increase the maximum apparent current densities. The advantage of the porosity is to maintain high current densities when the solution is stirred.
- The electro-oxidation of ethylene glycol at gold and the two Gold 990 electrodes is similar. The titanium content of 4 at% may be too low to have a significant influence on the electrochemical behaviour of gold. The titanium may be in the passive condition (Fig 2.21) or the titanium may have dissolved selectively from the Gold 990 alloy resulting in a pure gold surface.

The following conclusions on the electro-oxidation of ethylene glycol can be made based on the electrolysis of ethylene glycol at a fixed potential:

- Electrode poisoning occurs rapidly and the current densities drop to low values in a matter of seconds.
- The observation that Au-Pt electrodes in the solid solution condition are more effective for the electro-oxidation of ethylene glycol than the two-phased electrodes was confirmed.

- Stirring of the solution results in a faster decay of the current densities at all the electrodes. The effect is much less pronounced with porous electrodes.
- The observation that the electro-oxidation of ethylene glycol at gold and Gold 990 electrodes is similar was confirmed.

The following conclusions on the electro-oxidation of ethylene glycol can be made based on electrolysis using the potential pulsing technique:

- Potential pulsing is successful in removing the poisoning species formed at the pure gold and pure platinum electrodes. The activities of these two electrodes remain high over a period of 100 cycles.
- High apparent current densities are found during the first few cycles at the Au-Pt alloy electrodes. Unfortunately, these high current densities lead to the formation of more poisoning species than at both pure gold and platinum. The cleaning cycles are too short (or not aggressive enough) to remove all the poisons and the current densities decline. The activity of the Au-Pt electrodes can decline to levels lower than the pure metals within a hundred-cycle period. A longer cleaning cycle is able to remove most of the poisons at the electrode and the current densities increase.
- Slightly more ethylene glycol is oxidised at the Gold 990 electrode (solid solution) than at pure gold. This is probably due to the higher current densities obtained at the Gold 990 electrode at the end of the cycle prior to the cleaning procedure. Gold-titanium electrodes with a higher titanium content than Gold 990 have to be studied to indicate whether this observation is significant or not.

Chapter 7

CONCLUSIONS AND RECOMMENDATIONS

The electrochemistry of gold-based alloys in different heat treatment conditions were investigated in this study. Based on the heat treatment results (Chapter 3), the following conclusions can be made:

- The solid solution heat treatment of the two-phased 60Au-40Pt alloy leads to Kirkendall porosity. This porosity increases the surface area of the sample.
- Conventional nucleation and growth of the platinum-rich areas occurs when the 60Au-40Pt alloy samples are heat treated in the miscibility gap.
- Spinodal decomposition occurs when the 50Au-50Pt alloy samples are heat treated in the miscibility gap.
- The solid solution heat treatment of the two-phased 50Au-50Pt alloy does not lead to Kirkendall porosity.
- The Gold 990 sample in the solid solution condition has a Vickers hardness of HV_5 = 50 kg/mm^2. It is possible to increase the hardness to 150 kg/mm^2 by a precipitation-hardening heat treatment.

The electrochemical properties of the gold-based alloys were determined in acid (Chapter 4) and alkaline (Chapter 5) solutions without an organic in the solution. The main conclusions from these experiments are:

- The cyclic voltammograms of the Au-Pt alloy electrodes have features corresponding to both pure gold and platinum.
- The extra surface area of the porous Au-Pt electrodes results in higher currents. Higher apparent current densities are therefore obtained with these electrodes.
- The electrochemical behaviour of gold and Gold 990 are similar.

The electro-oxidation of ethylene glycol in an alkaline solution at the gold-based electrodes were investigated in Chapter 6. The main conclusions of these experiments are:

- The platinum region of the Au-Pt alloys is more active for ethylene glycol electro-oxidation than pure platinum after anodic activation. The gold region of the alloys is less active than pure gold after anodic activation.
- The solid solution Au-Pt electrodes are more active for the electro-oxidation of ethylene glycol than the two-phased electrodes. This can perhaps be explained by the "third-body effect".
- Poisoning of all electrodes occurs. Poisoning is thought to occur by linearly bonded CO.
- Stirring of the solution reduces the current densities at non-porous electrodes. Stirring presumably causes an accelerated transportation of intermediates into the solution, resulting in lower current densities.
- Stirring does not have a great effect on the current densities at porous electrodes. The solution inside the pores is probably not affected much by stirring.
- The porosity does not increase the maximum apparent current densities. The advantage of the porosity is to maintain high current densities when the solution is stirred.
- The electro-oxidation of ethylene glycol at gold and the two Gold 990 electrodes is similar. The titanium content of 4 at% may be too low to have a significant influence on the electrochemical behaviour of gold. The titanium may be in the passive condition (Fig 2.21) or the titanium may have dissolved selectively from the Gold 990 alloy resulting in a pure gold surface.
- Potential pulsing is successful in removing the poisoning species formed at the pure gold and pure platinum electrodes. The activities of these two electrodes remain high over a period of 100 cycles.
- High apparent current densities are found during the first few cycles at the Au-Pt alloy electrodes. Unfortunately, these high current densities apparently lead to the formation of more poisoning species than at both pure gold and platinum. The cleaning cycles are too short (or not aggressive enough) to remove all the poisons and the current densities decline. The activity of the Au-Pt electrodes can decline to levels lower than the pure metals within a hundred-cycle period. A longer cleaning cycle is able to remove most of the poisons at the electrode and the current densities increase.

The following recommendations are made based on the results obtained in this study:

- The 60Au-40Pt alloy in the "ductile" heat treatment condition needs to be studied. It will be interesting to see whether Kirkendall porosity is formed when such a sample is solutionised.
- The mechanism for oxide formation and oxide reduction at Au-Pt alloys in the solid solution condition has to be investigated. It is surprising that two oxide reduction peaks are observed at alloys in the solutionised condition.
- The poisoning phenomena at Au-Pt alloys during ethylene glycol oxidation have to be studied. The solid solution electrodes give higher current densities for ethylene glycol oxidation than the two-phased electrodes, presumably due to the "third-body effect". However, the solid solution electrodes also poison during electrolysis. The exact role of poisoning at Au-Pt alloys therefore has to be determined.
- The cleaning cycle (potential and time at potential) has to be optimised for electrolysis by potential pulsing.
- Gold-titanium alloys with a higher titanium content than Gold 990 have to be studied to determine how titanium will influence the electrochemical properties of pure gold. It is possible to have 10 at% titanium in solid solution with gold (see Fig. 3.20). A higher solutionising heat treatment temperature (approximately 1000°C) will be needed to obtain a Au-10at% Ti solid solution.